Universidade de Aveiro

2014

Departamento de Biologia

Maria Helena Almeida Braz da Silva

Modulation of TG/(GL+FFA) cycle as a therapeutic strategy in obesity

Modulação do ciclo TG/(GL+FFA) como alvo terapêutico na obesidade

DECLARAÇÃO

Declaro que este relatório é integralmente da minha autoria, estando devidamente referenciadas as fontes e obras consultadas, bem como identificadas de modo claro as citações dessas obras. Não contém, por isso, qualquer tipo de plágio quer de textos publicados, qualquer que seja o meio dessa publicação, incluindo meios eletrónicos, quer de trabalhos académicos.

Universidade de Aveiro

2014

Departamento de Biologia

Maria Helena Almeida Braz da Silva

Modulation of TG/ (GL+FFA) cycle as a therapeutic strategy to obesity

Modulação do ciclo TG/ (GL+ FFA) como alvo terapêutico na obesidade

Dissertação apresentada à Universidade de Aveiro para cumprimento dos requisitos necessários à obtenção do grau de Mestre em Biologia Molecular e Celular realizada sob a orientação científica da Doutora Anabela Pinto Rolo, Professora Auxiliar do Departamento de Biologia da Universidade de Aveiro, e sob a co-orientação científica do Doutor João Paulo Soeiro Terra Teodoro, Investigador de Pós-Doutoramento do Centro de Neurociências e Biologia Celular da Universidade de Coimbra.

Aos meus pais.

Por todo o amor, amizade e apoio incondicional. Por todos os ensinamentos que formaram os alicerces da minha vida. Sem vocês nada disto seria possível.

o júri

presidente

Professora Doutora Maria de Lourdes Pereira
Professora associada com agregação no Departamento de Biologia da Universidade de Aveiro

Professor Doutor Carlos Manuel Marques Palmeira
Professor Catedrático do Departamento de Ciências da Vida da Faculdade de Ciências e Tecnologia da Universidade de Coimbra

Professora Doutora Anabela Pinto Rolo
Professora Auxiliar do Departamento de Biologia da Universidade de Aveiro

agradecimentos

Em primeiro lugar, gostaria de agradecer ao Professor Doutor Carlos Palmeira e à minha orientadora Professora Doutora Anabela Rolo por esta oportunidade, pela confiança depositada neste trabalho, por todos os ensinamentos, pela orientação e toda a disponibilidade! Obrigada também pela amizade, simpatia e carinho com que me receberam no MitoLab!

Ao Doutor João Soeiro, o meu co-orientador pela amizade, disponibilidade, apoio e por todos os conselhos e sugestões feitas ao longo deste trabalho.

À Faculdade de Ciências e Tecnologia da Universidade de Coimbra e ao Centro de Neurociências e Biologia Celular, pelo acolhimento.

Ao Professor Doutor Rui de Carvalho e ao Laboratório de Ressonância Magnética Nuclear da Universidade de Coimbra, pela grande (enorme!) ajuda na análise dos espectros de ressonância magnética nuclear.

Aos meus colegas de laboratório, por toda ajuda, paciência e sobretudo amizade! Por me fazerem sorrir todos os dias e sentir como se sempre tivesse feito parte do MitoLab! Obrigada: Ana, Catarina, Filipe, Inês, João, Leka, Rui e Rute!

À Inês, pela amizade, ajuda e muita paciência ao longo deste trabalho. Obrigada pelo grande impulso inicial! Foi um prazer trabalhar contigo.

A todos os meus colegas, amigos e companheiros que foram deixando a sua marca ao longo da minha vida, fazendo de mim uma pessoa melhor!

Ao Tiago. Por ter sido a chave de todo o incentivo e força nos momentos mais difíceis. Por todo o amor, amizade e companheirismo. Meine liebe, Ich liebe dich!

Aos meus avós, por fazerem parte do meu mundo, por todo o amor, carinho, amizade e suporte ao longo da minha vida. Levo-vos sempre no meu coração!

E por fim, um obrigado do fundo do coração aos meus pais. Não há palavras que descrevam o amor que sinto por vocês. Obrigada por fazerem de mim aquilo que sou hoje. Esta conquista é igualmente vossa!

palavras-chave CDCA, Ciclo TG/ (GL+FFA), Obesidade, Adipócitos 3T3-L1, UCP-1, Mitocôndria

resumo

A obesidade é um dos principais problemas de saúde pública a nível mundial. A grande maioria da população obesa desenvolve patologias associadas que consequentemente levam à diminuição da esperança média de vida. Estas incluem diabetes tipo 2 (T2DM), aterosclerose, esteatose hepática, doenças cardiovasculares e ainda alguns tipos de cancro, Dado que as estratégias atuais são ainda pouco eficazes, no que se refere ao tratamento da obesidade, é urgente que se investiguem novas terapias, nomeadamente a modulação do tecido adiposo branco (WAT). No WAT, as vias metabólicas da glicose e dos lípidos convergem no ciclo dos glicerolípidos/ácidos gordos livres (TG/ (GL+FFA)), sendo este considerado um ciclo fútil dado que não gera produtos enquanto consome substratos energéticos. A diminuição da atividade deste ciclo em situações de obesidade e diabetes diminui a oxidação de substratos e aumenta o armazenamento de ácidos gordos (FFA) no WAT. Assim, a estimulação deste ciclo fútil surge como um potencial alvo terapêutico. Porém, a oxidação de substratos implica a estimulação simultânea do ciclo fútil e da função mitocondrial sendo que, até à data, não existe um mecanismo capaz de acoplar estes processos. O ácido quenodesoxicólico (CDCA) é um ácido biliar conhecido pelos seus efeitos anti-obesidade, no entanto, o seu mecanismo de ação é ainda controverso. O CDCA activa dois reguladores da transcrição de genes metabólicos envolvidos no ciclo TG/ (GL+FFA), na capacidade oxidativa mitocondrial e na β-oxidação, o PPARα e o PPARγ. Assim, a nossa hipótese propõe que o CDCA medeia o acoplamento do ciclo fútil com o gasto energético no WAT, aumentando simultaneamente as taxas de atividade do ciclo fútil e de oxidação mitocondrial de substratos.

Este trabalho foca-se na avaliação das alterações metabólicas no ciclo TG/ (GL+FFA), na linha celular 3T3-L1, induzidas pelo CDCA. Especificamente, avaliou-se se a exposição ao CDCA altera a atividade deste ciclo, se essa alteração está relacionada com uma melhoria no perfil metabólico e ainda se o metabolismo mitocondrial está envolvido.

As células expostas ao CDCA demonstraram uma diminuição na acumulação de lípidos e um aumento no conteúdo de proteína desacopladora-1 (UCP-1), o que por sua vez diminui a produção de espécies reactivas de oxigénio (ROS). Adicionalmente, a exposição ao CDCA induziu um aumento na gliceroneógenese, sugerindo, assim, um aumento na atividade do ciclo TG/ (GL+FFA). Dessa forma, a administração de CDCA parece ser uma estratégia terapêutica atrativa no combate à obesidade e à T2DM. No entanto, uma questão mantém-se, o que leva à redução da acumulação dos triglicerídeos (TG)? Com base nos resultados obtidos, o CDCA aumenta a expressão dos genes envolvidos na β-oxidação e na biogénese mitocondrial, mas não existem diferenças na oxidação dos FFA entre o controlo e as células expostas ao CDCA. Uma possível explicação é que os lípidos estejam a ser exportados para o meio. No entanto, este é um estudo *in vitro*, logo seria interessante perceber o destino destes lípidos *in vivo*. Finalmente a possível ocorrência de compartimentalização metabólica abre novas perspectivas para trabalhos futuros.

keywords CDCA, TG/ (GL+FFA) cycle, Obesity, 3T3-L1 adipocytes, UCP-1, mitochondria

abstract

Obesity is one of the leading causes of health care issues all over the world. A large slice of the worldwide population develops co-morbidities as a consequence of this condition, such as type 2 diabetes mellitus (T2DM), atherosclerosis, fatty liver, cardiovascular diseases and even some cancers, conditions that are associated with reduced life expectancy. The inefficiency of current therapies that aim to treat obesity leads to further investigation on novel therapeutic targets for this condition, including modulation of white adipose tissue (WAT). In WAT, glucose and lipid metabolism converge into triglyceride/ glycerol + free fatty acid (TG/ (GL + FFA)) cycle, which is considered a futile cycle since it doesn't generate products while consuming energy substrates. The decreased activity of this cycle in obesity, decreases substrates oxidation and increases free fatty acids (FFA) storage in WAT. If coupled to increased mitochondrial β-oxidation, modulation of TG/ (GL+FFA) cycling provides an attractive therapeutic target to stimulate fat mobilization and prevent WAT dysfunction. Currently there are no known strategies that simultaneously stimulate both these processes. Chenodeoxycholic acid (CDCA) is a bile acid known for its anti-obesity effects; however the mechanism of action is still controversial. CDCA activates both peroxisome proliferator activating receptor (PPAR) α and PPARγ, regulators of the transcription of key metabolic genes involved in the TG/ (GL+FFA) cycle, mitochondrial oxidative capacity and FFA oxidation. As such, we hypothesized that CDCA mediates the coupling of futile cycles with energy expenditure in WAT, increasing simultaneously futile acid activity and mitochondrial substrates oxidation.

This work focused on evaluating the metabolic alterations of TG/ (GL+FFA) cycle, in culture 3T3-L1 cells exposed to CDCA. Specifically, we addressed if CDCA supplementation alters the TG/ (GL+FFA) cycle activity, if this was related to improved metabolic status and if mitochondrial metabolism was involved.

Cultured 3T3-L1 cells exposed to CDCA exhibit decreased lipid accumulation and an increase in uncoupling protein-1 (UCP-1) content, which in turn leads to a decrease in reactive oxygen species (ROS) generation. CDCA also leads to an increase in glyceroneogenesis, suggesting an increase activity in TG/ (GL+FFA) cycle activity. Indeed, these results show that administration of CDCA seems to be an attractive therapy to obesity and T2DM. However, a question still remains, what leads to a reduction in triglycerides (TG) accumulation? Based on our results CDCA up-regulates genes involved in β-oxidation and mitochondrial biogenesis, but there are no differences in fatty acid oxidation between control and cell exposed to CDCA. A possible explanation is that lipids are being exported to the medium. However this is an *in vitro* study, it would be interesting understand the destination of this lipids *in vivo*. Finally the possible occurrence of metabolic compartmentalization opens new perspectives in futures works.

Index

List of figures

List of tables

List of abbreviations

6-ECDCA - 6a-ethyl-chenodeoxycholic acid

ACC - Acetyl-CoA carboxylase

ACS - Acetyl-CoA syntethase

ADP - Adenosine diphosphate

aP2 - Adipocyte protein 2

ATCC - American Type Culture Collection

ATGL - Adipose triglyceride lipase

ATP - Adenosine triphosphate

BA - Bile acids

BAT - Brown adipose tissue

BCA - Bicinchoninic acid

BMI - Body mass index

BSA - Bovine serum albumin

C/EBP - CCAAT enhancer binding proteins

CA - Cholic acid

cAMP - Cyclic AMP

CD36 - Cluster of differentiation 36

CDCA - Chenodeoxycholic acid

CoQ - Coenzyme Q

COX - Cytochrome *c* Oxidase

CPT1α - Carnitine palmitoyltransferase I alpha

CREB - cAMP response element binding protein

Cu^{+} - Copper cation

CYP7A1 - Cytochrome P450 enzyme cholesterol 7α-hydroxylase

CYP8B1 - Microsomal sterol 12α-hydroxylase

DAG - Diacylglycerol

DCA - Deoxycholic

DCF - 2', 7' –dichlorofluorescin

DCFDA - 2',7'–dichlorofluorescein diacetate

DEX - Dexamethasone

DMEM - Dulbecco's Modified Eagle Medium

DMSO - Dimethyl sulfoxide

DNA - Deoxyribonucleic acid

DNL - *De novo* lipogenesis

DNP - Uncoupler 2,4-dinitrophenol

FABP4 - Fatty-acid-binding protein 4

$FADH_2$ - Flavin adenine dinucleotide

FAS - Fatty acid synthase

FATP - Fatty acid transport protein

FBS - Fetal bovine serum

FCCP - Carbonyl cyanide-*p*-trifluoromethoxyphenylhydrazone

FFA - Free fatty acids

FID - Free Induction Decay

FXR - Farnesoid X receptor

GLP1 - Glucagon-like peptide

GLUT4 - Glucose transporter 4 protein

GSPx - Glutathione peroxidase

H_2O_2 - Hydrogen peroxide

HDL - high-density lipoprotein

HSL - Hormone sensitive lipase

IBMX - Isomethylbutylxanthine

IGF-1 - Insulin-like growth factor 1

IL-6 - Interleukin-6

LCA - Lithocholic acids

LCFA – Long chain fatty acids

LDH - Lactate dehydrogenase

LPL - Lipoprotein lipase

MeOH/$CHCl_3$/H_2O - Methanol/chloroform/water

MG - Monoglycerides

MGL - monoglyceride lipase

MRC - Mitochondrial respiratory chain

mtDNA - Mitochondrial DNA

NADH - Nicotinamide adenine dinucleotide

NADPH - Dinucleotide phosphate-oxidase

NASH - Non-alcoholic fatty liver

NCS - Newborn calf serum

NMR - Nuclear magnetic resonance

NRF - Nuclear respiratory factor

O_2 - Molecular oxygen

$O_2\bullet^-$ - Superoxide anion

OXPHOS - Oxidative phosphorylation

PBS - Phosphate-buffered saline

PC - Pyruvate carboxylase

PDC - Pyruvate dehydrogenase complex

PEP - Phosphoenolpyruvate

PEPCK - Phosphoenolpyruvate carboxylase

PGC-1α - Peroxisome proliferator-activated receptor gamma coactivator 1-alpha

PKA - Protein kinase A

PPAR - Peroxisome proliferator activating receptor

PPARE - Peroxisome proliferator-activated receptor element

ROS - Reactive oxygen species

RPB-4 - Retinol protein binding 4

SHP - Short Heterodimer Protein

SRB - Sulforhodamine B

SREBP-1 - Sterol regulatory element binding protein

T2DM - Type 2 diabetes mellitus

T3 - Tri-iodothyronine

T4 - Thyroxine

TCA - Tricarboxylic acid

TFAM - Mitochondrial transcription factor A

TG - Triglycerides

TG/ (GL+FFA) - Triglyceride/ glycerol + free fatty acid

TGR5 - G-protein-coupled membrane receptor

TMPD - Tetramethyl-*p*-phenylenediamine

TMRM - Tetramethylrhodamine methyl ester

TNF-α - Tumor necrosis factor-α

TPI - Triose phosphate isomerase

TZDs - Thiazolidinediones

UCP - Uncoupling protein

VLDL - Very-low-density lipoprotein

WAT - White adipose tissue

WHO - World Health Organization

Δψ - Mitochondrial membrane potential

CHAPTER I

General Introduction

1. General Introduction

1.1 Obesity

1.1.1 An overview

Obesity is one of the leading causes of health care issues all over the world. According to World Health Organization (WHO), 205 million men and 297 million women over the age of 20 were obese in 2008, a total of more than half a billion adults worldwide (Soumaya, 2012; WHO, 2013). As such, it is safe to claim that we are in the midst of a worldwide epidemic of obesity.

One of the parameters for defining over-weightiness is the Body Mass Index (BMI), which is a measure of weight corrected for height and which reflects the total body fat (Nammi et al., 2004).

$$\text{BMI} = \frac{\text{Weight of an individual}\,(\text{in kg})}{\text{Height}^2\,(\text{m}^2)}$$

The WHO defines that a BMI equal or greater than 25 indicates excess of weight and a BMI equal or greater than 30 is considered obesity (WHO, 2013).

Several co-morbidities develop as a consequence of obesity like dyslipidemia, insulin resistance, type 2 diabetes mellitus (T2DM), atherosclerosis, fatty liver, cardiovascular diseases and even some cancers, conditions that are associated with reduced life expectancy (Scarpellini & Tack, 2012; Gesta et al., 2007). Obesity is also associated with metabolic syndrome, a cluster of disorders that require the presence of diabetes, impaired glucose tolerance (IGT), impaired fasting glucose or insulin resistance and any two of the following abnormalities: central obesity, dyslipidemia (high triglycerides or low high-density lipoprotein (HDL) cholesterol concentration), elevated blood pressure, or microalbuminuria (WHO, 1999).

Obesity is a multi-factorial disorder that involves complex ethological links between genetic, metabolic and neural frameworks on one hand, and behavior, food habits, physical activity and socio-cultural factors on the other (Nammi et al., 2004). In general, obesity is caused by energy imbalance, where energy intake exceeds energy expenditure for an extended period of time. This excess of energy intake compared to

energy usage leads to excessive accumulation of fat in adipose tissue, resulting in enlarged and/or increased number of fat cells (Bray, 2004; Sikaris, 2004; Nammi et al., 2004).

Fat distribution is a key to the development of metabolic syndrome, as shown in Figure 1. Increased intra-abdominal/visceral fat (central or apple-shaped obesity) promotes a high risk of metabolic syndrome, whereas increased subcutaneous fat in the thighs and hips (peripheral or pear-shaped obesity) exerts little risk (Gesta et al., 2007).

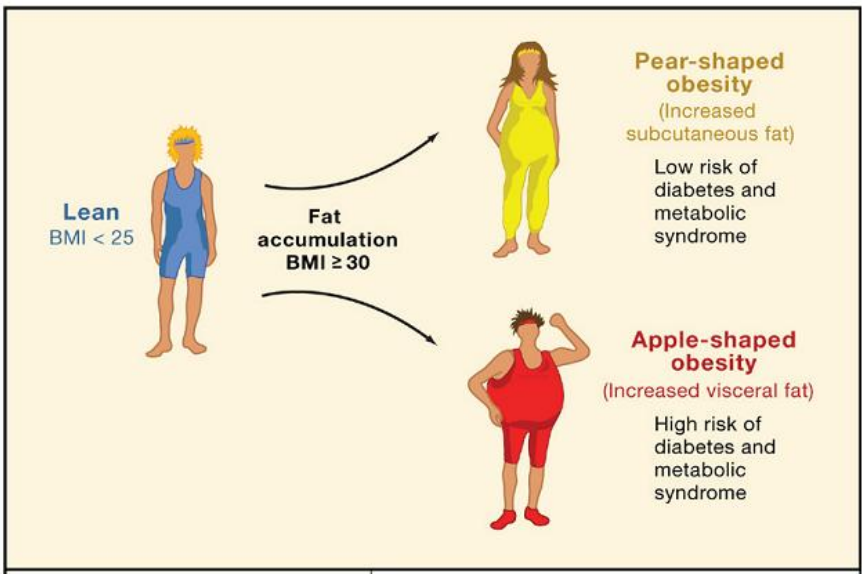

Figure 1 - Fat Distribution Influences risk of deveplopment of metabolic syndrome. Adapted from Stephane Gesta *et al*. 2007

Adipose tissue not only serves to store energy but is also one of the body's largest endocrine organs, affecting the function of cells and tissues throughout the body (Scarpellini & Tack, 2012). The excess adiposity and adipocyte dysfunction, leads to the dysregulation of expression of bioactive substances secreted by adipocytes, called adipokines. Adipokines, such as leptin, adiponectin, resistin, retinol protein binding 4 (RPB-4), tumor necrosis factor-α (TNF-α) and interleukin-6 (IL-6), to name a few, can either promote inflammation and metabolic dysfunctions, or contribute to the resolution of both these processes (Scarpellini & Tack, 2012). The imbalance of pro and anti-inflammatory adipokines is an important contributor to a chronic low-grade inflammatory state that has been associated to obesity (Scarpellini & Tack, 2012).

While on one hand, lipid storage is increased in obesity, the adipose tissue inflamed also releases more free fatty acids (FFA) that lead to fat accumulation in liver and muscle, contributing to insulin resistance (Rasouli & Kern, 2008; Guan et al., 2002a).

The glycerolipid/free fatty acid (TG/GL+FFA) cycle is associated with the flux of FFA in the organism. This process is intimately related with glyceroneogenesis, which rate-limiting step is regulated by phosphoenolpyruvate carboxykinase (PEPCK). In adipose tissue, glyceroneogenesis controlled by PEPCK contributes to the regulation of FFA release to the blood (Hsieh et al., 2011). The over-expression of PEPCK in white adipose tissue (WAT) lead to an increase of FFA re-esterification in adipose tissue and to obesity without insulin resistance (Franckhauser et al., 2002). The increased glyceroneogenesis reduced the availability of FFA to the muscle and thus prevented impaired glucose tolerance. Therefore, the regulation of (TG/GL+FFA) cycle seems to be important in the development of obesity and T2DM, and for this reason an attractive therapeutic target.

Taking into account these findings, obesity and associated conditions are linked to disorders in the metabolism of glucose, which in turn are closely related with disturbances in the metabolism of lipids. Since adipose tissue plays a crucial role in the regulation of fatty acid homeostasis, this organ may be a primary site where the early metabolic disturbances leading to the development of insulin resistance take place, followed by the development of insulin resistance in other tissues follows (Cahová et al., 2007).

1.1.2 Regulation of glucose and lipid metabolism

Obesity and associated pathologies are characterized by an unbalance in carbohydrate and lipid metabolism (Saltiel, 2001). Insulin and glucagon act in concert to ensure that glucose homeostasis is maintained throughout a wide variety of physiological conditions (Vance, 2002). Insulin stimulates glucose uptake, utilization, and storage, while suppressing hepatic glucose production, thus reducing plasma glucose levels (Prentki & Madiraju, 2012). Glucagon promotes the release of stored and newly synthesized glucose into the bloodstream. Pancreatic β and α-cells regulate insulin and glucagon synthesis and release, respectively, even in response to small changes in plasma glucose levels, since they are extremely sensitive to glucose concentrations (Hsieh et al., 2011).

Following a meal, most glucose disposal occurs in skeletal muscle, whereas fasting plasma glucose levels are determined primarily by glucose output from the liver. The balance between the utilization and production of glucose is maintained at equilibrium by two opposing hormones, insulin and glucagon (Saltiel, 2001). After a meal, in response

to an elevation in plasma glucose and amino acids, insulin is released from the β-cells of the islets of Langerhans in the pancreas. The β-cells contain a specific glucokinase that exhibits a low affinity for glucose, and is not inhibited by product formation, thus enabling the enzyme to adjust its activity in response to a wide range of glucose concentrations (Prentki & Madiraju, 2012). After phosphorylation, glucose is oxidized and adenosine triphosphate/adenosine diphosphate (ATP/ADP) ratio increase, this leads to close potassium channels and consequently the cell becomes depolarized. This results in the opening of voltage-sensitive calcium channels, which increases intracellular calcium and insulin is released (Saltiel, 2001). During fasting or exercise, when plasma glucose level falls, glucagon is secreted by α-cells, which surround the β-cells in the pancreas. Glucagon promotes the release of stored and newly synthesized glucose into the bloodstream.

The primary targets for insulin are skeletal and cardiac muscle, adipose tissue and liver. Glucose uptake is the rate-limiting step in glucose utilization and storage. Insulin stimulates the transport of glucose into muscle and fat cells by increasing the concentration of glucose transporter 4 protein (GLUT4) at the cell surface (Vance, 2002). Upon entering the muscle cell, glucose is rapidly phosphorylated by hexokinase and either subsequently stored as glycogen due to the activation of glycogen synthase, or oxidized to generate ATP synthesis, via activation of enzymes such as pyruvate kinase (Saltiel, 2001). In adipocytes, glucose is stored primarily as lipid, due to increased uptake of glucose and activation of enzymes associated with lipogenesis. Insulin also inhibits lipolysis in adipocytes, primarily through inhibition of the enzyme hormone sensitive lipase (HSL) (Vance, 2002). Insulin inhibits the production and release of glucose by the liver, due to the blockade of gluconeogenesis and glyceroneogenesis. In addition to controlling the activities of metabolic enzymes through phosphorylation or dephosphorylation, insulin also regulates the expression of a number of genes encoding hepatic enzymes. On the other hand, glucagon increases hepatic cyclic AMP (cAMP), which in turn increases PEPCK gene expression during hypoglycemia. This results in augment rate of gluconeogenesis and glyceroneogesis that lead to an increase in plasma glucose levels (Franckhauser et al., 2002; Vance, 2002).

1.1.3 Metabolic imbalance associated with obesity

Insulin resistance, the failure to respond to normal circulating concentrations of insulin, is a common state associated with obesity and T2DM. When the effects induced by normal or elevated insulin levels are attenuated, β-cell secretion increase to maintain normal blood glucose levels, and so insulin resistance is associated with compensatory hyperinsulinaemia (Reaven, 2004).

A complex interaction between genetic and environmental factors underlies the development of insulin resistance, which affects whole-body metabolic homeostasis, with manifestations varying according to the dependence of the tissues on insulin for metabolic processes. Resistance to the antilipolytic effects of insulin causes increased lipolysis and FFA release from fat depots (Saltiel, 2001). This elevated plasma FFA attenuate the ability of insulin to suppress glucose production in the liver, but allow a continual increase in insulin-stimulated FFA synthesis. Initially, β-cell insulin secretion is also stimulated by elevated FFA, however, long-term exposure of pancreatic β-cells to elevated FFA ultimately impairs insulin secretion (Hsieh et al., 2011). Increased circulating levels of FFA are initially associated with increased rates of fatty acid oxidation in the skeletal muscle. However, the accumulation of metabolites from fatty acid oxidation in the cytoplasm of muscle cells (lipotoxicity) interferes with insulin signaling cascade and the ability to easily switch between glucose and fat oxidation in response to homeostatic signals (Hsieh et al., 2011). For example, increased generation of nicotinamide adenine dinucleotide (NADH), and ATP inhibit key regulatory enzymes in the glycolytic pathway such as pyruvate dehydrogenase complex (PDC), contributing to increased blood glucose concentration. The augment of FFA oxidation also blocks the recycling of GLUT4 to the surface of muscle cells and decreases glucose uptake, thus contributing to increased blood glucose levels (Hsieh et al., 2011).

The impaired uptake of glucose increases plasma glucose concentration leading to further insulin secretion and starting a vicious cycle with impaired regulation of energy substrate metabolism. This state of “metabolic inflexibility”, is defined as an impaired ability to switch easily between glucose and fat oxidation according to the metabolic needs of the organism (Cahová et al., 2007); (Saltiel, 2001) (Figure 2).

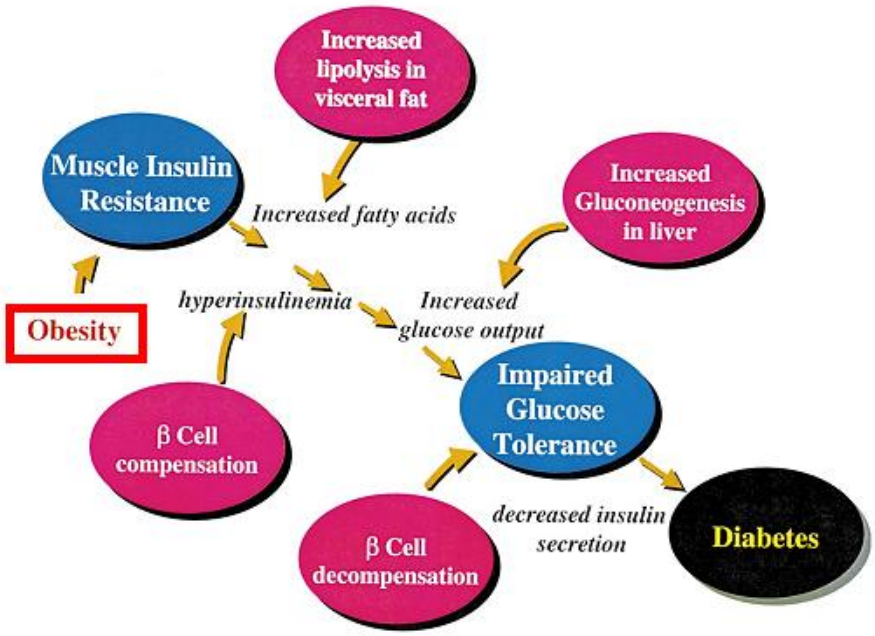

Figure 2 - Metabolic staging of T2DM. Adapated from Alan R. Saltiel 2001

T2DM is characterized by a progressive decrease in insulin action, followed by an inability of the β-cell to compensate for insulin resistance. Insulin resistance is the first lesion due to metabolic changes produced by obesity. Insulin resistance in visceral fat leads to increased fatty acid production, which exacerbates insulin resistance in liver and muscle. The β-cell compensates for insulin resistance by secreting more insulin. Ultimately, the β-cell can no longer compensate, leading to impaired glucose tolerance, and diabetes.

1.2 Adipose Tissue

1.2.1 Structure and physiologic function

Adipose tissue is a dynamic organ at the center of nutritional adaptation and metabolic regulation (Sethi & Vidal-puig, 2007; Harwood, 2012). In mammals, adipose tissue exists in many different locations through the body and typically in areas of lose connective tissue, such as subcutaneous layers between muscle and dermis. Moreover, adipose-specific depots surround vital organs like heart and kidneys (Casteilla et al., 2008).

The classical roles of adipose tissue are to insulate the body, provide mechanical support and to store FFA after food intake, which are also released during the fasting state to maintain energy levels (Hajer et al., 2008).

There are two types of adipose tissue: WAT and brown adipose tissue (BAT) (Figure 4). WAT constitutes the major component of body's adipose tissue and is responsible for the storage of energy in large unilocular droplets (mainly constituted by TG) and the release of FFA. Several types of cells constitute WAT: mature adipocytes and a variety of other cells (i.e., preadipocytes, fibroblasts, endothelial cells, and macrophages), usually described as the "stroma vascular fraction". The adipocytes, preadipocytes, and macrophages have metabolic and inflammatory functions, which render WAT able to release several adipokines with effects on WAT and other tissues and metabolic processes, as described in previous section and as illustrated in Figure 3.

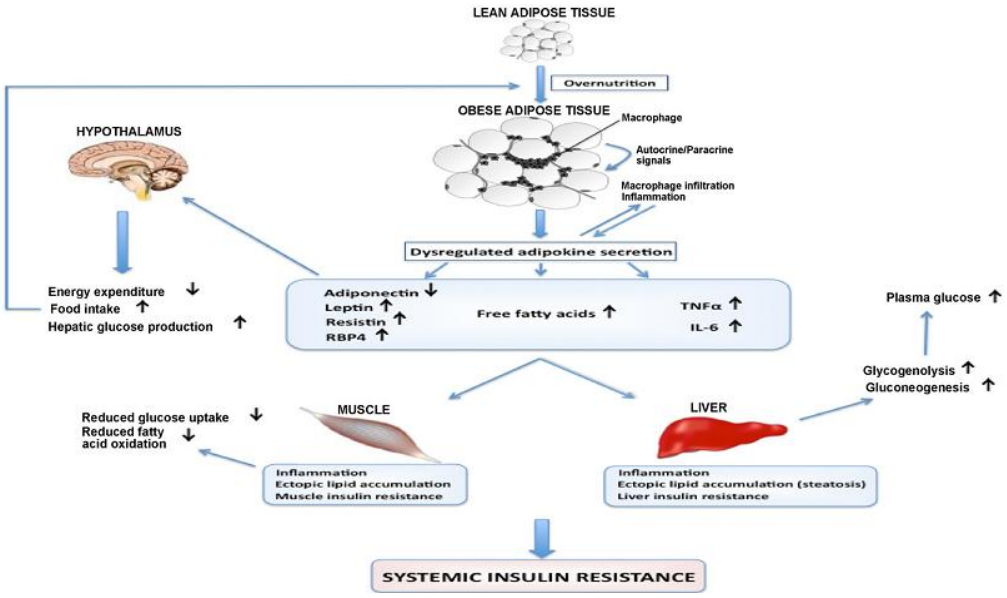

Figure 3 - Obesity-induced changes in adipokine secretion and leads to the development of insulin resistance. Adapted from Galic et al. 2009

In general, obesity is accompanied by an increased release of FFA and plasma concentration levels of adipokines (Leptin, Resistin and Retinol protein binding-4), with the exception of adiponectin, which plasma levels are lower. This rise on the level of adipokines leads to a chronic inflammatory state and insulin resistance in peripheral tissues, accompanied by infiltration of a large number of macrophages Although the majority of adipokines is adipocyte-derived, there are others which are also produced by macrophages (TNF-α and IL-6), interacting in a paracrine way to control adipocyte metabolism.

Unlike WAT, BAT typically has a smaller number of adipocytes, which are multilocular, containing many cytoplasmic lipid droplets of varying sizes. BAT also has a richer vascular supplies with more abundant mitochondrial chromogens, responsible for the brown color (Sethi & Vidal-puig, 2007; Medina-gómez, 2012; Torres et al., 2008; Gesta et al., 2007; Redinger, 2009; Balistreri et al., 2010). BAT is considered a thermogenic tissue, with its specialized heat production through mitochondrial "uncoupling" of oxidative phosphorylation, by the action of uncoupling protein 1 (UCP-1). BAT mitochondria are enriched in UCP-1, while it is minimally present in WAT (Yehuda-shnaidman et al., 2010). UCP-1 is present on the internal mitochondrial membrane and creates a proton leak that diminishes the electrochemical gradient needed for oxidative phosphorylation. As a consequence, BAT affects energy use by producing heat from uncoupled oxidative phosphorylation (Sethi & Vidal-puig, 2007; Medina-gómez, 2012; Torres et al., 2008; Gesta et al., 2007; Redinger, 2009; Balistreri et al., 2010).

In humans, BAT was thought not to be present postnatally, but recently studies using positron emission tomography have clearly shown active BAT depots in adult humans metabolically, in the cervical, supraclavicular, axillary and paraventral regions (Yoneshiro et al., 2013; Lichtenbelt et al., 2009; Taittonen et al., 2009).

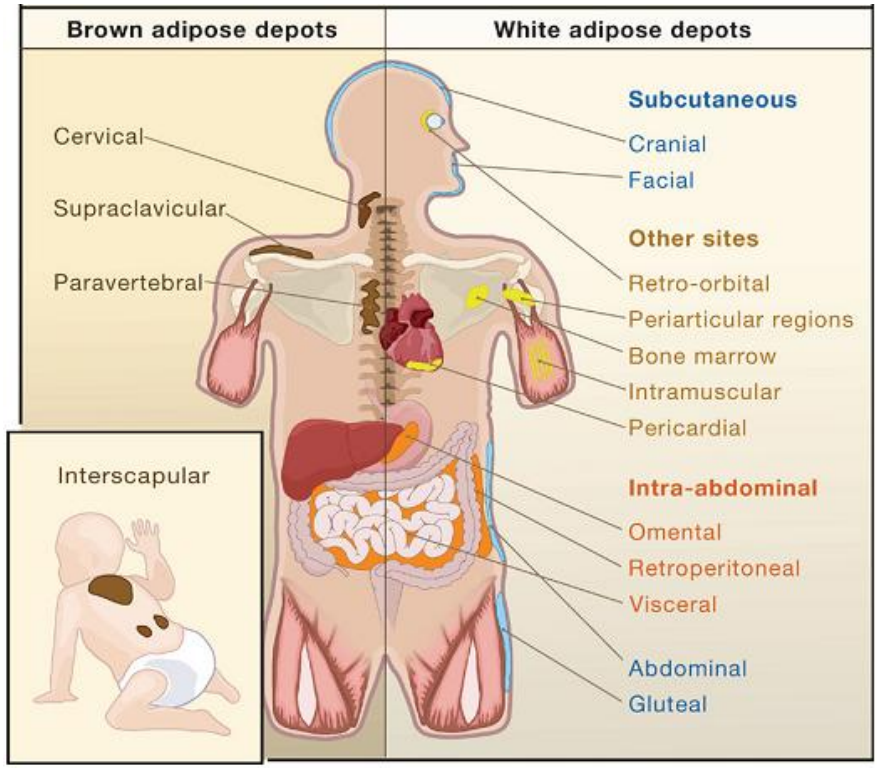

Figure 4 - Distribution of the WAT and BAT depots. Adapted from Stephane Gesta *et al.* 2007

Recently, the concept of two distinct forms of adipose tissue has also been challenged through the recognition, in mouse and humans, that some fat depots have both white and brown adipocytes, and by the identification of a third form of fat cell, the "brite" (or beige) adipocyte. These "brite" (from the joining of the words "brown" and "white") cells express UCP-1, but do not possess the complete molecular characteristics of brown adipocytes (Barbatelli et al., 2010; Wu et al., 2012; Petrovic et al., 2010). In humans, the amount of BAT is inversely correlated with BMI, so the conversion of white adipocytes into-"brite"-cells associated with their activation seems to be an attractive strategy to increase energy expenditure and reduce obesity (Wu et al., 2012).

1.2.2 Adipogenesis

Adipogenesis is the formation of adipocyte from precursor cells, as shown in Figure 5. Hormonal activity and transcription factors induce proliferation and differentiation of preadipocytes into mature adipocytes. In humans, preadipocytes are converted into adipocytes in the late embryonic stage origin. However, the ability of differentiation of

preadipocytes is always present in all species depending on the body energy status and the storage needs (Torres et al., 2008; Moreno-Navarrete & Fernández-real, 2012).

Development of adipocytes has been studied using two distinct cell lines. One refers to pluripotential fibroblasts that originate myocytes, chondrocytes and adipocytes. The other is a unipotential cell line (3T3-L1 origin) that can only give rise to mature adipocytes (Ntambi & Kim, 2000). Before converting into adipocytes, 3T3-L1 cells are maintained undifferentiated by the preadipocyte factor 1 (Pref-1) (Sul et al., 2000). When the differentiation program is initiated, CCAAT enhancer binding proteins (C/EBP-β/δ) expression is mildly increased. These are key early regulators of adipogenesis and promoters of the genes encoding C/EBP-α and Peroxisome Proliferator Activating Receptor Gamma (PPARγ), critical factors that maintain the phenotype of the adipocyte inducing the expression of genes involved in insulin sensitivity, lipogenesis and lipolysis, including those encoding GLUT4, fatty-acid-binding protein (FABP4, also known as adipocyte protein 2, aP2), lipoprotein lipase (LPL), perilipin and the secreted factors adiponectin and leptin (Lowe et al., 2011). Furthermore, differentiation of adipocytes is accompanied by an increase in the expression of sterol regulatory element binding protein (SREBP-1). SREBP-1 is a transcription factor that participates in adipocyte differentiation by stimulating PPARγ expression. The role of SREBP-1 has been clearly established in the liver as the key lipogenic transcription factor that regulates the expression of enzymes of FFA biosynthesis such as fatty acid synthase (FAS) and acetyl-CoA carboxylase (ACC) (Ntambi & Kim, 2000). Previously studies demonstrated that the accumulation of TG, characteristic of mature adipocytes, is due an increase in lipogenic rate determined by an augmented expression of these enzymes (Student et al., 1980; Mackall et al., 1976). However, in adipocytes, the function of SREBP-1 is not clear.

Maximal differentiation of 3T3-L1 fibroblast cells is obtained by stimulating preadipocytes with a mixture that includes insulin, dexamethasone (DEX), and isomethylbutylxanthine (IBMX) (Ntambi & Kim, 2000). Insulin is known to act through the insulin-like growth factor 1 (IGF-1) receptor, a protein that regulates muscle growth through activation of PI3/AKT pathway (Nakae et al., 2003). DEX, a synthetic glucocorticoid agonist, is traditionally used to stimulate the glucocorticoid receptor pathway and activate the transcription factor C/EBP-β. IBMX, a cAMP-phosphodiesterase inhibitor, is traditionally used to increase intracellular cAMP. At the nuclear level, treatment with IBMX results in activation of the related transcription factor C/EBP, such C/EBP-β and δ in turn induce transcription of C/EBP-α and PPARγ. After 5 to 7 days of stimulation,

adipocytes acquire a round shape and the enzymes involved in lipolysis and lipogenesis (Ntambi & Kim, 2000).

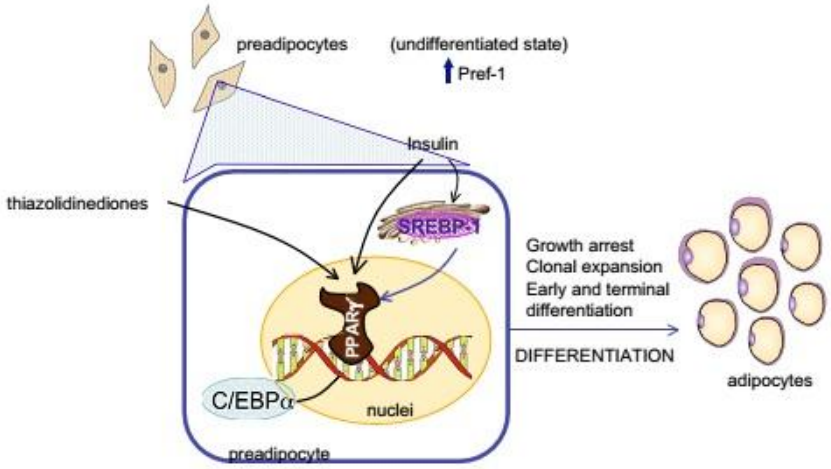

Figure 5 – Adipogenesis, Adapted from Vázquez-Vela *et al.* 2008

PPARs are ligand-activated transcription factors that belong to the nuclear hormone receptor super-family. The name PPAR derives from the ability of the first identified family member, PPARα, to induce peroxisome proliferation in rodent hepatocytes (Christodoulides & Vidal-Puig, 2010). PPARα is predominantly expressed in the liver and to a lesser extend in the heart, skeletal muscle, small intestine, and kidney and it has a crucial role in inducing the expression of genes involved in FFA oxidation (Torres et al., 2008). This factor is expressed at low levels in WAT but its expression level in BAT is four times higher than in the liver, being sensitive to peroxisome proliferator agents and fasting (Christodoulides & Vidal-Puig, 2010). *In vitro*, the levels of PPARα are similarly very low and when pharmacologically stimulated, it failed to promote differentiation of 3T3-L1 cells (Berger et al., 1999). However when co-expressed with peroxisome proliferator-activated receptor gamma coactivator 1-alpha (PGC-1α), this nuclear factor induces the expression of FFA oxidation enzymes in 3T3-L1 preadipocytes (Vega et al., 2000). *In vivo*, when rats are exposure to a bezafribate (Christodoulides & Vidal-Puig, 2010), a PPARα activator (Peters et al., 2003), the expression of genes involved in FFA uptake and β-oxidation are increased. On the other hand, WAT is normally over-developed in animals lacking the PPARα gene and are susceptible to development late onset obesity despite a stable caloric intake, associated with adipocyte hypertrophy. In parallel, when PPARα is pharmacologically activated, there is a reduction of adiposity in mouse models of diet-induced and genetic obesity (Christodoulides & Vidal-

Puig, 2010). PPARα has also been shown to down-regulate apoliprotein C-III, a protein which inhibits TG hydrolysis by LPL (Lee et al., 2003). This effect of PPARα further contributes to the lipid-lowering effect. These results strongly indicate that reduction in obesity due PPARα activation is correlated with an increase in β-oxidation, which make this receptor a possible therapeutic target to this condition.

Relatively to PPARγ there are two distinct isoforms, PPARγ1 and PPARγ2. PPARγ1 is predominantly present in adipose tissue, but is also detected in other tissues as immune cells, intestine, kidney and liver. On the other hand, PPARγ2 is produced almost exclusively in WAT and BAT (Christodoulides & Vidal-Puig, 2010; Semple et al., 2006). Interestingly, PPARγ2 knockout mice still have WAT, suggesting a role of PPARγ1 to compensate the lack of PPARγ2 to sustain adipogenesis (Tontonoz et al., 1994). An increase in PPARγ expression is sufficient to initiate adipogenesis *in vitro* in 3T3-L1 fibroblasts and *in vivo* (Tontonoz et al., 1994). On the other hand, adipose-specific deletions of the PPARγ gene leads to lipodystrophy; and dominant-negative versions of PPARγ, in other words, an altered gene product that acts antagonistically to the wild-type allele, inhibit the conversion of preadipocytes into adipocytes (Torres et al., 2008). These works prove the importance of this nuclear factor in adipogenesis. PPARγ also plays a key role in adipose tissue lipid metabolism. Its expression is increased postprandially (Vidal-Puig et al., 1996), and its activation leads to the upregulation of genes that mediate FFA uptake and storage, such as: cluster of differentiation 36 (CD36, also known as fatty acid translocase), LPL, fatty acid transport protein (FATP) family and acetyl-CoA syntethase (ACS) (Schoonjans et al., 1996; Oakes et al., 2002; Olswang et al., 2002). PPARγ may also promote futile cycling in adipocytes between TG esterification and re-esterification (Guan et al., 2002a).

Thiazolidinediones (TZDs), like rosiglitazone, are antidiabetic agents and PPARγ ligands that induce differentiation of preadipocytes (Zebisch et al., 2012; Berger et al., 1996). The promotion of adipogenesis decreases insulin resistance by increasing the capacity to store lipids. This is due in part to PPARγ action that augments the levels of GLUT 4, uncoupling proteins, and adiponectin expression, all of which contributes to a lower risk of developing insulin resistance (Lee et al., 2003). Thus, equilibrium between PPARα and PPARγ activities is necessary to maintain the balance between lipid synthesis and oxidation. If such balance is lost, the risk of developing obesity and insulin resistance could be increased (Ferre, 2004).

1.2.3 Adipose tissue metabolism, TG/(GL+FFA) cycle and glyceroneogenesis

The process of storage and mobilization of energy to supply the needs of organs and tissues is the responsibility of WAT. Contrarily, BAT also stores energy, but to a far lesser extent. It also produces heat by oxidizing FFA within the adipocytes, rather than supplying FFA for other cell types. Lipids, particularly fatty acids, are an exceptionally efficient fuel storage molecules (Vance, 2002), so is important to focus on what regulates the flux of FFA between tissues and organs, as illustrated in Figure 6.

The TG/ (GL+FFA) cycle, also known as triglyceride/fatty acid cycling regulates the flux of FFA between tissues and organs, and is the central pathway that interlink TG and glucose metabolism. Most tissues are involved in fatty acid metabolism, but three are quantitatively more important than others: adipose tissue, skeletal muscle and liver. The TG/(GL+FFA) cycling is a process of fatty acid esterification (lipogenesis) with glycerol-3-phosphate to form TG, followed by the hydrolysis (lypolysis) of TG to regenerate glycerol and fatty acids, which can re-enter the cycle, a process that occurs in each tissue referred previously (Prentki & Madiraju, 2012). It is known that in various tissues most of the FFA released in the cytoplasm upon lipolysis is immediately re-esterified, even at steady state levels of TG and FFA. Thus, this process is considered futile as 7 ATP molecules are consumed per each complete turn of the cycle (Prentki & Madiraju, 2012). This cycle is important for whole body homeostasis since lipogenesis and lipolysis generate products, such as glycerol, FFA and many lipid signaling molecules with influence in other organs and tissues, making it fundamental to have balance between these pathways (Prentki & Madiraju, 2012). Abnormalities associated with this cycle lead to pathological conditions such as insulin resistance, T2DM, non-alcoholic fatty liver disease, and even cancer (Prentki & Madiraju, 2012), what makes this cycle a possible therapeutic target to these metabolic diseases.

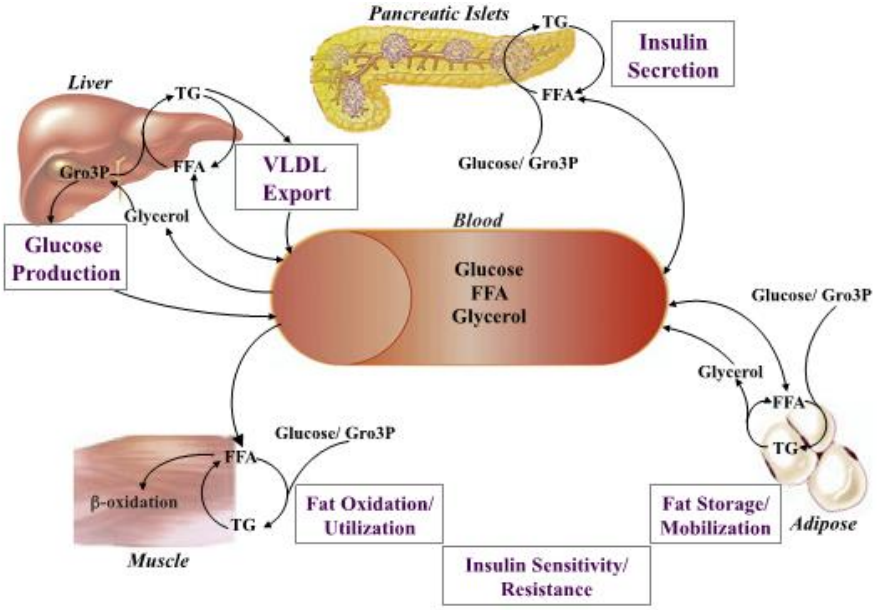

Figure 6 - Role and interrelationship of TG/ (GL/FFA) cycle in various organs. Adapted from Prentki *et al.* 2011

There is a continual flow of fatty acids between the three tissues described above. Dietary fat enters the plasma from the small intestine in the form of chylomicron-triacylglycerol. The chylomicrons are the largest of the lipoprotein particles and have a very fast turnover. They deliver triacylglycerol-fatty acids to tissues expressing the LPL. The remaining 'remnant' particles (that have lost perhaps two-thirds of their triacylglycerol) are mainly taken up by the liver. This is the starting point for fatty acid metabolism in the tissues. Adipose tissue takes up fatty acids via the action of LPL. It releases fatty acids by the hydrolysis (lipolysis) of stored TG, by the action of the enzyme known as HSL and other lipases, to liberate FFA into the plasma. Plasma FFA circulate bound to albumin. The liver takes up fatty acids in various forms and liberates triacylglycerol-fatty acids as VLDL (very-low-density lipoprotein) particles. In this scenario, skeletal and heart muscle (and other oxidative tissues not considered here) are the only pure consumers, taking up fatty acids either from lipoprotein-triacylglycerol or from the plasma FFA pool and using them ultimately for oxidation.

i. Adipose Tissue metabolism: Lipogenesis and Lipolysis

The FFA stored in human adipose tissue reflect dietary intake (Frayn et al., 2006). *De novo* lipogenesis is the synthesis of FFA from carbohydrates or other energy sources acquired in the diet. Glucose is the major substrate for lipogenesis and this process occurs predominantly in the liver and to a lesser extent in adipose tissue. The contribution of adipose tissue to *de novo* fatty acid synthesis is less well defined in human and particularly in pathological situations such as diabetes and obesity (Torres et al., 2008). There's discussion about the contribution of *de novo* lipogenesis to adipose tissue fat

stores but, at the whole-body level, it only operates significantly when carbohydrate intake exceeds energy requirements. However, it is clear that the key enzymes for fatty acids synthesis, FAS, ACC and malic enzyme are present in human adipose tissue (Torres et al., 2008; Large et al., 2004). Thus in adipocytes, most of FFA used for TG synthesis are taken from the plasma either as FFA bound to plasma albumin, or as TG incorporated in TG-rich lipoproteins, mainly chylomicrons (carrying diet fat) in the postprandial state and VLDL (secreted from the liver) in the post-absorptive state (Mead et al., 2002). FFA are released from lipoproteins through the hydrolysis of TG by LPL, which expression and activity in adipose tissue are increased in fed state (Mead et al., 2002). Then FFA liberated from TG can be taken up by the adipocyte and esterified to form new TG. LPL is synthesized within adipocytes and exported to its site of action, the luminal side of the capillary endothelial cells. Contrary to the fed state, in fasting more LPL becomes inactive (perhaps via monomerization) (Frayth, 2003). In contrast, LPL in skeletal and cardiac muscle is activated during fasting (Frayn et al., 2006).

Within the adipocyte, FFA can be taken into the mitochondrial matrix and be oxidized to acetyl-CoA through the fatty acid β-oxidation (Torres et al., 2008). In spite of LPL generating excess of FFA, adipocytes only take up a proportion depending on nutritional state. There is always an "overspill" of FFA to the circulation, so the insulin levels increase proportionally to FFA taken up by the tissue (Frayth, 2003). However in the postprandial state typically approximately 50% may be released as FFA, clearly shown by enrichment of the plasma FFA pool with dietary fatty acids soon after a meal (Frayn et al., 2006). These fatty acids are then available for uptake by other tissues including muscle and liver. It also involves stimulation of FFA esterification to make new TG within the adipocyte. In addition, insulin may stimulate glucose uptake and glycolysis, which supplies the glycerol-3-phosphate necessary for FFA esterification (Frayn et al., 2006).

Lipolysis is responsible by controlling the availability of FFA and TG in nonadipose tissues, mostly in situations of energy needs. During intracellular lipolysis, TG are broken down in a stepwise manner, to form three molecules of FFA and one of glycerol per unit of completely hydrolyzed TG (Large et al., 2004).

First, TG stored in the lipid droplet are hydrolyzed by the enzyme adipose triglyceride lipase (ATGL), also known as desnutrin, releasing a diacylglycerol (DAG) and FFA. This enzyme is induced under fasting condition and inhibited after feeding. After hydrolysis by ATGL, DAG are then hydrolyzed by the HSL, so named because of its

responsiveness to the hormones insulin and catecholamines, and monoglyceride lipase (MGL), producing FFA and glycerol. HSL is one of the major regulatory points of lipolysis. HSL is regulated in the long-term by transcriptional control, since mRNA abundance increases during starvation, and is decreased in obesity (Frayn et al., 2006). But the most important aspect of HSL on a day-to-day basis is its regulation by reversible phosphorylation, described in Figure 7 (Torres et al., 2008; Frayn et al., 2006).

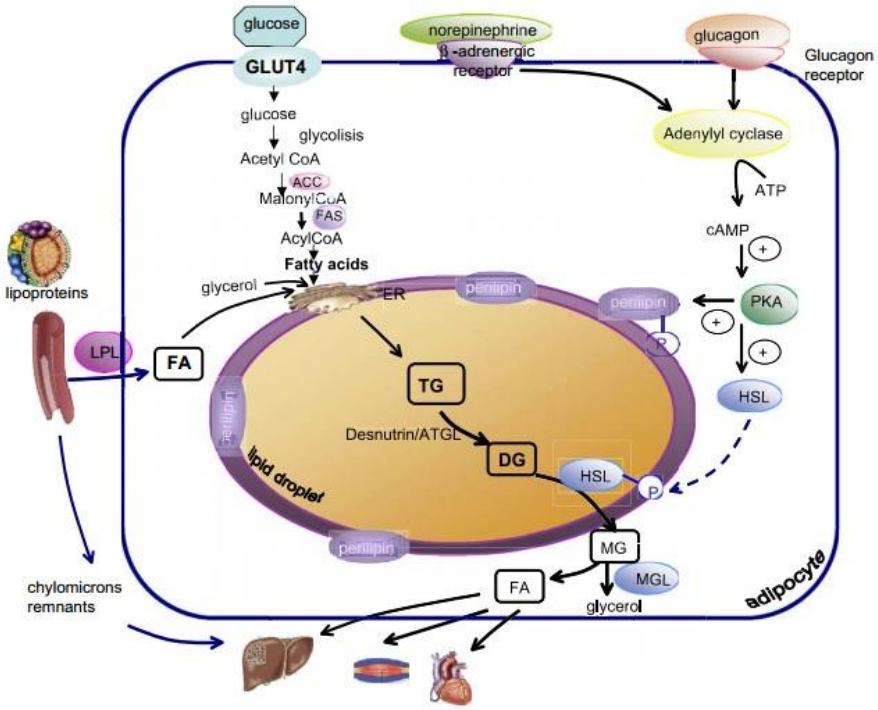

Figure 7 - Lipogenesis and lipolysis. Adapted from Vázquez-Vela *et al.*, 2008.

In the adipocyte, glucose is oxidized via glycolysis to pyruvate, which is converted to acetyl-CoA. Alternatively, fatty acids from lipolysis can be taken into the mitochondrial matrix and be oxidized to acetyl-CoA through the fatty acid β-oxidation. The acetyl groups are converted into acyl-CoA, which are esterified in the endoplasmic reticulum to TG. These are then translocated into the lipid droplet. Under fasting conditions, lipolysis is activated by G-protein-coupled receptors resulting in an increase in cAMP, which activates PKA. PKA phosphorylates the protein perilipin located in the membrane of the adipocyte fat droplet. PKA also phosphorylates the HSL triggering its translocation from the cytoplasm to the lipid droplet and inducing the hydrolysis of diglycerides produced by the ATGL to form monoglycerides (MG). Then MG are hydrolyzed by MGL producing FFA and glycerol. FFA are released to supply the energy needs of organism. On the other hand, in the fed state insulin suppresses HSL activity by activation of a particular phosphodiesterase, PDE3B, which reduces the cAMP concentration.

Different lipases get access to the lipid droplet when proteins that coat the lipid droplet, called perilipins, are phosphorylated. Usually, Perilipin A prevents lipolysis of TG by surrounding the lipid droplet, preventing the access of lipases. β-adrenergic stimulation of adipocytes leads to the activation of adenyl cyclase, which in turns increases cAMP concentrations. Increased cAMP levels promote the activation of cAMP dependent protein kinase A (PKA) and the subsequent phosphorylation of HSL and perilipin. This leads to the translocation of HSL from the cytoplasm to the lipid droplet and induce neutral lipid hydrolysis (Torres et al., 2008; Large et al., 2004).

During fasting, glucagon and catecholamines levels are increased, leading to the stimulation of lipolysis in the adipocytes by activating several lipases via PKA, leading to FFA mobilization from the adipocyte into circulation. FFA are then bound to albumin and transported to muscle, liver, heart and other tissues for its oxidation or re-esterification. β-adrenergic receptors induce lipolysis, whereas α2-adrenergic receptors mediate lipogenesis. In postprandial state, high insulin concentrations inhibit lipolytic enzymes, decreasing lipid mobilization from adipose tissue. These effects are mediated by the activation of phosphodiesterase 3B that degrades cAMP, preventing the stimulation of several lipases, and by activating protein phosphatase-1 that causes dephosphorylation of HSL, in both instances reducing the rates of lipolysis (Torres et al., 2008; Large et al., 2004).

ii. Glyceroneogenesis

Quantitative estimates of TG/(GL+FFA) cycle activity in human adults, newborn infants and in animals show that only a small portion of the FFA released as a result of lipolysis in the WAT are oxidized, and the majority are re-esterified to TG in various tissues (Reshef et al., 2003). The fraction of FFA released that is recycled back to TG remains relatively constant (75%). However, marked changes were verified in the rate of total TG/(GL+FFA) cycle during different metabolic states, including the deceleration on the TG/(GL+FFA) cycle in experimental models of obesity and diabetes (Reshef et al., 2003) and acceleration of cycle by acute exercise (Schenk & Horowitz, 2007). The metabolic significance of the rate of triglyceride/fatty acid recycling remains to be determined, however it is clear that TG/(GL+FFA) recycling requires the constant generation of glycerol-3-phosphate for triglyceride synthesis, particularly in situations when cycling is increased (Figure 8) (Reshef et al., 2003).

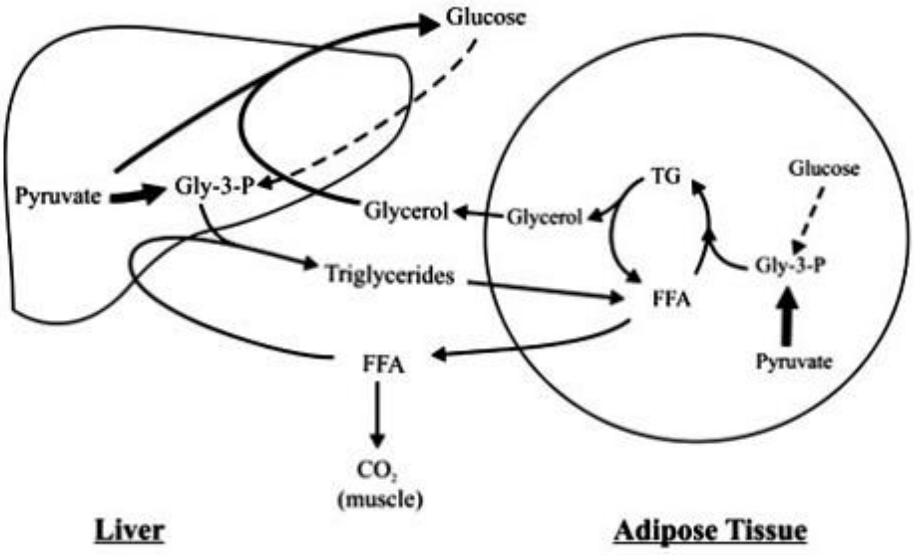

Figure 8 - The triglyceride/fatty acid cycle in mammals. Adapted from Reshef *et al.* 2003

In the fed state glucose is metabolized to glycerol-3-phosphate via glycolysis and esterified with three FFA to generate TG. This occurs both in the liver and in WAT, being the FFA derived both from the diet or *de novo* lipogenesis. FFA yield energy through β-oxidation or can be stored as TG in adipose tissue for energy supplying at a later time. However, during fasting, approximately 65% of FFA are re-esterified back to TG in WAT (Hsieh et al., 2011). Since glucose levels are decreased during fasting, the synthesis of glycerol-3-phosphate from glucose is minimal. Moreover, in WAT the glycerol released during lipolysis cannot be phosphorylated and used for triglyceride synthesis because the activity of glycerol kinase in this tissue is negligible (Reshef et al., 2003). Thus, an alternative source of 3-glycerol phosphate during fasting other than glucose is necessary (Reshef et al., 2003). Some studies demonstrated that exists an alternative pathway called that glyceroneogenesis, which is defined as the conversion of precursors other than glucose or glycerol, such as pyruvate and lactate, into glycerol 3-phosphate for triglyceride synthesis. Thus, this pathway is exceptionally important in situations of fasting (Reshef et al., 2003; Reshef et al., 1970).

Glyceroneogenesis, like gluconeogenesis, is regulated by PEPCK, a key enzyme which is expressed in liver, WAT and BAT and catalyzes the conversion of oxaloacetate to phosphoenolpyruvate, in both pathways (Reshef et al., 2003). This is supported by a study where the deletion of the binding site for the PEPCK (proliferator-activated receptor element, PPARE), abolished glyceroneogenesis in the WAT, as determined by their inability to synthesize glyceride-glycerol from pyruvate (Olswang et al., 2002).

Furthermore, glyceroneogenesis seems to be important in the control of triglyceride turnover in WAT (Reshef et al., 2003).

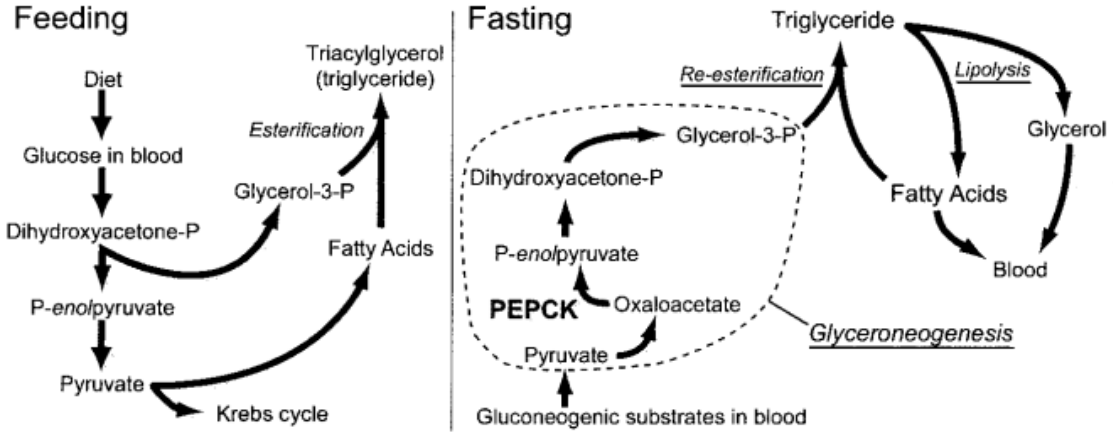

Figure 9 - Glyceroneogenesis modulates fatty acid release during periods of fasting. Adapted from Beale et al. 2002

When fuel is not available from the diet, lipolysis releases glycerol and fatty acids from triglyceride stores in fat cells. Fasting lowers insulin and increases intracellular cAMP, which leads to decreased glucose utilization and increased PEPCK production. Fatty acid release is restrained due to increased glyceroneogenesis and re-esterification. In contrast, almost 100% of the glycerol is released because it is not phosphorylated significantly in adipocytes.

Although insulin resistance is associated with TG mobilization from the adipose tissue, GLUT4-deficient mice do not exhibit TG depletion in the WAT, which may be explained by an enhanced activity of glyceroneogenesis (Abel et al., 2001). Moreover, over-expression of PEPCK in WAT has been shown to increase FFA re-esterification, leading to obesity, without insulin resistance (Franckhauser et al., 2002). Thus, increased glyceroneogenesis leads to a reduction in plasmatic FFA levels.

BAT has a tenfold activity of PEPCK compared to the WAT, but the physiological significance has not been formally established (Reshef et al., 2003). Findings suggest that glyceroneogenesis plays a critical role in thermogenesis in BAT by controlling the rate of formation of glycerol-3-phosphate required for triglyceride synthesis. It has been shown that rats fed with high protein content diet and low on carbohydrates, exhibit increased glyceroneogenesis from alanine, pyruvate, and lactate in BAT, and a fourfold increase in PEPCK activity of, leading to increased re-esterification of FFA (Brito et al., 1999). Additionally, rats fed a carbohydrate free diet exhibit reduced BAT thermogenic capacity (Brito et al., 1992). As such, this pathway may play a critical role in determining the rate of FFA released from TG to BAT mitochondria for thermogenesis, since this FFA seems to

increase the expression of UCP-1 (Millward et al., 2010). Contrarily to WAT, BAT has an enhanced activity of glycerol kinase so form glycerol-3 phosphate for triglyceride synthesis directly from glycerol (Reshef et al., 2003). However, most of the preformed FFA are re-esterified to TG using glycerol-3-phosphate generated via glyceroneogenesis. Thus glyceroneogenesis seems to play a important role in providing glycerol-3-phosphate required to ensure TG synthesis from dietary FFA in BAT during the fed state (Brito et al., 1999). Finally, ablation of PEPCK in WAT and reduced expression of PEPCK in BAT resulted in increased plasma FFA, thus contributing to the development of insulin resistance (Millward et al., 2010).

1.3 Mitochondria

1.3.1 General overview

Mitochondria are essential organelles in all eukaryotic cells and are involved in many processes that are critical for cell survival and functioning, including metabolic pathways, redox control and calcium homeostasis. These organelles are also the main sources of reactive oxygen species (ROS) and play a key role in cell death mechanisms (Dalgaard & Pedersen, 2001).

The main source of cell energy is the synthesis of ATP from ADP and inorganic phosphate (Pi) by oxidative phosphorylation (OXPHOS) or coupled respiration, carried out in the inner mitochondrial membrane. The mitochondrial respiratory chain (MRC) is located in the inner mitochondrial membrane, and is constituted by four multienzymatic complexes and two proteins responsible for electron transport, coenzyme Q (CoQ), and cytochrome *c* (Figure 9) (Coutinho et al., 2012). The protein subunits can be grouped in four complexes:

- Complex I or NADH dehydrogenase;
- Complex II or succinate dehydrogenase;
- Complex III or cytochrome c reductase;
- Complex IV or cytochrome c oxidase.

The total number of polypeptides involved directly in OXPHOS is 91 when cytochrome *c* is included. Of these proteins, some are nuclear-encoded and others are mitochondrial-encoded in the mtDNA (Attardi & G., 1988). The mitochondrial genome encodes for essential proteins for the complex I, III, IV and V, but complex II subunits are all encoded by the nuclear genome. Because of its limited coding capacity, mtDNA relies on nuclear genes for structural components and biological functions (Duarte, 2012). Furthermore, nuclear-encoded genes also regulate mitochondrial transcription, translation, and mtDNA replication, thus the precise cooperation of nuclear and mtDNA expression is critical to regulate OXPHOS capacity in response to different physiological demands and disease states (Scarpulla, 2008; Peralta et al., 2011).

Transcription of the mitochondrial genome is under the control of a single transcription factor, mitochondrial transcription factor A (TFAM), which is encoded by the nuclear genome (Bengtsson et al., 2001). Nuclear respiratory factor (NRF)-1 and NRF-2,

which specifically activate numerous nuclear-encoded genes involved in mitochondrial respiration (Lee & Wei, 2005). Through NRF-stimulated expression of TFAM, occurs simultaneously the transcription of the mitochondrial genome and of nuclear-encoded mitochondrial genes (Patti & Corvera, 2010). The expression of mitochondrial genes is also controlled by additional nuclear transcription factors, including PPARα and PPARδ, which can induce expression of mitochondrial genes in a tissue-dependent and physiological context-dependent manner (Patti & Corvera, 2010). A high level of transcriptional coordination is required to ensure coupling of mitochondrial activity to other metabolic activities within the cell and to mediate appropriate parallel changes in all components of multiprotein complexes (Scarpulla, 2008). This coordination is accomplished through the action of transcriptional coactivators and corepressors (Patti & Corvera, 2010). The most studied coactivator of mitochondrial gene transcription is the PGC-1α (Knutti & Kralli, 2001), activated in cellular energy-requiring conditions such as cell growth, hypoxia, glucose deprivation, and exercise to activate transcription factors promoting mitochondrial remodeling and/or biogenesis, thus increasing cellular energetic capacity (Patti & Corvera, 2010). For example, PGC-1α is highly expressed in muscle, liver, and BAT and expression is further increased in these tissues in response to exercise, fasting, and cold exposure, respectively (Knutti & Kralli, 2001). PGC-1α seems do not be required for mitochondrial biogenesis during development, however is necessary for the expression of the full complement of proteins of mitochondrial OXPHOS and β-oxidation pathways in muscle and BAT (Sonoda et al., 2007).

OXPHOS involves the coupling of electron transport, by means of the complexes I-IV of the MRC, to the active pumping of protons across the inner mitochondrial membrane, and ATP formation by ATP synthase (Complex V). During mitochondrial respiration, the electron transport chain oxidizes reduced coenzymes (NADH and flavin adenine dinucleotide ($FADH_2$) at Complexes I and II level, respectively) by donating electrons to the MRC. The movement of electrons through the MRC is driven by a redox potential that is found across the chain. Complexes I, III, and IV pump protons across the inner membrane as electrons pass down the MRC. This produces an electrochemical potential difference across the inner membrane, known as proton motive force, consisting mostly of an electrochemical gradient (membrane potential) and a chemical gradient (pH difference). The energy that is conserved in the proton gradient across the inner membrane is used by ATP synthase to synthesize ATP as protons are transported back from the intermembrane space into the mitochondrial matrix. The final destination of the

electrons is molecular oxygen (O_2), which is reduced to water by complex IV, in the last step of the MRC.

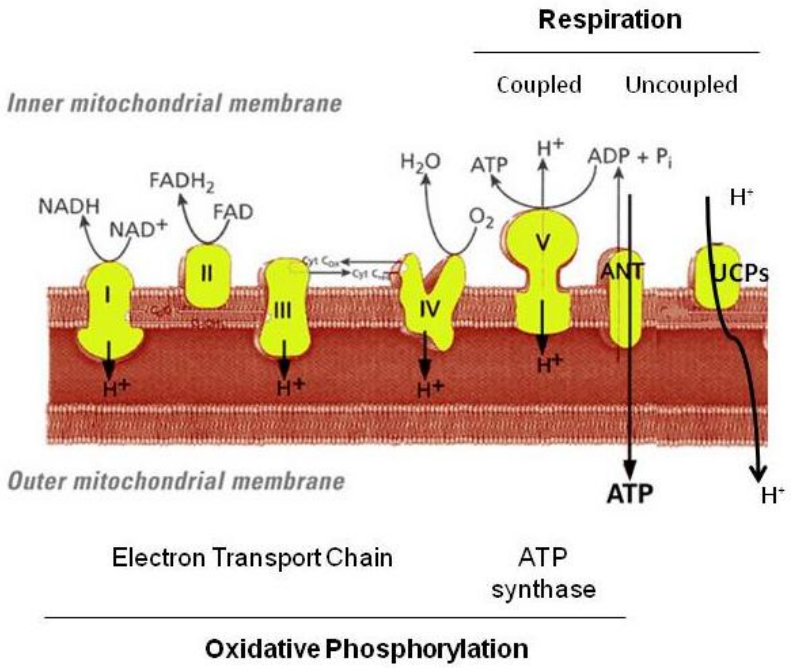

Figure 10 – Schematic representation of coupled and uncoupled respiration. Adapted from Pati et al. 2010

Complex I accept fuel from the citric acid cycle in the form of NADH, which donates electrons to the chain. Complex II accepts electrons from $FADH_2$ and passes to Complex III via CoQ. The electro is then passed to Complex IV via cytochrome *c*. This proton electrochemical gradient is consumed by demand pathways via the ATP synthase to produce ATP or by proton leak pathways, which release energy in the form of heat. Proton leak pathways can be mediated by UCPs or by ANT.

ROS are formed as a natural byproduct of the normal metabolism of oxygen and correspond to a variety of molecules and free radicals (chemical species with one unpaired electron) (Coutinho et al., 2012), such as superoxide anion ($O_2^{\bullet -}$) and hydrogen peroxide (H_2O_2). ROS normally exist in all aerobic cells in balance with biochemical antioxidants (Coutinho et al., 2012), and they are formed in response to various stimuli (Fridovich, 1978), since they play a role in different physiological processes (Pinkus et al., 1996). However when this balance is broken, due an increase in ROS production, a decrease in antioxidants or both, oxidative stress occurs (Coutinho et al., 2012) with significant damage to cell structures. Mitochondria are the main sources of ROS, what

makes these organelles particularly susceptible to oxidative damage (Kirkinezos & Moraes, 2001).

Mitochondria have their own ROS scavenging mechanisms that include superoxide dismutase, glutathione peroxidase (GSPx), glutathione dismutase and vitamin C (Kirkinezos & Moraes, 2001). However it has been demonstrated that they generate ROS at a rate higher than their scavenging capacity, resulting in the incomplete reduction of approximately 1–3% of the consumed oxygen (Kirkinezos & Moraes, 2001). This indicates that ROS production is a physiologic process that occurs in the sequence of aerobic metabolism (Lee & Wei, 2005). Complexes I and III produce most of ROS (Kirkinezos & Moraes, 2001). Specifically, is during the transfer of electrons from CoQ to complex III that the most significant production of superoxide anion occurs. Thus, inhibition of the MRC results in an increase in ROS (Turrens et al., 1985).

The coupling of respiration to ATP synthesis is not 100% efficient, and some of the energy is dissipated as heat. Partial uncoupling of respiration from ATP synthesis, also known as proton leak, can be mediated by UCPs. Thus an increase in UCPs content could have severe consequences for cellular function, due to the decrease in ATP synthesis. On the other hand, a beneficial effect that may result from the proton "leak" is to prevent excessive accumulation of ROS (Teodoro, 2007).

1.3.2 Uncoupling proteins

Uncoupling proteins (1, 2, 3, 4 and 5) are a subfamily of the mitochondrial solute carrier family, and are located in the inner mitochondrial membrane (Azzu & Brand, 2010). These proteins have similarities in their structures, but different tissue expression in mammals. The UCP-1 was the first discovered and is mainly expressed in BAT (Coutinho et al., 2012). UCP-2 was mainly identified in liver (Dalgaard & Pedersen, 2001), whereas UCP-3 is mainly restricted to the skeletal muscle. More recently, UCP-4 and UCP-5 were identified, being mainly expressed in brain (Coutinho et al., 2012).

The main function of these proteins is decrease metabolic efficiency through uncoupling of ATP synthesis from the MRC. However, depending on tissue, this uncoupling effect has different consequences, such as thermogenesis and energy expenditure (UCP-1), regulation of FFA metabolism (UCP-2 and UCP-3), reduction in

ROS generation (UCP1-3 and UCP-5), and regulation of ATP dependent processes (UCP-2) (Coutinho et al., 2012).

The uncoupling activity of UCP-1 is explained by its ability to transport protons across the inner mitochondrial membrane, in particular when FFA bind to the protein (Silva, 2006). However, the precise mechanism by which FFA regulate transport through UCP-1 is still unclear. There are two mechanisms proposed: the FFA protonophore (*or flip-flop*) model, and the channel (or *proton buffering*) model. In the *flip-flop* model, UCP-1 is a carrier of fatty acid anions, which are transported by this protein from the mitochondrial matrix to intermembrane space. In this model, each fatty acid anion combines with a proton, becomes electrically neutral and flips back through the membrane, releasing the proton in the matrix. The channel model predicts a two domain structure of UCP-1 with a pore domain and a gating domain, which allows protons to pass through the UCP-1. In this model, fatty acid carboxyl groups are involved in the proton transport by providing H^+ buffering capacity (Frayn et al., 2006).

UCP-1 gene expression is increased by cold, adrenergic stimulation, β3-agonists, retinoid and thyroid hormones, cAMP and bile acids (Frayn et al., 2006; Watanabe et al., 2006; Ockenga et al., 2012; Teodoro et al., 2013). Moreover, its expression is activated by FFA and inhibited by purine nucleotides such as, ATP and ADP (Coutinho et al., 2012).

1.3.3 Mitochondrial activity in WAT and BAT

Mitochondrial metabolism is both the origin and target of multiple nutrient signals that coordinate integrated physiological responses to maintain cellular insulin sensitivity (Kusminski & Scherer, 2012) and play key roles in the metabolism of adipose tissue, both in WAT and BAT (Figure 11). WAT has less mitochondrial content when compared to BAT. This tissue interprets nutritional and hormonal signals in its microenvironment and then coordinates its mitochondrial response, either to oxidize incoming FFA and carbohydrate fuels through the tricarboxylic acid (TCA) cycle and the respiratory chain, or to store these fuels in the form TG until their release in situations of energy requirements (Kusminski & Scherer, 2012). Mitochondria play an important role in lipogenesis by providing acetyl-CoA for FFA synthesis, before their esterification into TG. Furthermore, mitochondria provide a key intermediary for the synthesis of TG, glycerol-3-phosphate through the glyceroneogenic pathway. This organelle is also involved in the regulation of

lipolysis with FFA resulting from lipolysis being oxidized by β-oxidation pathway in the mitochondrial matrix. This process of removal of FFA within white adipocytes by fatty acid-induced mitochondrial β-oxidation would protect the organism against FFA leakage out of adipocytes, thereby preventing lipotoxicity-induced insulin resistance in other organs such as liver, muscle or beta cells (Medina-gómez, 2012). Furthermore, the synchronized initiation of adipogenic process and mitochondrial biogenesis indicates that mitochondria play a pertinent role in the differentiation and maturation of adipocytes (De Pauw et al., 2009).

On the other hand, BAT is known to generate heat through dissipation of chemical energy, a process known as thermogenesis. When animals are subjected to cold stimulus or ingest surplus energy, their sympathetic nervous is stimulated and catecholamines are released. Catecholamines activate adenyl cyclase, which is able to convert ATP to cAMP. In addition, cAMP also activates lipases to release FFA from TG (Silva, 2006). These FFA act as fuel for the thermogenic process and are endogenous activators of UCP-1 (Silva, 2006).

Since the discovery of UCP-1 in BAT, and its capacity to increase energy expenditure through thermogenesis (Nicholls, 1983), many studies have focused its attention in this protein as a target in obesity and related disorders (Enerbäck et al., 1997; Bradford et al., 1993; Floryk et al., 1999; Kopecky et al., 1995; Silva, 2006; Matthias et al., 2000). By discharging the proton gradient that is produced across the inner mitochondrial membrane during substrate oxidation without producing ATP, BAT exhibits higher rates of oxidation, particularly fatty acids. In this way, animals with active BAT can partition excess energy intake toward oxidation and thus away from storage as body fat (Schoeller, 2001).

In humans, UCP-1 expression in the intraperitoneal fat of obese subjects is 50% lower than in normal weight subjects, in spite of the fact that the amount of BAT interspersed in WAT depots in adult individuals is relatively low (Frayn et al., 2006). Other works have shown that UCP-1 may be ectopically induced to be expressed in WAT, and thus could be exploited to increase the capacity to oxidize fatty acids in white adipocytes, and thereby regulate body fat mass. Induction of UCP-1 expression in white adipocytes has been achieved *in vitro* (Tiraby et al., 2003) and *in vivo* (Kopecky et al., 1995). *In vivo*, the fat-specific ap2 promoter has been used to construct transgenic mice that express UCP-1 in both BAT and WAT. These mice were resistant to genetic obesity and possess WAT cells with an increased mitochondrial content (Kopecky et al., 1995). *In vitro*,

expression of PGC-1α in white adipocytes not only induced UCP-1 expression, but also stimulated mitochondrial biogenesis and the expression of mitochondrial enzymes of the respiratory chain and fatty acid oxidation (Tiraby et al., 2003). Together, these findings suggested that UCP-1 could be an integral component of cellular energy control but the specific role of UCP-1 remains to be fully elucidated.

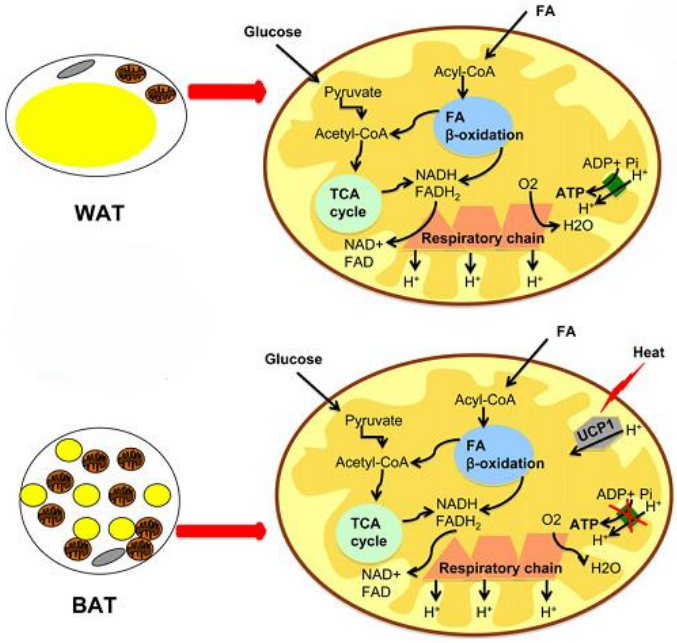

Figure 11 - Mitochondrial functions in WAT and BAT. Adapted from Medina-Gómez *et al.*, 2012

1.3.4 Mitochondrial dysfunction in obesity and T2DM

Obesity and T2DM are associated with an increase in ROS production and consequently mitochondrial damage in various organs, such as adipose tissue, liver and muscle (Patti & Corvera, 2010; Kusminski & Scherer, 2012; Alfadda & Sallam, 2012), which results in oxidative damage and irreversible loss of mitochondrial function (Teodoro, 2007). Impaired mitochondrial function is associated with insulin resistance and secretion of proinflammatory adipokines (Kusminski & Scherer, 2012).

In the adipose tissue, reduction in mitochondrial mass is usually associated with obesity and T2DM (Kusminski & Scherer, 2012). This is related to a reduction in both FFA β-oxidation and OXPHOS rates, leading to an increase of cytosolic FFA levels that alter glucose uptake and consequently lead to insulin resistance (Medina-gómez, 2012;

Kusminski & Scherer, 2012). In fact, mitochondrial content in white adipocytes derived from epididymal fat-pads of ob/ob mice arise approximately 50% lower than in lean control mice (Wilson-fritch et al., 2004). At a cellular level, the lost of function of mitochondria leads to glucose and lipid management disorders, which in turn result in lipid accumulation in non-adipose tissues, such as liver and muscle (Listenberger et al., 2003). This lipotoxicity process alters the metabolism of these tissues, contributing to development of insulin resistance.

Studies have also revealed that several mitochondrial genes crucial for mitochondria function and replication, including PGC-1α, are downregulated in obese, high-fat diet-fed, insulin-resistant mice, and in db/db mice. This suggests that mitochondrial biogenesis is highly compromised in WAT of obese insulin-resistant mouse models (Keller & Attie, 2010). Furthermore, an excessive caloric intake increases ROS production and causes deleterious effects in cells. ROS reduce oxygen consumption in adipocytes (Wang et al., 2010) and have been demonstrated to inhibit preadipocyte 3T3-L1 cell line model's proliferation (Carrière et al., 2003) and differentiation (Carrière et al., 2004). In these conditions, the expression of PPARγ and adiponectin was down-regulated and the expression of proinflammatory adipokines was up-regulated. Furthermore, increased ROS production has been found in mouse models of obesity, with increased expression of NADPH oxidase and inhibition of antioxidant enzymes such as superoxide dismutase, glutathione peroxidase and catalase (Furukawa et al., 2004). Likewise, increased levels of TNF-α decrease endothelial nitric oxide synthase expression and mitochondrial biogenesis, in adipose tissue from obese mice (Valerio et al., 2006).

1.4 Therapeutic interventions to obesity and associated disorders

1.4.1 Current therapies

Therapeutic strategies to improve adipocyte mitochondrial function could lead to improvements on whole-body insulin sensitivity. Currently there are some therapeutic strategies that aim to improve adipose tissue mitochondrial function and effectively treat obesity-induced T2DM. One of these strategies is a pharmacological intervention, such as the use of TZDs that increase mitochondrial mass (Kusminski & Scherer, 2012). As previously described TZDs are antidiabetic drugs since they increase the insulin sensitivity of WAT and skeletal muscle, in part because they are PPARγ agonists (Zebisch et al., 2012; Berger et al., 1996). Besides promoting adipocyte differentiation these drugs lead to an increase in mitochondrial biogenesis (Wilson-fritch et al., 2004).

In addition to TZDs, the process of 'browning' the WAT is an emerging and promising therapeutic strategy against obesity. Browning is the process by which brown-like adipocytes appear at anatomical sites characteristic of WAT. This strategy focuses in inducing a switch of WAT to a BAT-like phenotype through, amongst other, enhancement of mitochondrial biogenesis (Kusminski & Scherer, 2012). Mitochondrial biogenesis is driven in part through the activity of PGC-1α, which serves as coactivator of nuclear transcription factors, such PPARγ and PPARα, that are involved in the induction of lipid accumulation and β-oxidation, respectively (Kusminski & Scherer, 2012). This therapeutic manipulation aims to promote weight loss and insulin sensitivity, while preventing lipid accumulation through UCP-1 mediated mitochondrial thermogenic uncoupling.

Other therapeutic strategy was enhancing adipocyte mitochondrial function through the use of chemical uncouplers to dissipate energy as heat, reducing ATP synthesis by increasing proton leakage. Indeed, a study in 1930's used the chemical uncoupler 2,4-dinitrophenol (DNP) as a dietary drug and this created massive weight losses, as much as 3 kg per week (Harper et al., 2001). However, such uncoupling effects must be tightly controlled because a hypermetabolic state can lead to fatal uncontrolled thermogenesis in many tissues, including WAT, leading to chronically elevated body-temperatures (Hsiao et al., 2005). Thus, the use of uncouplers was discontinued, but the rationale behind it stands.

Aerobic endurance exercise is another strategy that improves whole-body glucose homeostasis by stimulating skeletal muscle mitochondrial respiratory activity and

mitochondrial biogenesis, by increasing gene expression levels of PGC-1α and TFAM. In addition to exercise, caloric restriction can also induce mitochondrial biogenesis, oxygen consumption and ATP synthesis; such effects have additional ROS-reducing benefits (Kusminski & Scherer, 2012).

All strategies described have the same aim that it is stimulate fuel oxidation in WAT and shift the balance toward less fuel storage and more substrates consumption. Thus, taking into account what was described in the previous two sections, if one could increase both the TG/(GL+FFA) cycle activity while removing one of its end products towards oxidation, it is possible that further cycling will occur and thus lead to decreased obesity. In other words, stimulate glyceroneogenesis pathway to increase glycerol-3-phosphate production and consequently augment FFA uptake; and at the same time, increase FFA β-oxidation. However, to increase the oxidation of substrates, the stimulation of futile cycle and mitochondrial function must occur in parallel. Currently there is no known strategy to the coupling of these processes.

1.4.2 Bile acids

i. Metabolism

Bile acids (BA), together with cholesterol, phospholipids and bilirubin, are the main constituents of bile (Thomas et al., 2008). They are synthesized from cholesterol in the liver and secreted from hepatocytes into the bile canalicular system and subsequently stored in the gall bladder. After meals, bile flows into the duodenum, where it contributes to the solubilization and digestion of fats and lipid-soluble nutrients. Of the BA pool, 95% are then absorbed by passive diffusion and active transport from the terminal ileum and transported back to the liver, in the so-called enterohepatic circulation. The remaining 5% of the BA pool is lost with the feces and replaced by hepatic *de novo* synthesis (Staels & Fonseca, 2009). After a meal, BA levels increase in the intestine and liver, and also in the systemic circulation (from ~5 μM to ~15 μM in humans), which might exert systemic effects. Serum bile-acid levels therefore vary during the day following a rhythm that is dictated by the ingestion of meals. Taking into account these observations, systemic bile acids inform the peripheral tissues that a meal has been ingested and that energy will become available (Thomas et al., 2008).

The immediate products of the bile acid synthetic pathways are referred to as primary BA. Cholic acid (CA) and chenodeoxycholic acid (CDCA) are the primary bile acids formed in humans. The action of intestinal bacterial flora on primary BA results in the formation of secondary bile acid species: deoxycholic (DCA) and lithocholic acids (LCA), derived from CA and CDCA, respectively. Due to previously discussed recycling of BA, these species are by far the most abundant in humans. The synthesis of BA involves two distinct pathways, classic (neutral) and alternative (acidic) pathways, as illustrated in Figure 11. The first is characterized by hydroxylation of cholesterol, catalyzed by the cytochrome P450 enzyme cholesterol 7α-hydroxylase (CYP7A1), in the first step. The activity of CYP7A1 is subject to complex modes of control. This pathway is the main source of cholesterol-derived BA synthesis. On the other hand, BA synthesis can also occur by the alternative pathway, which is governed by the enzyme CYP27A1 and converts oxysterols to BA. Unlike CYP7A1, CYP27A1 isn't regulated by BA but it is estimated that only 6% of bile acid synthesis occurs via this pathway (Lefebvre et al., 2009). The subsequent conversion of bile acid intermediates from either the classical or alternative pathways to CA or CDCA is governed by microsomal sterol 12α-hydroxylase (CYP8B1). The interaction of primary BA with this enzyme determines the amount of CA versus CDCA formed. Hydroxylation via CYP8B1 results in the formation of the more hydrophilic CA molecule. Thus, the CA/CDCA ratio determines the general hydrophobicity of the BA pool. Since BA are powerful detergents, at high concentrations they might be cytotoxic. For this reason, BA exert negative feedback on their own synthesis (Lefebvre et al., 2009).

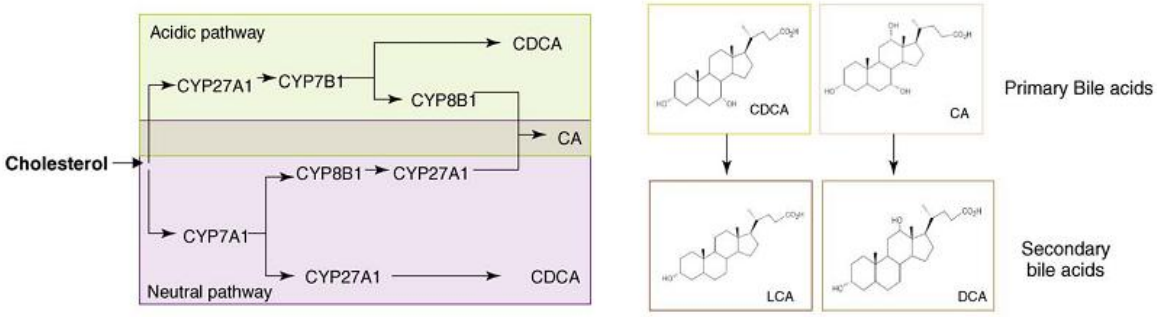

Figure 12 - Bile acids biosynthetic pathways. Adapted from Fiorucci *et al.* 2009

Apart from their role in dietary lipid and cholesterol homeostasis, a growing body of evidence suggests that BA also act as a signaling molecules and are involved in the regulation of energy expenditure (Ockenga et al., 2012; Watanabe et al., 2006). Moreover, BA metabolism seems to be altered in T2DM patients and the manipulation of the BA pool

can improve glucose metabolism, insulin sensitivity, energy homeostasis as well as lipid metabolism in such patients (Prawitt et al., 2011). Although BA are involved in the activation of many signaling pathways, two major BA-regulated signaling mechanisms have been receiving the most attention in the scientific literature, the G-protein-coupled membrane receptor (TGR5) and the orphan nuclear receptor, farnesoid X receptor (FXR) (Thomas et al., 2008).

ii. Bile acids as regulatory molecules and their clinical significance

As described before, the most studied BA receptors are the nuclear receptor FXR and membrane receptor TGR5 which are involved in lipid and glucose metabolism (Porez et al., 2012), summarized in Figure 13. FXR is a member of the orphan nuclear hormone receptor superfamily and is mainly expressed in liver and intestine, the main sites of bile acid metabolism, but also in adipose tissue, pancreas and adrenals glands (Porez et al., 2012). CDCA is the most effective natural activator of FXR, effective at a concentration of 10μM, while LCA, DCA and CA bind with lower affinity and specificity(Prawitt et al., 2011; Fiorucci et al., 2009). Upon ligand-binding, FXR acts either as a homodimer or forms a heterodimer with RXR (retinoid X receptor) to subsequently activate or repress the expression of genes that contain a specific FXR response element in their promoter (Fiorucci et al., 2009). Furthermore, numerous FXR functions are mediated by the induction of Short Heterodimer Protein (SHP) which in turn represses target genes in bile acid, lipid and glucose metabolism. FXR was originally characterized for its ability to regulate genes involved in BA synthesis, detoxification and excretion. However, nowadays is known that FXR is involved in glucose metabolism, insulin sensitivity, energy and lipid metabolism (Fiorucci et al., 2009).

Several studies have tried to understand the role of FXR. In the 1970's, it was observed that CDCA administration to gallstone-suffering patients solubilizes cholesterol-rich stones and decreased blood TG levels (Iser et al., 1975). This effect has now been linked to FXR activation (Kast et al., 2001). Also, this nuclear factor seems to be responsible for changes in transcription of several genes involved in FA and TG synthesis, such as FAS and ACC, and lipoprotein metabolism (Teodoro et al., 2011). The administration of synthetic FXR agonists (as GW4064, 6a-ethyl-chenodeoxycholic acid (6-ECDCA) and WAY-362450) to rats or mice reduces plasma TG and cholesterol levels (Fiorucci et al., 2009). Furthermore, FXR deficiency results in an increased plasmatic level of TG, cholesterol, high-density lipoprotein (HDL) and FFA. By using GW4064, it is

possible to inhibit hepatic TG synthesis, in a mechanism that involves alterations of SREBP1c expression levels with the concomitant downstream effects. However, FXR might impact TG metabolism by other mechanisms, including induction of PPARα and PGC-1α (Fiorucci et al., 2009). FXR might also involved in the modulation of gluconeogenesis in liver, muscle and adipose tissue, since administration of CDCA decreases gluconeogenesis in fed mice by reducing the expression and/or activity of PEPCK, glucose-6-phosphatase and fructose-1,6-biphosphatase (Yamagata et al., 2004). Moreover, loss of FXR disrupts normal glucose homeostasis and leads to insulin resistance (Ma et al., 2006). Indeed, FXR activation, trough administration of CDCA, was shown to increase the insulin-mediated uptake of glucose (Rizzo et al., 2006).

Due to the importance that FXR seems to have to lipid and glucose metabolism and insulin sensitivity, this nuclear factor appears to be also involved in some pathologies like obesity, T2DM and non-alcoholic fatty liver (NASH). Pharmacological studies in obese *fa/fa* Zucker rats, a model of NASH and T2DM, showed that administration during 12 weeks of 6-ECDCA reduced body weight gain, hyperglycemia and hyperlipidemia, hepatic lipid content and serum insulin, glucose, FFA, triglyceride and cholesterol levels, and ameliorated liver histology (Cipriani et al., 2010). Moreover, the expression of FXR itself is decreased in rat models of type 1 and T2DM (Duran-Sandoval et al., 2004). Even though adipose tissue is not a tissue classically involved in BA metabolism, it expresses FXR. In FXR-deficient mice, adipose tissue mass and adipocyte size are reduced, indicating a role for FXR in adipocyte biology (Cariou et al., 2006) and basal lipolysis is increased whereas lipogenesis is reduced (Abdelkarim et al., 2010). Indeed, FXR controls adipocyte differentiation and function by promoting the expression of several genes, including C/EBPα, PPARγ and SREBP1c (Teodoro et al., 2011). Furthermore, as described previously obesity is characterized for a state of inflammation where adiponectin expression is decreased, whereas TNF-α, IL-6, leptin, resistin and RBP-4 are increased. FXR agonism leads to an increase in adiponectin expression and a repression in TNF-α. Thus, FXR seems to have a important role in control of adipokines release, both in normal conditions as in situations of obesity (Teodoro et al., 2011).

FXR is also involved in the regulation of PPARα and PPARγ. PPARα, as described in the previous section, is a key regulator of lipid metabolism by positively regulating FFA uptake and β-oxidation. Indeed, activation of PPARα leads an increase in β-oxidation, lipolysis, energy uncoupling and expenditure, while decreases lipogenesis, TG secretion and adiposity (Teodoro et al., 2011). However, future works are required, since exist some

controversy between studies exist. If on the one hand, there is evidence suggesting that PPARα might activate FXR expression (Zhang et al., 2004), on the other in C57BL/6J and KK-A^y mice treated with CA, there was no increase in expression of genes involved in β-oxidation; in fact, expression of some genes decreased in C57BL/6J mice (Watanabe et al., 2004). PPARγ, as also previously discussed, is a key regulator in lipid metabolism and it was recently reported that FXR is necessary for full PPARγ activation, and some of the beneficial effects of FXR activation on adipose tissue are mediated by PPARγ (Abdelkarim et al., 2010).

TGR5 is a member of the rhodopsin-like superfamily of G protein coupled receptors that transduces signals through G_s protein (α–βγ subunits), and was recently identified as a BA receptor (Fiorucci et al., 2009). TGR5 is mainly expressed in the gall bladder, ileum, colon, BAT and WAT, and to a lesser extent in skeletal muscle, liver and immune cells; and is activated by nanomolar concentrations of LCA and TLCA and micromolar concentrations of CA, DCA and CDCA (Prawitt et al., 2011). After ligand binding to plasma membrane-bound TGR5, the receptor is internalized, the $G\alpha_s$ subunit released and adenyl cyclase activated. The accumulation of cAMP leads to activation of PKA or the transcription factor CREB (cAMP response element binding protein), mediating BA functions in energy and glucose homeostasis (Prawitt et al., 2011).

There are some evidences that TGR5 is involved in the regulation of glucose homeostasis. One study observed that activation of TGR5 stimulates the secretion of glucagon-like peptide (GLP1). GLP1 belongs to the family of incretins, a group of insulinotropic gastrointestinal hormones secreted by intestinal entero-endocrine cells into the bloodstream within minutes after eating. The main physiological role of incretins is to regulate insulin secretion in response to meals. The authors demonstrated that LCA and DCA TGR5-dependently induced intracellular cAMP concentrations and GLP1 secretion from intestinal L-cells (Katsuma et al., 2005). In a second study, the TGR5 agonist oleanolic acid reduced obesity and improved insulin resistance in mice upon high-fat diet-feeding (Strehle et al., 2007). Further support comes from a study that show that glucose tolerance reduced by TGR5-deficiency and improved by TGR5 overexpression in high-fat diet-fed mice via increased GLP1 and insulin secretion (Thomas et al., 2010).

TGR5 also seems to play a role in energy homeostasis (Watanabe et al., 2006; Ockenga et al., 2012). Watanabe and colleagues have shown that BA increase energy expenditure by acting in thermogenically competent tissues, such as BAT in mice and

muscle in humans (Watanabe et al., 2006). This effect has been linked to the prevention of diet-induced obesity and insulin resistance in mice fed a high-fat diet. The authors hypothesize that induction of energy expenditure by CA requires a TGR5-dependent increase in intracellular cAMP and induction of Dio2, a gene whose protein product is the enzyme 2-iodothyronine deiodinase or D2.

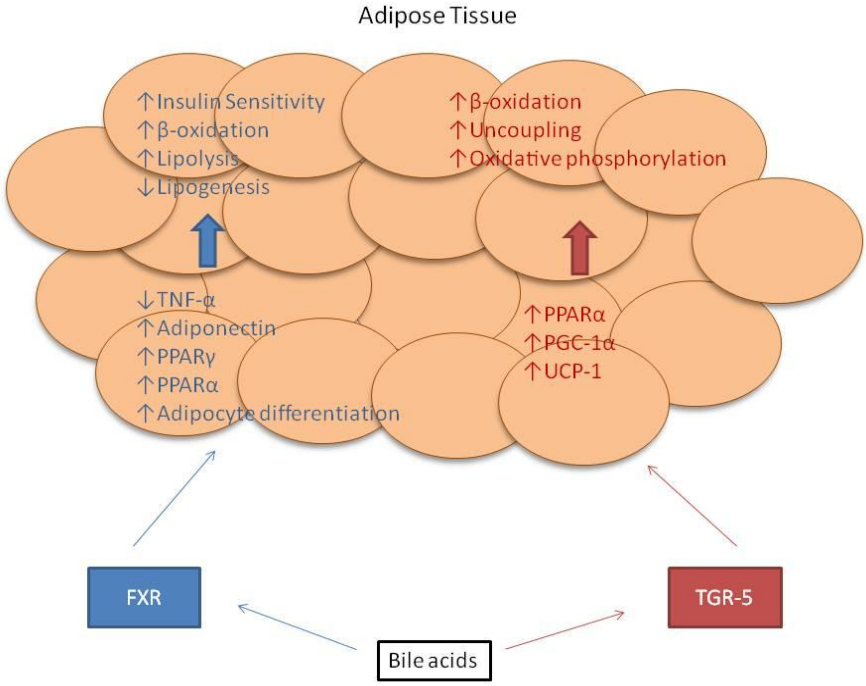

Figure 13 - Role of FXR and TGR-5 in adipose tissue.

Agonism of FXR leads to a repression of TNF-α, an increase in adiponectin, PPARγ, PPARα expression and adipocyte differentiation; which in turn leads to an improvement in insulin sensitivity, an increase in β-oxidation and lipolysis and a decrease in lipogenesis. On the other hand, agonism of TGR-5 increases expression of PPARα, PGC-1α and UCP-1 leading to an augment in β-oxidation, energy uncoupling and oxidative phosphorylation.

BA induce D2 expression in thermogenically relevant tissues described before, because only these tissues co-express both TGR5 and D2. D2 then converts locally available thyroxine (T4) to tri-iodothyronine (T3), resulting in increased energy expenditure without leading to changes in circulating thyroid hormone levels. In addition to D2, several genes involved in the regulation of energy expenditure were increased in brown adipose tissue after BA treatment, such as PPARα, PGC-1α and UCP-1 (Watanabe et al., 2006). The stimulation of energy expenditure by bile acid is observed only when mice are fed a

high-fat diet and not in D2 knockout mice (Watanabe et al., 2006). Exactly how T3, mediates an increase in energy expenditure remains to be clarified. One potential mechanism is T3-mediated induction of UCP-1 expression, leading to dissipation of the proton gradient generated by the electron transport chain, resulting in a decrease in ATP synthesis (Watanabe et al., 2006). Ockenga and colleagues have shown also there is a consistent relation between administration of BA and energy expenditure in humans, through thyroid function and activation of TGR-5 (Ockenga et al., 2012). However, even though that this evidences are an attractive concept, the current explanation for the mechanism by which this happens is being contested. Neither the overexpression nor the absence of TGR5 in mice leads to a difference in body weight and the susceptibility to diet-induced obesity is gender-specific (Maruyama et al., 2006). Taking into account these findings, BA seems to have a high potential to act as signaling molecules in the improvement of glucose metabolism, insulin sensitivity, energy homeostasis and lipid metabolism. In addition to studies that demonstrated that BA seems to have anti-obesity effects (Watanabe et al., 2006; Ockenga et al., 2012), a recent study revealed that CDCA, could in fact reduce obesity and associated metabolic disorders (Teodoro et al., 2013).

1.5 Aims / Objectives

Nowadays, obesity is considered a major worldwide concern since associated to this condition is other co-morbidities that contribute to reduce life expectancy. The failure of current therapies towards a significant and stable reduction in global obesity and diabetes leads to further investigation on novel therapeutic targets for these conditions. One of such targets is the "acceleration" triglyceride/glycerol-free fatty acid (TG/(GL+FFA)) cycle. If one could increase both the TG/(GL+FFA) cycle activity while removing one of its end-products towards oxidation, it is possible that further cycling will occur and thus lead to decreased obesity. To further this idea, the deceleration and alterations on the TG/(GL+FFA) cycle have been demonstrated in experimental models of obesity and diabetes. Thus, since the current explanation for the mechanism by which CDCA induces energy expenditure is controversial, one possible explanation is that CDCA could affect TG/(GL+FFA) cycle activity. CDCA activates both PPARγ and PPARα, two transcription factors that are involved in the transcription of key metabolic genes, like the some enzymes of the TG/(GL+FFA) cycle and of mitochondrial oxidative capacity; and of genes involved in FFA oxidation, respectively.

Thus, this work will focus on evaluating the metabolic alterations to the TG/(GL+FFA) induced by CDCA. Specifically, we will address if CDCA supplementation alters the TG/(GL+FFA) cycle activity, if this is related to improved metabolic status and if mitochondrial alterations are involved.

CHAPTER II

Methods and Materials

2. Methods and Materials

2.1 Materials

Except when noted, all compounds were purchased from Sigma-Aldrich (St. Louis, MO). All reagents and chemicals used in this work were of the highest grade of purity commercially available.

2.2 Studies with cellular culture of 3T3-L1 cells

2.2.1.1 Cell culture

The fibroblast cell line 3T3-L1 was originally developed by clonal expansion from murine Swiss 3T3 cells. It has a high potential to differentiate from fibroblasts to adipocytes, for this cell line has been widely used in studies about adipogenesis, biochemistry of adipocytes and metabolism (Zebisch et al., 2012).

3T3-L1 cells were obtained from American Type Culture Collection (ATCC). All cells care and maintenance was done according to the protocol recommended by ATCC. The cells were grown in 75-cm^2 culture flasks (Sarstedt AG & Co., Germany) at 37°C in a humidified atmosphere with 5% CO_2 and maintained in maintenance medium consisting of Dulbecco's Modified Eagle Medium (DMEM), supplemented with 25 mM Glucose, 18 mM Sodium Bicarbonate, 2 mM L-glutamine, 1 mM Sodium pyruvate, Antibiotic/antimycotic 1% (Invitrogen, Carlsbad, CA) and 10% of newborn calf serum (NCS) (Invitrogen). Cells were passaged or harvested for experiments when reaching 70-80% of confluence, by detachment with 0,05% trypsin and 0,5 mM EDTA (Invitrogen). Reseeding was took into consideration ATCC's recommendations for this specific cell line, two times per week, with a dilution factor of between 1:5 and 1:8 of original cell content. Cells were counted with an automated cell counter (Bio-Rad TC10^{TM} Automated Cell Counter, Bio-Rad, Hercules, CA) and seeded in 12-well plates (Orange Scientific, Braine-l'Alleud, Belgium) at a density of 5 x 10^4 cells/well. This cell count method uses the trypan blue exclusion method, which is based on membrane integrity determined by the uptake of the dye to which the cell is normally impermeable. Thus viable cells will exclude trypan blue dye, while dead cells will have blue cytoplasm and dark nuclei.

At this point, was let cells grown during 48h hours and when cells reached confluence the medium was replaced for the first time. After 48h, cell differentiation was induced by changing the medium to DMEM containing glicose 25 mM, 18 mM Sodium

Bicarbonate, 2mM L-glutamine, 1mM Sodium pyruvate, Antibiotic/antimycotic 1%, 10% of fetal bovine serum (FBS) (Invitrogen, Carlsbad, CA), 0,5 mM IBMX, 0,25 µM DEX, 1µg/ml insulin (Invitrogen, Carlsbad, CA) and 2 µM rosiglitazone (Cayman Chemical Company, Michigan, USA). According to ATCC recommendations differentiation medium doesn't contain rosiglitazone, however when trying to differentiate the cells to adipocytes using conventional protocol, we encountered the following problem: the differentiation efficiency was low and declined rapidly with the passage number. So the protocol differentiation used in this work was based in protocol defined by Zebish and coworkers (Zebisch et al., 2012), that concluded that supplementation of rosiglitazone in differentiation medium leads to a complete and efficiency differentiation of 3T3-L1. After 48 h, the medium was changed to DMEM-similar to. On day 7, the medium was changed to Differentiation medium 2, equal to Differentiation medium 1 minus IBMX and DEX. This medium was refreshed every 48 hours until cells were totally differentiated, usually between 7 and 10 days, as evidenced by observation of lipid droplet formation (Figure 12).

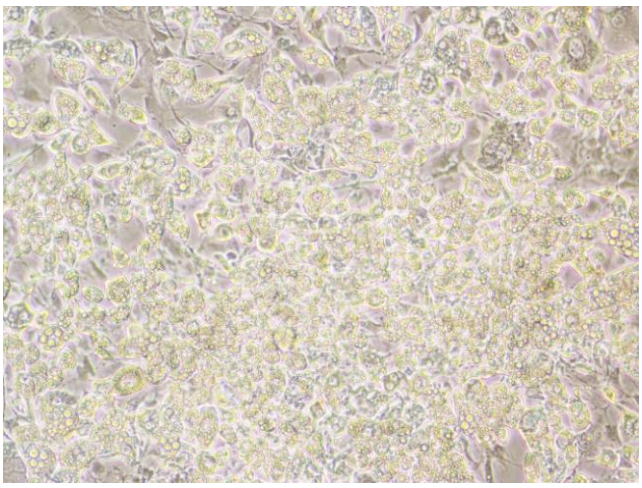

Figure 14 – Optical microscopy photography of differentiated 3T3-L1 cells, day 8.

When cells were totally differentiated the treatment with CDCA was initiated. The cultures were maintained in the Differentiation medium 2 supplemented with CDCA, according to figure 13, for 96 h after which the assays were performed.

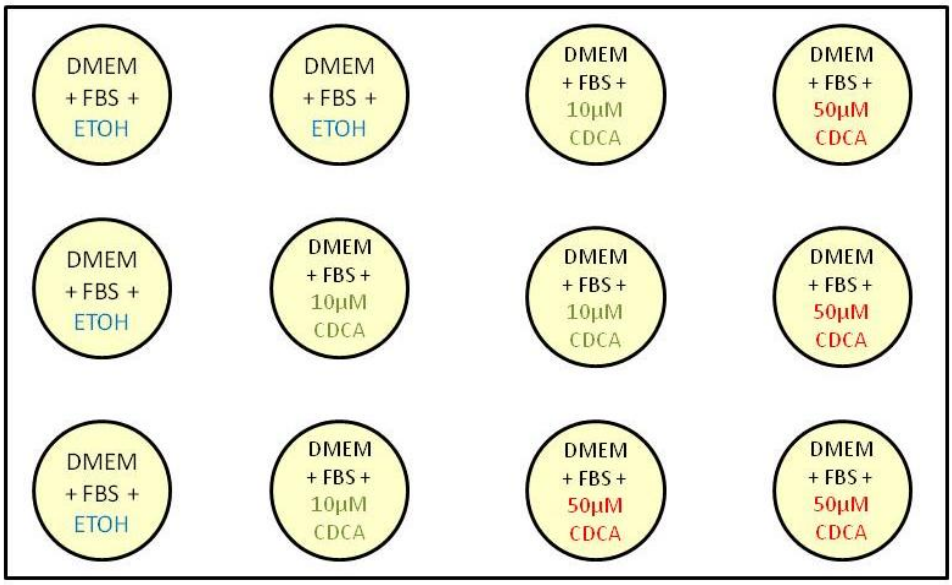

Figure 15 - Scheme of CDCA treatment in 12- well plate.

The first four wells were maintained with FBS and CDCA vehicle, ethanol (ETOH) and were considered the controls; the next four wells were treated with 10 µM CDCA and the last four with 50 µM CDCA.

2.2.2 Oil red O Staining

To document lipid accumulation, Oil Red O staining was performed according to the method described by González and coworkers (González et al., 2012). This technique detects neutral lipids and lipid droplets, allowing an easy estimation of cells lipid content and distribution (Mehlem et al., 2013). Firstly, an Oil Red O stock solution was prepared by stirring 0.5% Oil Red O in isopropanol overnight. The solution was filtered through a 0.2-µm filter and stored at 4°C. Then fresh Oil Red O working solutions were prepared by mixing stock solution with distilled water (6:4), followed by incubation for 20 minutes and further filtration (Zebisch et al., 2012). At the end of the experiment, 3T3-L1 differentiated cells were washed with phosphate-buffered saline (PBS) (pH 7.2) twice, fixed in 10% (v/v) *p*-formaldehyde for 30 minutes, rinsed twice in PBS and once in distilled water, and then, stained with Oil Red O for 1 hour, in constant horizontal agitation. After staining, the wells were washed three times with distilled water. Finally isopropyl alcohol was added to he weels, extracting the total lipid content, which was measured in a 96 multiwell plate using colorimetric assay in a Victor^3 1420 series plate reader (Perkin-Elmer, Waltham, MA), at 490 nm. To obtain an estimate of lipid content/viable cells, the relative fluorescence units from the Oil Red data were normalized using the absorbance values from the viability data measured by the Sulforhodamine B method, described in section 2.2.5.

2.2.3 Mitochondrial membrane potential evaluation

To evaluate mitochondrial membrane potential (Δψ), after 96 h of CDCA treatment the medium was aspirated and the cells were loaded with 6,6 μM tetramethylrhodamine methyl ester (TMRM) in dimethyl sulfoxide (DMSO) in 1 mL of DMEM without NCS or FBS at 37 ºC, in a humidified atmosphere with 5% CO2 and in the dark, during 30 minutes. TMRM is a membrane-permeable cationic fluorophore that accumulates electrophoretically in mitochondria in proportion to their Δψ. After this incubation period, the medium with TMRM was removed and was added 1 mL the same medium but without the fluorescent dye. Fluorescence was measured using excitation and emission wavelengths of 485 and 590 nm respectively, at 37 ºC in the same plate reader as described before. Since TMRM increases or decreases fluorescence intensity proportionally to a stimulus that increases or decreases the levels of Δψ, it's imperative to measure fluorescence intensity of this probe at the baseline level and after the application of a specific stimulus. Thus, after 5 minutes of recording basal fluorescence, cells were incubated with 1mM Carbonyl cyanide-*p*-trifluoromethoxyphenylhydrazone (FCCP), a mitochondrial uncoupler. Δψ was estimated taking into account the complete depolarization caused by FCCP (Rolo et al., 2003)'(Joshi & Bakowska, 2011). To normalize, the relative fluorescence units from the mitochondrial membrane potential data were divided by absorbance values from the viability data measured by the Sulforhodamine B method, described in section 2.2.5.

2.2.4 Mitochondrial ROS generation

ROS generation was fluorometrically determined using 2',7'–dichlorofluorescein diacetate (DCFDA), a fluorogenic dye that measures hydroxyl, peroxyl and other ROS species within the cell. After diffusion in to the cell, DCFDA is deacetylated by cellular esterases to a non-fluorescent compound, which is later oxidized by ROS into 2', 7' –dichlorofluorescin (DCF). DCF is a highly fluorescent compound which can be detected by fluorescence spectroscopy with maximum excitation and emission spectra of 488 nm and 515 nm, respectively (Joshi & Bakowska, 2011). After the 96 h treatment, the medium was aspirated and the cells were loaded with 50 mM DCFDA in DMSO in 1 mL of DMEM without NCS or FBS at 37 ºC, in a humidified atmosphere with 5% CO2 and in the dark, during 30 minutes. After this incubation period, the medium with DCFDA was removed and was added 1 mL the same medium but without the fluorescent dye.

Fluorescence was measured using excitation and emission wavelengths described above, at 37 ºC and in the same plate reader as before. As described in mitochondrial membrane potential evaluation, in this assay it is necessary the application of a specific stimulus after reading the basal fluorescence. Thus, after 5 minutes of recording basal fluorescence, cells were incubated with 1mM Antimycin A, a well-known specific inhibitor of mitochondrial respiratory chain Complex III which induces inhibition of cell respiration, thus inducing heightened ROS generation (Carrière et al., 2009). Mitochondrial ROS generation was estimated taking into account the ROS overproduction caused by Antimycin A. To normalize, the relative fluorescence units from the mitochondrial ROS data were divided by absorbance values from the viability data measured by the Sulforhodamine B method, described in section 2.2.5.

2.2.5 Sulforhodamine B colorimetric assay

The sulforhodamine B (SRB) assay is used for cell density determination, based on cellular protein content. The SRB assay provides a colorimetric end point that is nondestructive, indefinitely stable, and visible to the naked eye. SRB strongly absorbs light excitation at 488 nm, providing a sensitive measure of drug-induced cytotoxicity (Vichai & Kirtikara, 2006).

First, cells were briefly washed with PBS and fixed in 10% (v/v) *p*-formaldehyde for 30 minutes. After fixation the wells were rinsed twice in PBS and once in distilled water, and air-dried. Then SRB solution (0,5% in 1 % acetic acid) was added to each well in sufficient amount to cover the culture surface area, about 500 µL. The plate was incubated at room temperature and in agitation, for 30 minutes. After the incubation period, unbound dye was removed by four washes with 1% acetic acid before air-drying one more time. Finally, the protein-bound dye was solubilized in 10 mM Tris (pH 10) using a volume equal to the original volume of culture medium (1 mL), during 5 minutes at room temperature and in agitation. The absorbance was read at 540 nm and blank background optical density was measured in wells incubated with growth medium without cells.

2.2.6 Cell viability assay – LDH

Cell viability was determined fluorometrically by estimating release of lactate dehydrogenase (LDH) into the medium trough a LDH activity detection kit (Hospitex Diagnostics s.r.l., Italy). LDH is a cytosolic enzyme present in many different cell types. Plasma membrane damage releases LDH into the cell culture media. Extracellular LDH in the media can be quantified by a coupled enzymatic reaction in which LDH catalyzes the conversion of lactate to pyruvate via NAD^+ reduction to NADH (Moran & Schnellmann, 1996). The rate of conversion of NAD^+ into NADH, by monitoring NADH autofluorescence at 340 nm, is proportional to the amount of LDH released into the medium, which is indicative of cytotoxicity.

After incubation period, the supernatant was extracted and fresh reaction solution was made by mixing 5 mL of 0.60 mM pyruvate with 15mL of 0.18 mM NADH in phosphate buffer (pH 7.5). After that, 40 µL of the cell-free supernatant was added to 200 µL of fresh assay solution to initiate the reaction. The amount of LDH released into the media was expressed as percent of total LDH (Rolo et al., 2003).

2.2.7 Cell viability assay – LIVE/DEAD

Cell viability was also determined by the LIVE/DEAD® Viability/Cytotoxicity Assay Kit (Life technologies, Paisley, UK) by fluorescence microscopy. This kit is a quick and easy two-color assay to determine viability of cells in a population based on plasma membrane integrity. This assay discriminates live from dead cells by simultaneously staining with blue-fluorescent trihydrochloride to indicate double strand DNA and red-fluorescent ethidium homodimer-1 to indicate loss of plasma membrane integrity. After incubation period the medium was removed and the cells were loaded with of 2 mM trihydrocoloride and 4 µM ethidium homodimer-1 in PBS (pH 7.2), during 30 min in the dark. After 30 minutes, the medium with probes was replaced by PBS. Then, cultured cells were analyzed thought light microscopy (NIKON Eclipse TS100) and with appropriated software (NIS-Elements D4.11.01, NIKON). The results were expressed as percent of total viable cells.

2.2.8 Protein extraction and BCA quantification

After CDCA treatment cells were washed three times with PBS (pH 7.2) and lysed in cell lysis buffer (10 mM Tris–HCl, pH 7.5, 10 mM NaH_2PO4, 130 mM NaCl, 1% Triton X-100). Lysates were then passed through a syringe to aid in the lysis and centrifuged at 12 000 rpm for 10 min, at 4ºC. Then supernatant was removed for protein assays and the pellet was discarded.

The bicinchoninic acid (BCA) protein quantification method was used to determine the concentration of protein. This method combines the well-known reduction of Cu^{+2} to copper cation (Cu^{+}) by proteins in an alkaline medium (the biuret reaction) with the highly sensitive and selective colorimetric detection of the Cu^{+} using bicinchoninic acid. The purple-colored reaction product of this assay is formed by the chelation of two molecules of BCA with one cuprous ion. This water-soluble complex exhibits a strong absorbance at 540 nm that is nearly linear with increasing protein concentrations over a broad working range (20-2000µg/mL). First, a working solution was prepared by adding 1 part of copper reagent to 50 parts of BCA reagent. To prepare a standard curve, a BSA (Bovine Serum Albumin) 1 mg/ml stock solution was prepared, following were prepared serial dilutions as in Table 1.

Table 1 - Standard curve.

Tube	BSA dilution
1	200 µL BCA + 25 µL H_2O
2	50 µL BSA 0.1%
3	160 µL BSA 0.1% + 40 µL H_2O
4	150 µL tube 2 + 50 µL H_2O
5	133 µL tube 3 + 67 µL H_2O
6	100 µL tube 4 + 100 µL H_2O

The samples were diluted to fall within 20-2000 µg/mL, and 25 µL of samples diluted were added to 200 µL of BCA into duplicated wells in a 96 well plate. Then the plate was incubated at 37ºC for 30 minutes. Finally the absorbance was measured at 540 nm.

2.2.9 Cytochrome *c* oxidase activity

Cytochrome *c* oxidase (COX) activity of cultured cells was polarographically determined by oxygen consumption using an oxygraph respirometer (Hansatech Instruments Ltd, Norfolk, England), as previously described by Brautigan and coworkers (Brautigan et al., 1978). Mitochondrial electron transport has as final step the reduction of O_2 to water (at complex IV, cytochrome *c* oxidase), which can be evaluated by respirometry. Reduced 0.5 mM tetramethyl-*p*-phenylenediamine (TMPD) served as an electron donor to cytochrome *c*, and its concentration was held constant by the addition of 2 mM ascorbate. Auto-oxidation of ascorbate and TMPD is a function of oxygen pressure and was subtracted from the measured oxygen consumption as a chemical background (Gnaiger* et al., 1998). Reactions were performed at 25°C in a closed chamber reaction and thermostated, with 500 µL of a mixture with PBS (pH 7.2), 2 µM rotenone, 10 µM cytochrome *c* and 150 µg of protein. After addition of protein, the reaction was initiated with the addition of 5 mM of ascorbate + 0.25 mM of TMPD and data were recorded during 4 minutes.

2.2.10 Western blotting analysis

After protein extraction and quantification, samples were diluted in equal volume of Laemmli buffer (Bio-Rad) supplemented with β-Mercaptoethanol 5%. Equal amounts of protein were loaded and electrophoresed on SDS-polyacrylamide gel and transferred to a polyvinylidene difluoride membrane (Bio-Rad Laboratories). Membranes were blocked with 5% non-fat milk (Bio-Rad) and incubated with anti-COX I (1:100), anti-COX IV (1:1000), anti-UCP1 (1:500), anti-Caspase3 (1:1000), anti-α-tubulin (1:1000) and anti-β-actin (1:2500). Immunodetection was performed with WesternDot™ 625 goat anti-rabbit or goat anti-mouse western blot kits (Life Technologies). Membranes were imaged using Bio-Rad Gel Doc™ EZ Imager equipment and with aid of Image Lab 4.1 Bio-Rad software. Antibodies utilized are summarized in Table 2.

Table 2 - List of utilized antibodies for Western blot: source, reference and dilution.

Antibody	Supplier	Reference	Dilution
β-Actin	Santa Cruz Biotechnology	sc-47778	1:2500
Cox I	Abcam	Ab14705	1:100
Cox IV	Abcam	ab14744	1:1000
Caspase 3	Cell Signaling	Asp175	1:500

UCP1	Abcam	ab10983	1:500
α-Tubulin	Sigma-Aldrich	T6199	1:1000

2.2.11 RNA isolation and genetic expression evaluation by qPCR

RNA was isolated from cultured cells with resource to PureLink™ RNA Mini Kit (Life technologies). First, the culture medium was aspirated and the lysis and homogenization of cells was done through addition of 600 µL at each well of a fresh solution of Lysis Buffer with β-mercaptoethanol. Then wells were scraped and the suspension was transferred to a 1.5 mL eppendorf and passed through a syringe. Then RNA purification was completed following to kit instructions, through a column-based method. Total RNA yield was quantified in Qubit® 2.0 Fluorometer (Life Technologies) and cDNA was produced using 0.75 µg of RNA with a Bio-Rad iScript™ cDNA synthesis kit and Bio-Rad MyCycler™ Thermal cycler equipment. Gene expression was evaluated by real-time PCR, in a Mini Opticon (Bio-Rad), using a SYBRGreen SuperMix (Bio-Rad). Primers used and theirs sequences are described in Table 3.

Table 3 – Utilized primers and their respective nucleotide sequence.

Gene	Forward Primer	Reverse Primer
18S	GCCCGAGCCGCCTGGATAC	CCGGCGGGTCATGGGAATAAC
COX III	TCATCGTCTCGGAAGTCTTTTT	ATTAGTAGGGCTTGATTTATGTGG
COX IV	AGAAGGCGCTGAAGGAGAAGGA	CCAGCATGCCGAGGGAGTGA
CPT1α	GCAGCTCGCACATTACAAGGACAT	AGCCGTCCCCGCCACAGGACACATAGT
FAS	GGCTGCCTCCGTGGACCTTATC	GTCTAGCCCTCCCGTACACTCACT
Glut4	ACCGGCTGGGCTGATGTGTCT	GCCGACTCGAAGATGCTGGTTGAATAG
PEPCK	GGCAGCATGGGGTGTTTGTAGGA	TTTGCCGAAGTTGTAGCCGAAGAAG
PGC-1α	CCCAAAGGATGCGCTCTCGTT	TGCGGTGTCTGTAGTGGCTTGATT
PPARα	TGCGCAGCTCGTACAGGTCATCAA	CCCCCATTTCGGTAGCAGGTAGTCTTA
PPARγ	GGCGAGGGCGATCTTGACAGG	GGGCTTCCGCAGGTTTTTGAGG
TFAM	AGGAGCTGAAGGCATGCGGTGAAG	GTCCAGTGCGTGCGGGTGAAC
UCP1	CACGGGGACCTACAATGCTTACAG	GGCCGTCGGTCCTTCCTT

2.2.12 NMR analysis

Nuclear magnetic resonance (NMR) spectroscopy has been used to study triglyceride metabolism in 3T3-L1 cells incubated with isotopically labeled compounds. Indeed, after cells are totally differentiated, the 96h treatment was induced but the medium was replaced by DMEM with 10% FBS supplemented with 1 mM [U-$^{2}H_5$] glycerol (Cortecnet) and 25 mM [U-^{13}C] glucose (Cambrige Isotope Laboratories), with exactly same concentrations of CDCA. The rate of endogenous TG lipolysis was measured from the rate of appearance of non-deuterated glycerol in the medium and cell extracts as determined by ^{1}H NMR spectroscopy. The rate of FFA esterification to TG was assessed by quantifying the appearance partially protonated glycerol-TG by ^{1}H NMR spectroscopy of cell lipidic extracts. Glycerol synthesis from glucose and glyceroneogenesis from lactate was quantified by ^{13}C-isotopomer analysis of glycerol-TG present in cells lipidic extracts.

Aqueous soluble metabolites were extracted from 3T3-L1 cells using a previously published method (Dettmer et al., 2011). After treatment period cells were washed with PBS (pH 7.2) twice and loaded with 750 µL of a ice-cold solution of 80% methanol and 20% water (MeOH/H_2O 80:20), as extraction solvent, which caused protein precipitation and hence cell disruption. Wells were then lightly scraped using a rubber tipped cell scraper (Armin Baack, Schwerin, Germany) and the suspension transferred to a 2 mL eppendorf tube. The wells were washed one more time with 750 µL ice-cold MeOH/H_2O and the wash solution was added to the extract. The cell suspension was centrifuged at 5725×g and 4 °C for 5 min and the supernatant was transferred to a new eppendorf tube, corresponding to aqueous phase. The sample was lyophilized and kept in an excicator until being dissolved in the adequate solvent (200 µL of 10 mM sodium fumarate phosphate buffered $^{2}H_2O$ (99.9%) solution) for NMR analysis.

In a second phase, was added to the pellet 1 mL of Methanol/chloroform/water 1:1:0,1 (MeOH/$CHCl_3$/H_2O), this mixture generates a mono-phase that carries the advantage that cell debris can be spun down and is not located in the interphase between chloroform and water. The suspension was centrifuged at 5725×g and 4 °C for 5 min and the supernatant was transferred to a new tube, corresponding to organic phase. This sample was also lyophilized and kept in an excicator until being dissolved in 600 µL deuterated chloroform plus 25 mL a solution of pyrazine in chloroform used as internal standard, for evaluation of lipid absolute contents.

Finally was added to pellet 200µL 8M Urea at room temperature overnight. In the next day, the samples were sonicated at 3W for 20s using the Sonicator 3000 (Misonix Inc., Farmingdale, USA), to avoid protein aggregates, and was added 600µL of lysis buffer supplemented with a cocktail of protease and phosphatase inhibitors. Then was quantified the protein by BCA quantification, described in section 2.3.8.

Proton (^{1}H) NMR spectra of aqueous extracts: ^{1}H NMR spectra of cell aqueous extracts were acquired on a 14.1 Tesla Varian spectrometer using a 3mm broadband NMR probe. Each spectrum consisted of 32k points defining a 7.2 k spectral width. A radiofrequency observe pulse of 30º was used and an interpulse delay of 10 seconds was allowed in order to warrant full relaxation of all nuclei in the sample. A total of 128 scans were averaged to provide adequate signal-to-noise ratios. Before Fourier transformation each FID ("Free Induction Decay") was multiplied by a 0.2 HZ Lorentzian to improve signal/noise ratios.This spectrum allows the observation of all intracellular aqueous soluble metabolites and is crucial for an evaluation of the cytosolic redox (measured through the ratio of lactate/alanine) and for detection of the appearance of unenriched glycerol. Metabolic compartmentation issues can also be addressed through the comparison of the ^{13}C enrichments of lactate and alanine pools and glutamate and glutamine pools.

Carbon 13 (^{13}C) NMR spectra of aqueous extracts: ^{13}C NMR spectra of cell aqueous extracts were acquired on a14.1 Tesla Varian VNMRS spectrometer using a 3mm broadband NMR probe. Each spectrum consisted of 131 k points defining a 37 kHz spectral width. A radiofrequency observe pulse of 45º was used and an interpulse delay of 3 seconds was allowed in order to warrant full relaxation of all aliphatic carbon nuclei in the sample. The number of averaged scans ranged from 5k to 20k to provide adequate signal-to-noise ratios towards a ^{13}C NMR isotopomer analysis. Before Fourier transformation each FID was multiplied by a 0.5 HZ Lorentzian apodization function to improve signal-to-noise ratios. Easily observed metabolites included lactate, alanine, glutamate and glutamine, as well as other metabolic intermediates from the krebs cycle and metabolites in exchange with these. A ^{13}C-isotopomer analysis of glutamate provides information on Krebs cycle kinetics. The glutamate C4 resonance, composed by a doublet (D45) and a quartet (Q), correlates intimately with tissue oxygen consumption rates and through its analysis one can easily appreciate how effective is oxidative metabolism in the cells. Higher ratios of C4Q/C4D45 are concurrent with a higher rate of Krebs cycle flux and denote a more oxidative phenotype. In condition of higher contributions from unriched

sources to the acetyl-CoA pool, there is a dilution of ^{13}C labeling in krebs cycle intermediates and multiply labeled isotopomers are less abundant, easily appreciated from the lowering in the C4Q/C4D45 multiplet ratio.

Proton (^{1}H) NMR spectra of cell lipidic extracts: ^{1}H NMR spectra of lipidic extracts were acquired on a 11.7 Tesla Brucker spectrometer using a 5 mm Broadband NMR probe. Each spectrum consisted of 65k points defining a spectral width of 6 kHz. A radiofrequency observe pulse of 30º was used and an interpulse delay of 10 seconds was allowed in order to warrant full relaxation of all nuclei in the sample. A total of 128 scans were averaged to provide adequate signal-to-noise ratios. Before Fourier transformation each FID was multiplied by a 0.2 Hz Lorentzian to improve signal/noise ratios. From these spectra it is possible to evaluate the incorporation of partially protonated glycerol, denoting incorporation of glycerol deuterated provided in the culture medium in TGs. The higher the ratio between partially protonated and non-deuterated glycerol the more active is the "futile" cycle of synthesis and degradation of TGs.

Carbon (^{13}C) NMR spectra of cell lipidic extracts: ^{13}C NMR spectra of lipidic extracts were acquired on a 11.7 Tesla Brucker spectrometer using a 5 mm Broadband NMR probe. Each spectrum consisted of 33k points defining a spectral width of 25 kHz. A radiofrequency observe pulse of 30º was used and an interpulse delay of 3 seconds was allowed in order to warrant full relaxation of all aliphatic carbons in the sample. A total of 5-15k scans were averaged to provide adequate signal-to-noise ratios. Before Fourier transformation each FID was multiplied by a 0.5 Hz Lorentzian to improve signal-to-noise ratios. From these spectra it is possible to evaluate the abundance of uniformly ^{13}C enriched glyceryl (Triplet, T) and doubly 13C enriched glyceryl ([2,3-13C2]glyceryl) (Doublet, D). The ratio D/T will be higher in conditions of higher rates of gliceroneogenesis.

2.2.13 Statistical analysis

Data is presented as Average ± SEM. Statistical significance was evaluated by use one-way ANOVA with Bonferroni post-hoc test (for 3 or more groups comparison) (GraphPad Prism, GraphPad Software Inc., San Diego, CA). A p value < 0.05 was considered statistically significant.

CHAPTER III

Results

3. Results

3.1 Cell death/viability

3T3-L1 cells viability was assessed in order to evaluate if the concentrations used caused cytotoxicity. As shown in figure 16, 3T3-L1 cells exposure to CDCA did not induce an increase in described ethidium homodimer-1 staining, excluding loss of plasma membrane integrity caused by CDCA exposure (Figure 17).

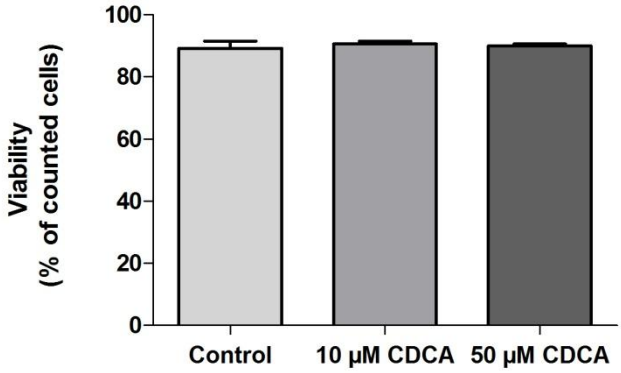

Figure 16 - 3T3-L1 cell death/viability after CDCA exposure.

3T3-L1 cells were cultured as described in Chapter 2. CDCA was added for 96h and Live/Dead assay was performed. Data are means ± SEM of four different experiments. No statistically significant differences were found ($P < 0.05$).

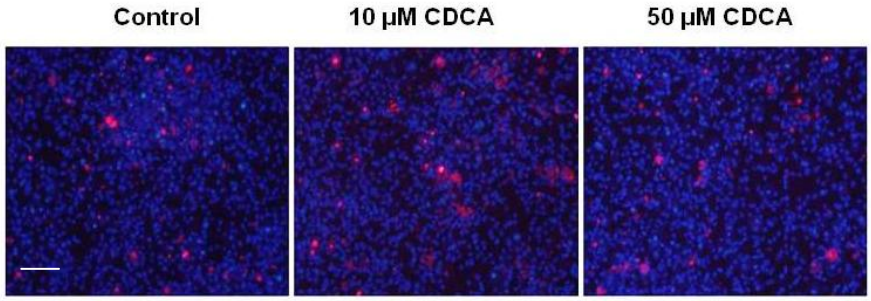

Figure 17 - Fluorescence microscopy images of 3T3-L1 cells treated with 10 µM CDCA and 50 µM CDCA for 96h.

3T3-L1 cells were exposed to CDCA and stained with trihydrochloride (blue) and ethidium homodimer-1 (red) as described in Chapter 2. Representative images are presented to show the viability of 3T3-L1 when exposed to CDCA. Scale bar, 40 µm

Furthermore, CDCA incubation didn't increase LDH release into the media, indicating that 96h of CDCA exposure doesn't induce necrotic cell in 3T3-L1 cells (Figure 18).

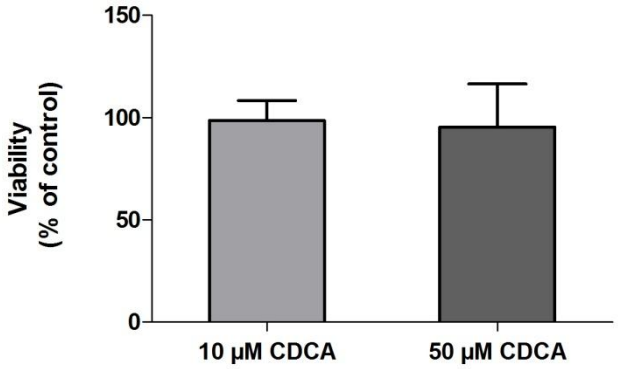

Figure 18 - Effects of CDCA exposure on LDH release.

3T3-L1 cells were cultured and treated for 96h with CDCA. Samples were collected and assayed for LDH release into the media and intracellular LDH using spectrophotometry, as described in Chapter 2. Data are means ± SEM of four different experiments. No statistically significant differences were found ($P < 0.05$).

In order to exclude the induction of programmed cell death in 3T3-L1 cells exposed to CDCA, caspase-3 content was determined by western blot analysis. Caspases are crucial mediators of apoptosis and among them caspase-3 is a downstream effector caspase, which in turn execute apoptosis by cleaving targeted cellular proteins (Li et al., 2011).

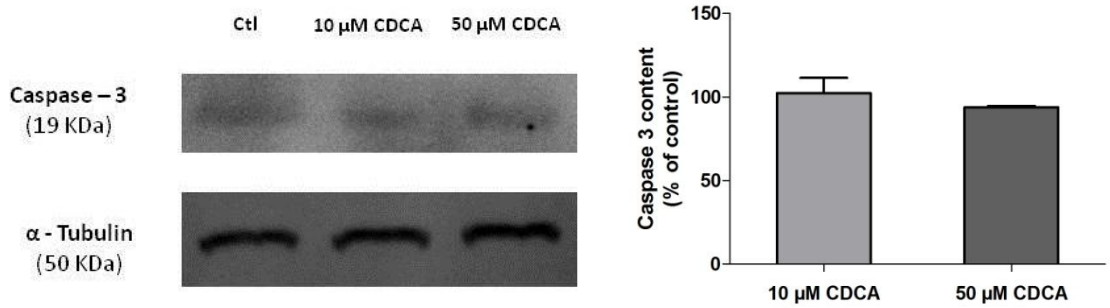

Figure 19 - Caspase-3 content evaluated by western blot analysis.

Caspase-3 content levels in 3T3-L1 cells detected by Western Blot which were performed as described in Chapter 2. (A) Graphic representation of relative density of caspase-3 protein levels in 3T3-L1 cells, which were normalized to those of α-Tubulin. (B) Data are means ± SEM of four different experiments. No statistically significant differences were found ($P < 0.05$).

No significant difference was observed in caspase-3 content between control and adipocytes exposed to the tested concentrations of CDCA (Figure 19), indicating that CDCA exposure doesn't cause apoptotic cell death at 96h of exposure.

3.2 Triglycerides accumulation

Culture of 3T3-L1 adipocytes in media containing high glucose resulted in a significant increase in the level of triglyceride (Wang et al., 2013). To evaluate if CDCA interferes with lipid accumulation, TG accumulation on 3T3-L1 cells was evaluated by oil-red o staining after 96h treatment, as described in section 2.2.2. Cells incubated with CDCA showed a significantly decrease in TG accumulation when compared to control, for both concentrations tested, at 96h of exposure, as shown in figure 20.

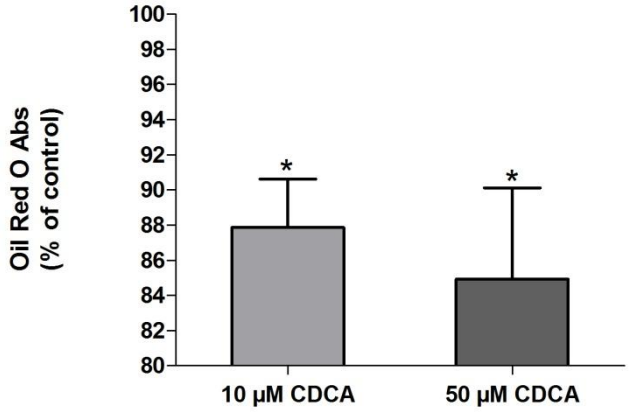

Figure 20 - Lipid accumulation in 3T3-L1 cells after CDCA exposure.

Cells were cultured and exposed to CDCA for 96h, and then assayed for lipid accumulation through colorimetric assay, as described in Chapter 2. Data are means ± SEM of seven different experiments. * indicates statistically significant difference versus control ($P < 0.05$).

3.3 Mitochondrial membrane potential

The decrease in TG content induced by CDCA could be explained by increased oxidative capacity, which could be related with stimulation of mitochondrial function. Therefore, mitochondrial membrane potential was evaluated in 3T3-L1 cells incubated with CDCA for 96h, by using the fluorescent dye TMRM, as described in section 2.2.3. This important physiologic mitochondrial parameter relates to cells' capacity to generate ATP by oxidative phosphorylation. Moreover, compromised mitochondrial energy

production is a major anomaly in obesity. The results showed that CDCA did not cause significant alterations in mitochondrial potential, after 96h treatment for both concentrations tested (Figure 21).

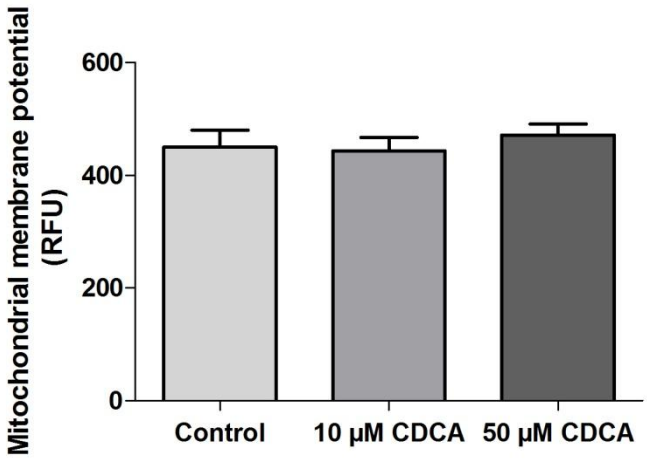

Figure 21 - Mitochondrial membrane potential (ΔΨ) in 3T3-L1 cells exposed to CDCA.

Cells exposed for 96h to CDCA were used to estimate ΔΨ fluorometrically with the probe TMRM, as described in Chapter 2. Data are means ± SEM of nine different experiments. No statistically significant differences were found ($P < 0.05$).

3.4 ROS generation

A pathological increase in ROS generation in adipocytes has been associated with obesity and it reflects an impairment of mitochondrial function. The results show that for both concentrations tested, 10 µM and 50 µM CDCA, ROS production is decreased (Figure 22) when compared to control. Despite the lower production in cells exposed to 10 µM CDCA, the decreased was only significant in cells exposed to 50 µM CDCA.

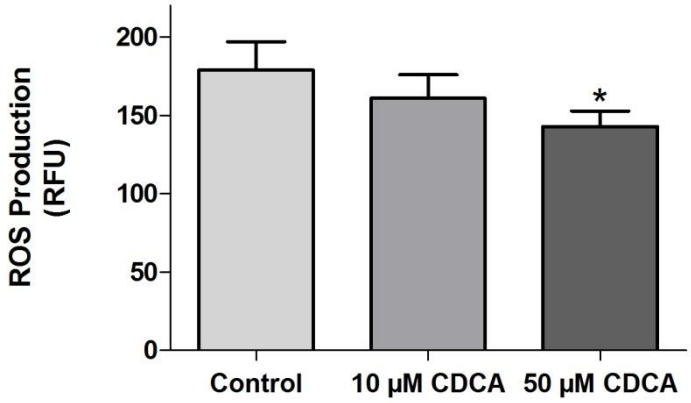

Figure 22 - ROS production in 3T3-L1 cells after exposure to CDCA.

Cells were cultured and exposed to CDCA for 96h, and then assayed for ROS production fluorometrically using the probe DCFDA, as described in Chapter 2. Data are means ± SEM of five different experiments. * indicates statistically significant difference versus control ($P < 0.05$).

3.5 Content in mitochondrial proteins

To further investigate the biochemical basis for the effects of CDCA in 3T3-L1 cells, mitochondrial protein content was evaluated. Since CDCA treatment induced both a decrease in TG accumulation and ROS generation for cells exposed to CDCA, UCP-1 content was determined. The results showed a significant increase for cells exposed to 50 µM CDCA (Figure 23).

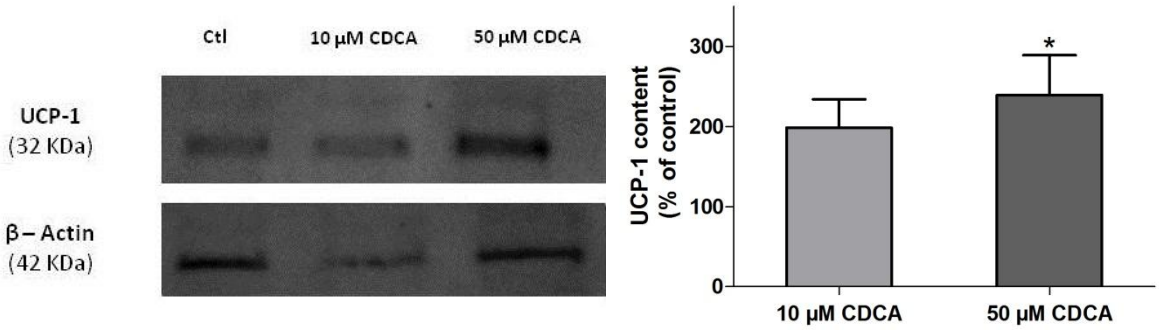

Figure 23 - UCP-1 content evaluated by western blot analysis in 3T3-L1 cells.

UCP-1 content levels in 3T3-L1 cells detected by Western Blot which were performed as described in Chapter 2. (A) Graphic representation of relative density of UCP-1 protein levels in 3T3-L1 cells, which were normalized to those of β-actin. (B) Data are means ± SEM of four different experiments. * indicates statistically significant difference versus control ($P < 0.05$).

The content in two subunits (I and IV) of COX, one of the four complexes of MRC that promotes the proton pumping and establishes the electrochemical gradient for the synthesis of ATP, was also determined.

Relatively to content of COX IV although there was a tendency to increase, a non statistically significant increase was observed between controls and cells treated with 10 μM CDCA and 50 μM CDCA (Figure 24).

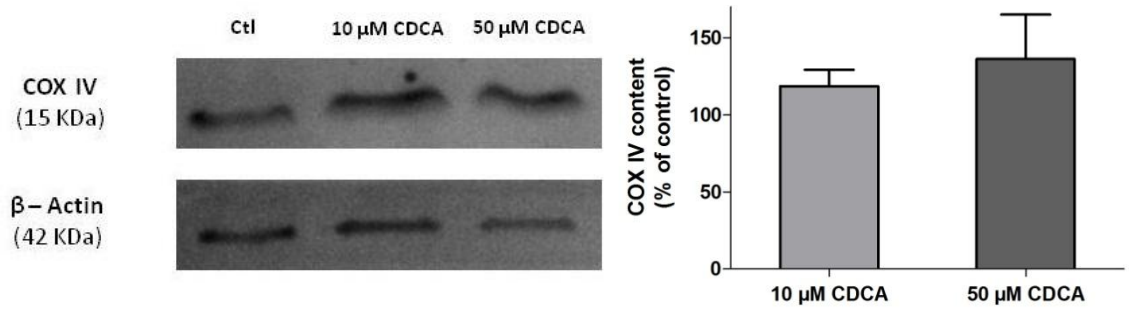

Figure 24- COX IV content evaluated by western blot analysis in 3T3-L1 cells.

COX IV content levels in 3T3-L1 cells detected by Western Blot which were performed as described in Chapter 2. (A) Graphic representation of relative density of COX IV protein levels in 3T3-L1 cells, which were normalized to those of β-actin. (B) Data are means ± SEM of four different experiments. No statistically significant differences were found ($P < 0.05$).

Similarly, the analysis done to the content in COX I showed no significant increase for both concentrations tested, as shown in figure 25.

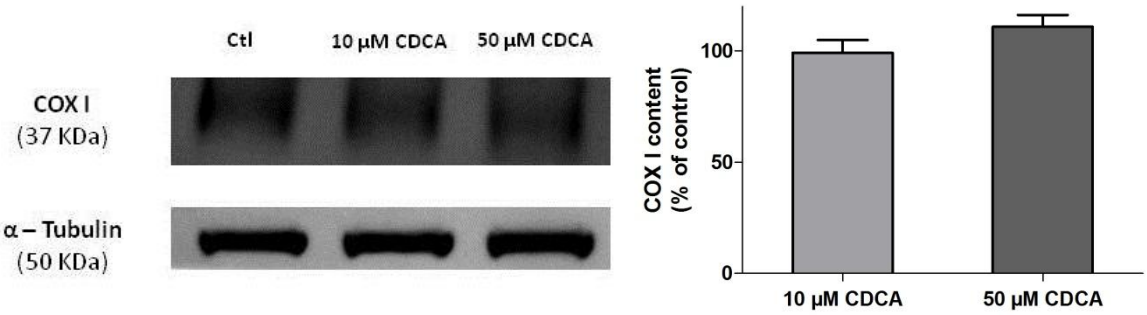

Figure 25 - COX I content evaluated by western blot analysis in 3T3-L1 cells.

COX I content levels in 3T3-L1 cells detected by Western Blot which were performed as described in Chapter 2. (A) Graphic representation of relative density of COX I protein levels in 3T3-L1 cells, which were normalized to those of α-Tubulin. (B) Data are means ± SEM of four different experiments. No statistically significant differences were found ($P < 0.05$).

So, taking into account this results the ratio between COX I (mtDNA encoded) and COX IV (nuclear encoded) was determined, since to form a functional holoenzyme with 1:1 stoichiometry of all 13 subunits, exact coordination is essential between the two genomes (Dhar et al., 2013). Furthermore, diseases such as obesity and T2DM have been associated to a decrease in mtDNA (Rolo & Palmeira, 2006). As shown in figure 26, the ratio between these proteins in not altered, in cells exposed to 10 μM CDCA and 50 μM CDCA.

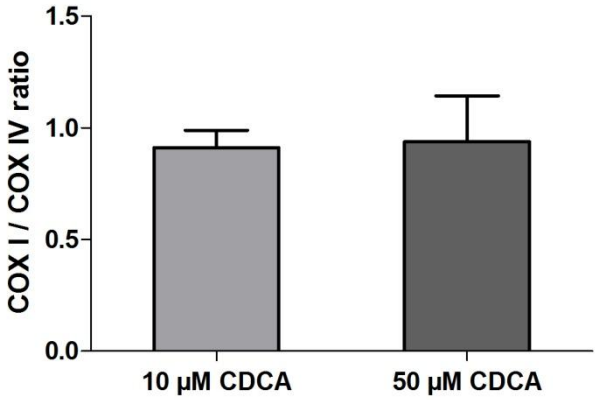

Figure 26 - COX I / COX IV ratio in 3T3-L1 exposed to CDCA.

Graphic representation of COX I / COX IV ratio in 3T3-L1 cells. Data are means ± SEM of four different experiments. No statistically significant differences were found ($P < 0.05$).

3.6 Cytochrome *c* Oxidase activity

Although Δψ and COX content were not altered by CDCA treatment, the decrease in ROS generation and increased UCP-1 content could be associated with increased activity of mitochondrial electron transport chain complexes. Therefore, COX activity was determined. However, no statistical significant differences were observed in cells exposed to CDCA, when compared to control (Figure 27).

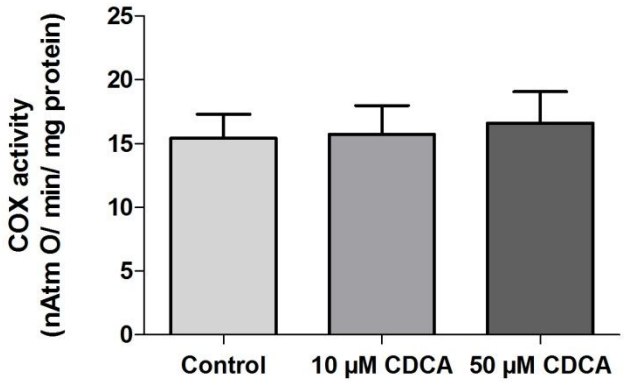

Figure 27 - Cytochrome c Oxidase activity.

Enzymatic activity was determined by oxygen consumption after incubation with CDCA using oxygen sensitive electrode, as described in Chapter 2. Data are means ± SEM of four different experiments and are expressed in nAtm O/ min/ mg protein. No statistically significant differences were found ($P < 0.05$).

3.7 Gene expression

To further investigate if the decrease in TG accumulation was associated with alterations in cellular metabolic capacity, expression of genes implicated in lipid metabolism was evaluated. One of them was the enzyme carnitine palmitoyltransferase I alpha (CPT1α), an isoform of CPT1, located in the outer mitochondrial membrane and responsible for the transfer of long-chain fatty acids (LCFA) into the mitochondria. The elevated concentration of FFA in plasma characteristic of obesity and T2DM are associated with an inhibition of LCFA oxidation (Rasmussen et al., 2002). The mechanism responsible for the decrease in LCFA oxidation is still poorly understood but most likely it involves the inhibition of CPT1α (Rasmussen et al., 2002). Other key genes were also evaluated. FAS, a key enzyme for FFA synthesis, GLUT4, the main insulin-responsive glucose transporter, PPARα and PPARγ, key transcriptional regulators of fatty acid oxidation and mitochondrial oxidative capacity, respectively. Lastly, the expression of PEPCK a key enzyme that regulates glyceroneogenesis was also assessed, as well as mitochondrial genes (UCP-1, COX IV and COX III) and biomarkers of biogenesis mitochondrial like TFAM and PGC-1α.

The results showed a tendency for increased expression in all genes, except COX III, for both concentrations, but only on PEPCK expression was statistically significant, as shown in figure 28. Since up-regulation of this enzyme is associated an increase

glyceroneogenesis, this results suggest that CDCA stimulates this pathway, which could be associated with increased TG/ (GL+FFA) cycle activity.

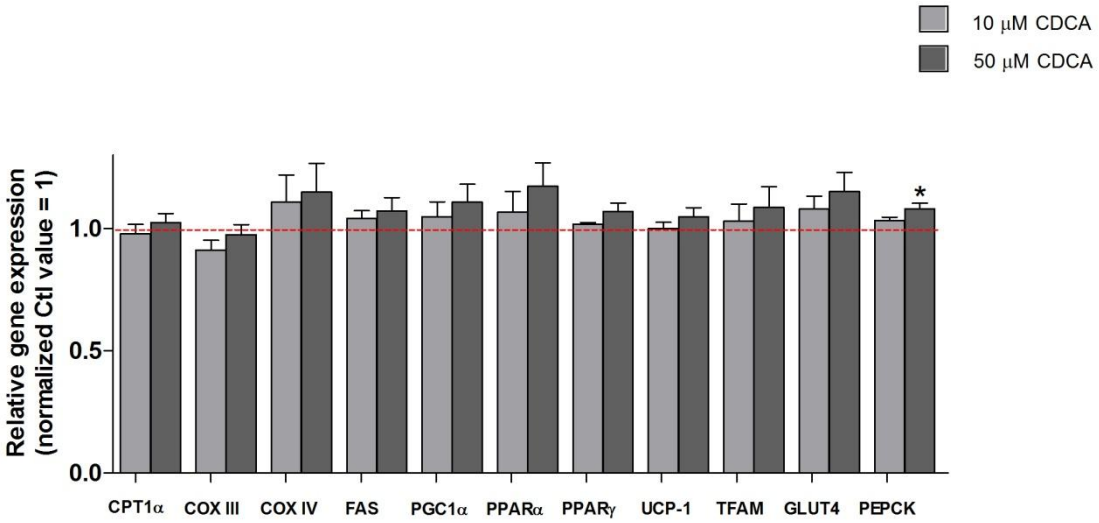

Figure 28 - Gene expression levels per cell in 3T3-L1 exposed to CDCA.

3T3-L1 cells were cultured and exposed to CDCA for 96h. Copy numbers for each gene were calculated based on standard curves and normalization was performed with respect to 18S RNA. Bars represent the mean ± S.E.M. for four different cell cultures. * Indicates statistically significant difference versus control ($P < 0.05$).

3.8 NMR analysis

To evaluate if CDCA supplementation alters the TG/(GL+FFA) cycle activity, cultured 3T3-L1 cells were exposed to CDCA in the presence of labelled compounds, [U-$^{2}H_5$] glycerol and [U-^{13}C] glucose, and followed their deposition by NMR. First analysis was to evaluate *de novo* lipogenesis (DNL). The synthesis of lipids from non-lipidic sources can be monitored by the detection of the incorporation of ^{13}C in lipids. Acetyl-CoA derived from [U-^{13}C] glucose will be enriched in both carbons of the acetyl moiety and can be used in the synthesis of lipids. These enriched lipids will be distinguishable from non-enriched by ^{1}H NMR spectroscopy due to the appearance of ^{13}C satellites in the lipidic methyl (-CH_3) resonance (Figure 29).

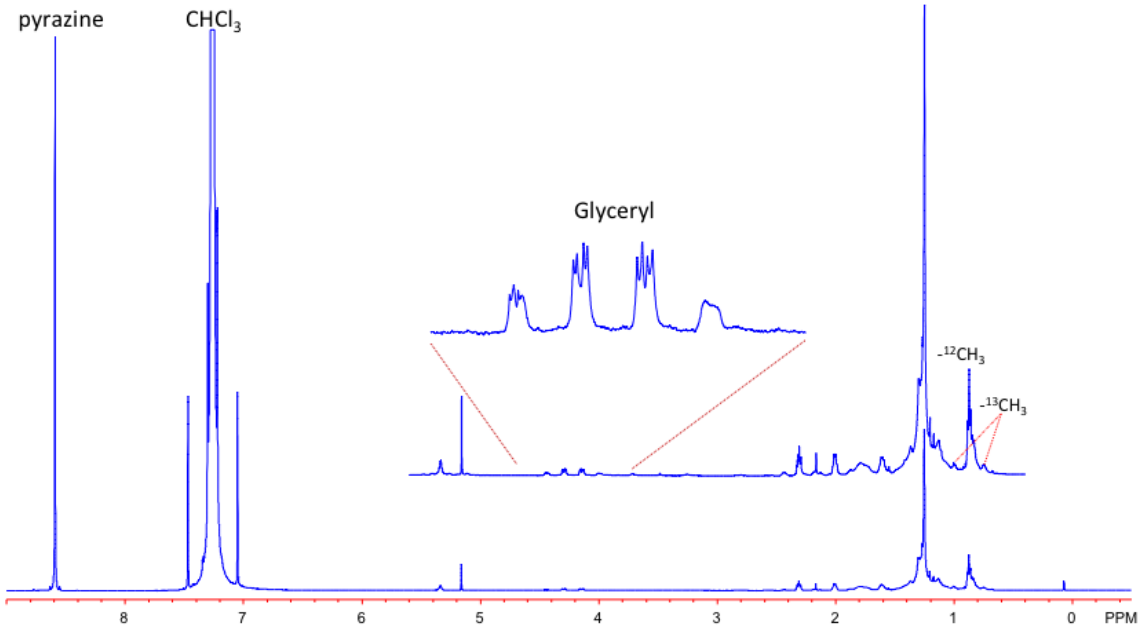

Figure 29 - 11.7 Tesla ^{1}H NMR spectrum of the cell lipidic extract.

The expansion shows the glyceryl moiety of TGs. Non-deuterated and partially protonated glycerol resonances are distinguishable and allow the quantification of TGs turnover.

Through the integration of the satellites, the relative DNL is quantified and upon comparison with the internal standard (pyrazine) absolute measures of DNL are also possible. An analysis of the effect of CDCA in lipid content revealed a considerable reduction both at 10 and 50 μM CDCA concentrations (Figure 30). No significant differences were observed in terms of relative DNL contributions (~20% in each experimental condition), however absolute measures of DNL show that the addition of CDCA leads to a significant reduction in absolute lipid synthesis and, concomitantly, the overall *de novo* synthesis of fatty acids (DNL) is also reduced.

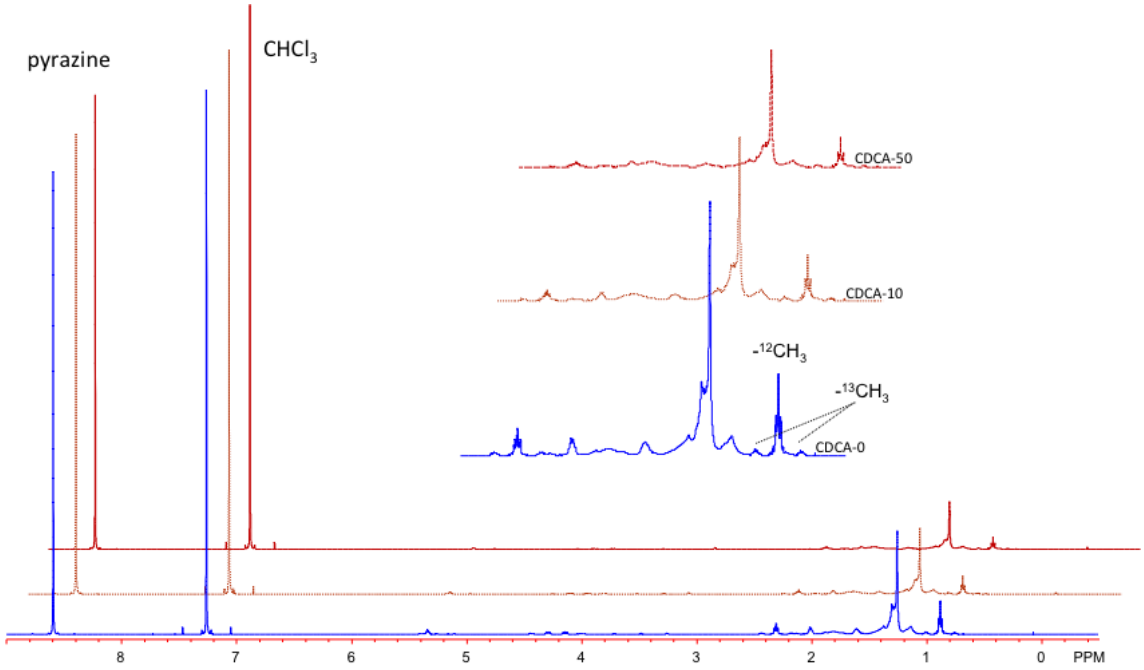

Figure 30 - 11.7 Tesla ^{1}H NMR spectrum of the cell lipidic extracts.

The expansions show the lipidic resonances (methyl and methylenic) and clearly demonstrate a reduction in lipid content due to CDCA treatment.

The incorporation of [U-$^{2}H_5$] glycerol in lipids is accompanied by the liberation into the media of unenriched glycerol. Thus an analysis of the deuterium enrichment of the glyceryl moiety of the TGs pool is the clearest evidence of the occurrence of a "futile" cycle of TG synthesis and degradation. Figure 31 shows the expansions of the glyceryl moiety of TGs for each of the experimental conditions.

A partial protonation of the [U-$^{2}H_5$] glycerol at the level of triose phosphate isomerase (TPI), due to incorporation from H_2O protons, allows its monitoring by ^{1}H NMR spectroscopy. A measure of this contribution to total glyceryl in TGs allows the monitoring of lipolysis followed by re-esterification. Thus, the more pronounced the turnover of the TGs pool the more extensive is the substitution of [U-$^{1}H_5$] glycerol by the partially protonated glycerol. With the increase in CDCA there is an increment in such contribution and more dynamic is the "futile" cycling.

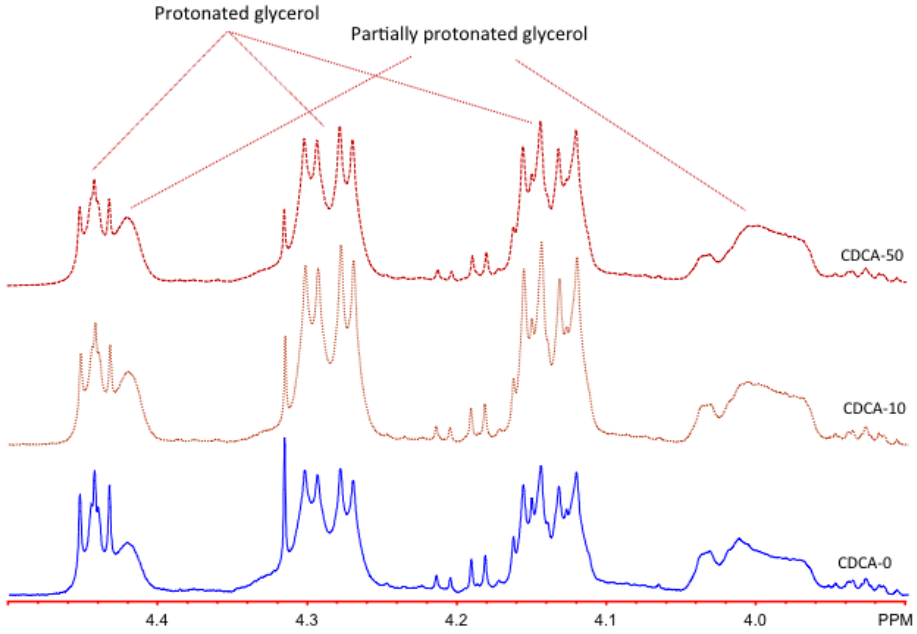

Figure 31 - Expansions of the glyceryl moiety of TGs ^{1}H NMR spectrum.

Partially protonated glycerol increases with CDCA treatment.

In a second phase, the synthesis of glycerol from glucose (direct synthesis) and glyceroneogenesis (indirect synthesis) was evaluated. [U-^{13}C] glucose can be used in the synthesis of glycerol. The direct synthesis produces [U-^{13}C] glycerol while the indirect prompts the appearance of the doubly labelled isotopomer [2,(3)-$^{13}C_2$]glycerol due to the action of backward scrambling at the level of the symmetric dicarboxylates (fumarate/succinate) in the TCA cycle. By the action of pyruvate carboxylase (PC) the [U-^{13}C] pyruvate forms [1, 2, 3-$^{13}C_3$] oxaloacetate. This isotopomer of oxaloacetate can subsequently be converted into [2, 3, 4-$^{13}C_3$] oxaloacetate by the combined actions of all enzymes involved in the conversion of all dicarboxylic Krebs cycle intermediates. Upon conversion to phosphoenolpyruvate (PEP), this oxaloacetate isotopomer looses one of the enriched carbons and originates the [2, 3-$^{13}C_2$]-enrichment pattern seen in glyceryl moiety of TGs. The amount of doubly labelled versus uniformly labelled glycerol will provide a measure of glyceroneogenesis versus direct synthesis from [U-^{13}C] glucose.

Figure 32 shows an expansion from the ^{13}C NMR spectra of the lipidic extract due to the carbons of the glyceryl moiety of TGs. The resonance due to carbon 2 of glyceryl is either a triplet (T), due to [U-^{13}C] glyceryl, or a doublet (D), due to the doubly labelled glyceryl isotopomer. The more pronounced this last component the higher the involvement

of glyceroneogenesis in the whole turnover of the glycerol pool. A higher turnover on the other hand suggests that lipolitic activity is more pronounced. The more reduced the TGs pool the more plausible is an increment in the doubly labelled pool and such could be used as an indirect measure of TGs turnover. This doublet component is more significant in the presence of CDCA both at 10 and 50 µM levels.

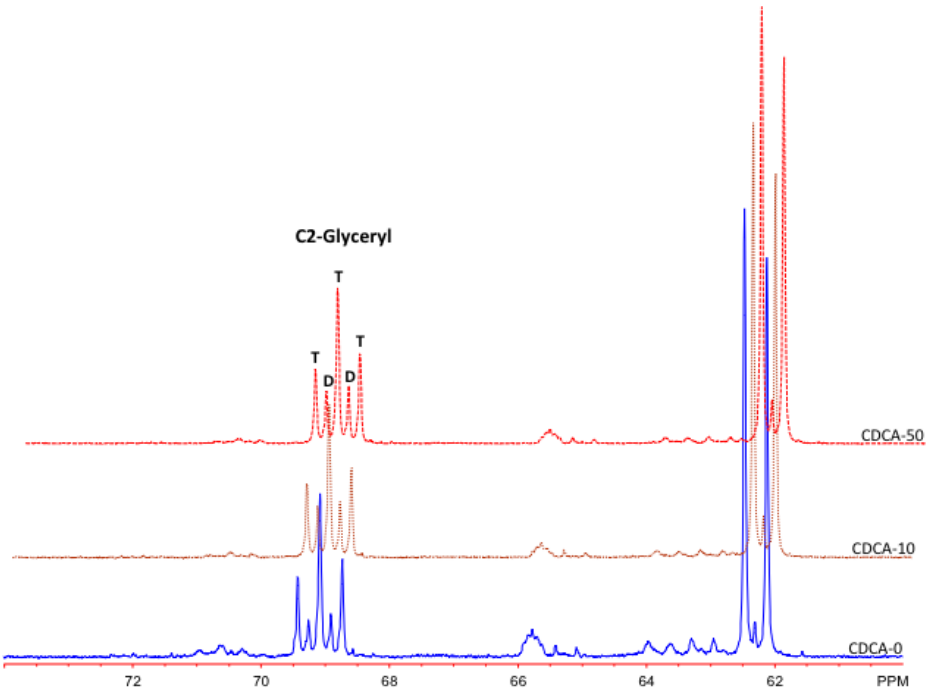

Figure 32 - Expansions of the glyceryl moiety of TGs 13C NMR spectrum.

Glycerol derived directly from [U-13C] glucose (T) and glycerol derived from glyceroneogenesis (D). CDCA treatment increases glyceroneogenesis.

Lastly, the fatty acid oxidation was measured indirectly. The [U-^{13}C] glucose oxidation in the Krebs cycle causes significant enrichment of cycle intermediates due to cycle turnover. However in the presence of non-enriched substrate competitors, there is considerable dilution of ^{13}C in cycle intermediates and rates of appearance of multiple-labelled intermediates are significantly diminished. An increased availability of FFA in adipocytes could favour their oxidation and in such case there should be a considerable dilution of ^{13}C labelling easily appreciated from the reduction in C4Q/C4D45 ratio seen in glutamate C4 resonance. Figure 33 shows the ^{13}C NMR spectrum of the aqueous cell extract and the expansions of the C4 resonance of glutamate. Figure 34 shows the expanded multiplets of C4 glutamate and C4 glutamine for each of the experimental conditions.

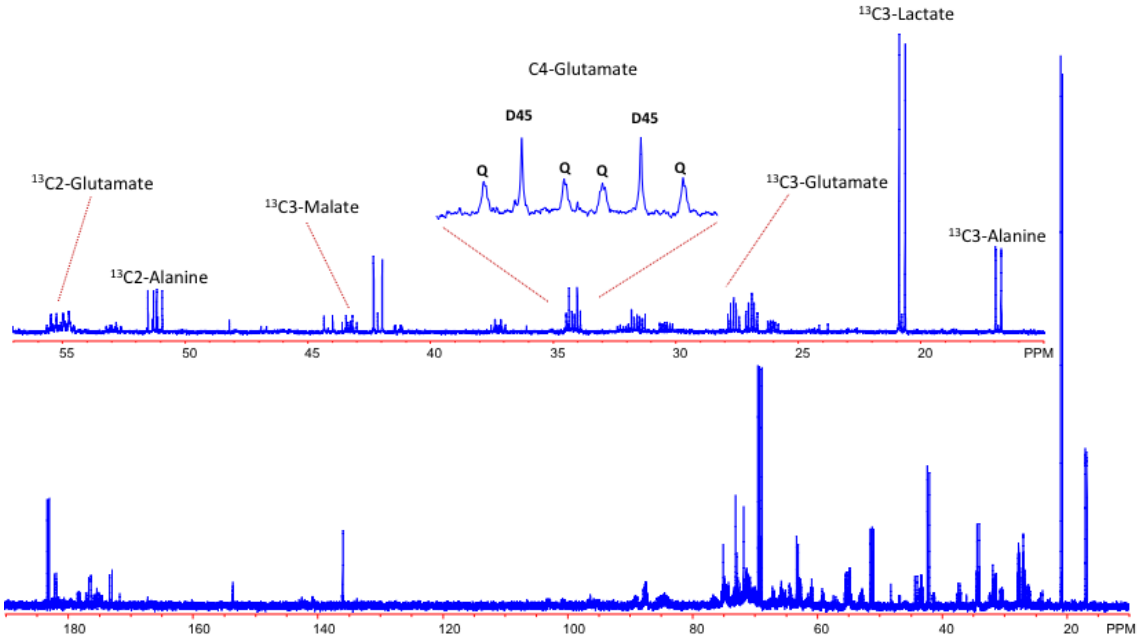

Figure 33 - ^{13}C NMR spectrum from an aqueous extract of adipocytes, treated with CDCA 50 µM.

Several carbons are signalled and the expanded resonance of glutamate shows the D45 and Q multiplet components used in the evaluation of Krebs cycle kinetics.

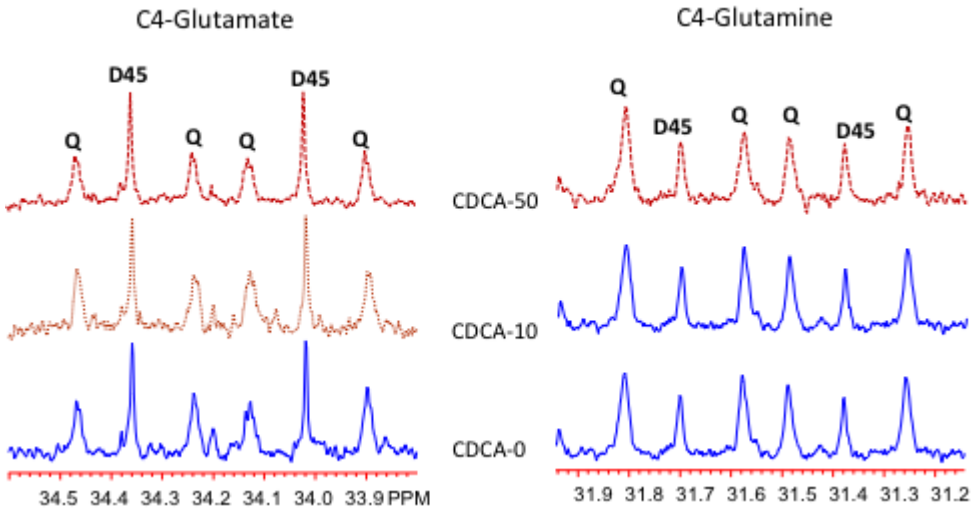

Figure 34 - Expansions of C4 glutamate and C4 glutamine resonances for the three experimental conditions.

There are no differences in multiplet composition between conditions but there is a significant difference among metabolites. Fractional 13C enrichment is higher for glutamine than glutamate, consistent with metabolic compartmentation issues in adipocytes.

Two major conclusions can be drawn from the analysis of these spectra. First, there is no difference in the ratios C4Q/C4D45 both for glutamate and glutamine. This suggests that there is no significant oxidation of unenriched fatty acids in the adipocytes in any of the experimental conditions. Second, the level of ^{13}C enrichment is higher in glutamine than in glutamate. Ratios of C4Q/C4D45 are higher in glutamine C4 than in glutamate. Since glutamine is derived from glutamate, such controversial finding suggests the occurrence of metabolic compartmentalization within adipocytes. The fast exchanging glutamine pool acquires significant levels of ^{13}C enrichment while glutamate shows a combination of slow and fast exchanging pools. The sizes of these pools are noticeably in the same order of magnitude and do not justify the differences in labelling patterns. This same compartmentalization issues are absent when analysing the lactate and alanine pools, as reported by the analysis of the ^{1}H NMR spectra of aqueous extracts (Figures 35 and 36), where no differences are seen in the relative fractions of ^{13}C enrichment for each metabolite.

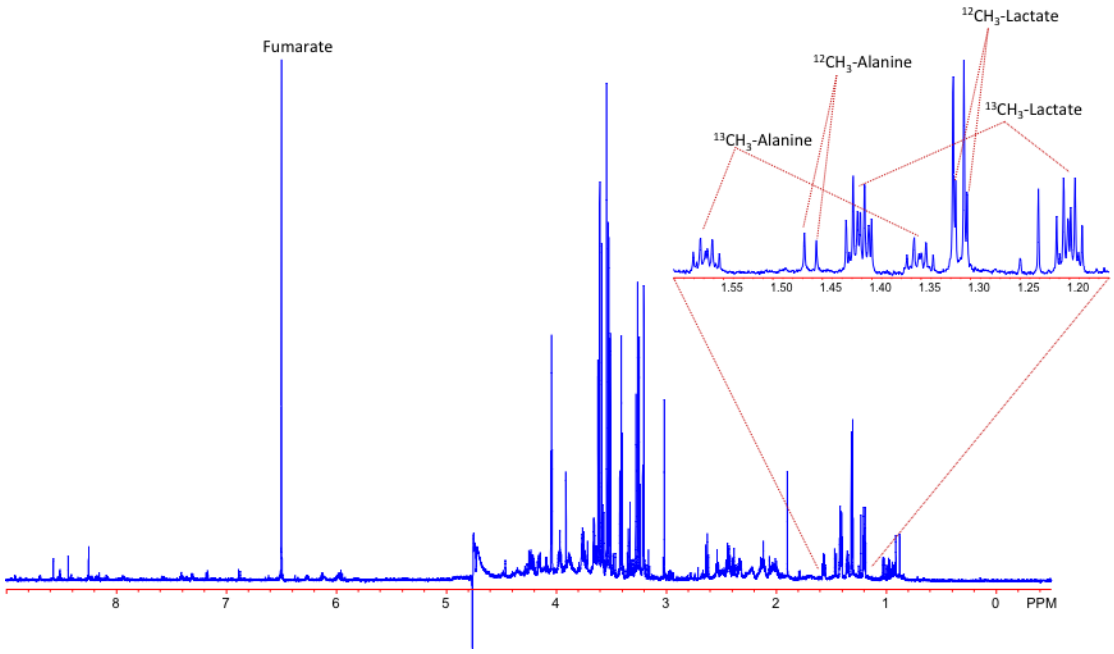

Figure 35 - 14.1 Tesla ^{1}H NMR spectrum from an aqueous extract of adipocytes.

The expansion shows the region of lactate and alanine methyl resonances.

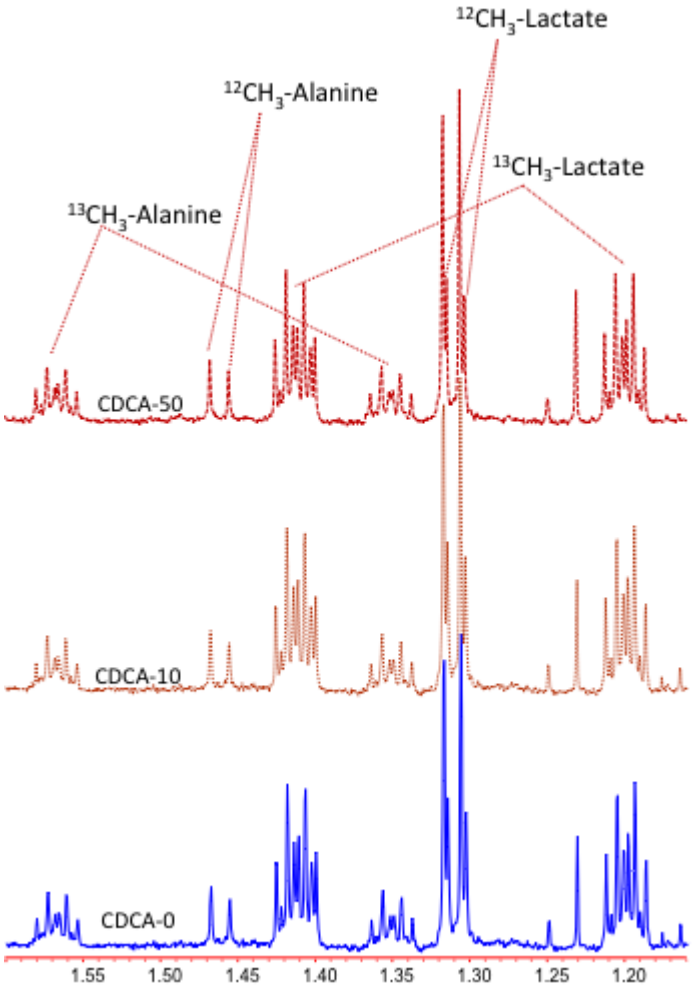

Figure 36 - Expansions of the region of lactate and alanine methyl resonances for the three experimental conditions.

CDCA does not interfere in ^{13}C enrichment of these two pools.

CHAPTER IV

Discussion

4. Discussion

Obesity is a worldwide epidemic; the WHO estimated that 400 million people were obese in 2005, and an increase is expected to 700 million in 2015 (Gesta et al., 2007). Thus, investigation on novel therapeutic targets for this condition assumes contours of urgency. This growing epidemic is a prelude to co-morbidities that develop as a consequence of this condition including hypertension, cardiovascular disease, insulin resistance and T2DM. Often these diseases occur together, so the term “metabolic syndrome” has been used to characterize this clustering of diseases (Scarpellini & Tack, 2012; Gesta et al., 2007; Schuster, 2010).

Obesity is associated with an excessive accumulation of TG in adipose tissue, resulting in enlarged and/or increased number of fat cells. While on one hand, lipid storage is increased in obesity, the adipose tissue inflamed also releases more FFA (Bray, 2004). Increased circulating levels of FFA are initially associated with increased rates of fatty acid oxidation in the skeletal muscle. However, the accumulation of metabolites from fatty acid oxidation in the cytoplasm of muscle cells (lipotoxicity) interferes with insulin signaling cascade and the ability to easily switch between glucose and fat oxidation in response to homeostatic signals (Hsieh et al., 2011). The impaired uptake of glucose increases plasma glucose concentration, leading to further insulin secretion and starting a vicious cycle with impaired regulation of energy substrate metabolism (Cahová et al., 2007).

Given the involvement of mitochondria in the metabolism of fatty acids, and its vital importance to the cell, any change in mitochondrial function induced by accumulation of fat in the adipose tissue, will certainly be reflected in the function cell. Indeed, many studies have been conducted within this thematic. These works indicated that adipose mitochondrial dysfunction associated with obesity is related to a reduction in both FFA β-oxidation and OXPHOS rates (Medina-gómez, 2012), a decrease in mitochondrial content (Wilson-fritch et al., 2004), an increase in ROS generation and also an inhibition of antioxidant enzymes such as superoxide dismutase, glutathione peroxidase and catalase (Wang et al., 2010; Furukawa et al., 2004). Moreover, the deceleration and alterations on the TG/ (GL+FFA) cycle have been demonstrated in experimental models of obesity and diabetes (Reshef et al., 2003). However, besides of extensive research is this area (Cahová et al., 2007; Kusminski & Scherer, 2012; Vankoningsloo et al., 2005), still remain

some doubts about primary site where dysregulation of mitochondrial function takes place and furthermore an efficient therapy to obesity.

Recently BA have been receiving a great attention in the scientific community and a growing body of evidence suggests that BA also act as a signaling molecules and are involved in the regulation of energy expenditure (Ockenga et al., 2012; Watanabe et al., 2006; Teodoro et al., 2013). Moreover, BA metabolism seems to be altered in T2DM patients and the manipulation of the BA pool can improve glucose metabolism, insulin resistance, energy homeostasis as well as lipid metabolism in such patients (Prawitt et al., 2011; Cariou et al., 2011). Until recently, it was thought that BA promoted increase energy expenditure via a TGR5-mediated signalling cascade in BAT (Watanabe et al., 2006). However the clinical relevance of this pathway has been challenged, once neither the overexpression nor the absence of TGR5 in mice leads to a difference in body weight and the susceptibility to diet-induced obesity is gender-specific (Maruyama et al., 2006). Nevertheless it's undeniable that BA, namely CDCA, has an effect anti-obesity (Teodoro et al., 2013; Ockenga et al., 2012; Watanabe et al., 2006; Watanabe et al., 2004), however the mechanism by which CDCA exerts this actions remains unknown. As such, a possible hypothesis is that CDCA could affect TG/ (GL+FFA) cycle activity. It is known that CDCA activates both PPARα and PPARγ, two transcription factors that are involved in the transcription of key metabolic genes, like some enzymes of the TG/ (GL+FFA) cycle and of mitochondrial oxidative capacity (PPARγ), and of genes involved in FFA oxidation (PPARα).

In order to assess if alterations in mitochondrial function and in TG/ (GL+FFA) cycle are induced by CDCA, an *in vitro* model was chosen, 3T3-L1 adipose like cell line, which have been used extensively to biological research in adipose tissue (Green & Meuth, 1974).

Since it is known that CDCA are particularly hepatotoxic (Rolo et al., 2003), cytotoxic assays were conducted in 3T3-L1 cells. Previously studies have been conducted in different types of cell cultures to understand the mechanisms involved in CDCA injury (Park et al., 2013; K. Ramaesh & Madigan, 1998; Powell et al., 2001; Rolo et al., 2003), but never in 3T3-L1 adipocytes cell line. Both concentrations tested, 10 μM and 50 μM CDCA, did not alter both necrotic (Figure 16,17,18) and apoptotic parameters (Figure 19), contrarily to what has been demonstrated by previous studies in other cell lines (Park et al., 2013; Powell et al., 2001; K. Ramaesh & Madigan, 1998; Rolo et al., 2004).

3T3-L1 adipocytes incubated with CDCA showed a significant decrease in TG accumulation, about 20%, when compared to control for both concentrations tested (Figure 20). These results are in agreement to other works realized *in vivo* (Cipriani et al., 2010) that observed that CDCA leads to a significant reduction in the weight of epididymal WAT and subcutaneous WAT, as well as interscapular BAT, indicating a decrease in adiposity in conditions of diet-induced obesity (Teodoro et al., 2013).

Impaired mitochondrial function, which includes decreased capacity to generate ATP and increased ROS production, are major anomalies in obesity (Vankoningsloo et al., 2005). Therefore, stimulation of mitochondrial oxidative capacity has been associated with improved WAT metabolic flexibility and decreased obesity in both humans and rodents (Teodoro et al., 2013). Although exposure to CDCA did not cause significant alterations in mitochondrial potential for 96h treatment for both concentrations tested (Figure 21), ROS production was decreased but was only significant in cells exposed to 50 µM CDCA (Figure 22). This suggested a CDCA effect at a mitochondrial level. A possible explanation to the decrease in ROS generation and TG accumulation, could be an increase in UCP-1 content and activity, since a previously study *in vivo* demonstrated that CDCA increases UCP-1 content in an animal model obesity (Teodoro et al., 2013). The increase in UCP-1 content induced by CDCA in our cell model (Figure 26) and its impact on TG content is further supported by data showing that a increase in chemical uncoupling in 3T3-L1 cells leads to a reduction of about 35% in TG accumulation (Si et al., 2009; Si et al., 2007; Senocak et al., 2007).

Surprisingly, UCP-1 mRNA levels in cells exposed to CDCA were not significantly increased by this concentration. Based on previously evidences (Jacobsson et al., 1987; Patel et al., 1987; Picó et al., 1994), this seems to be related to the fact that the effect of stimulus on UCP-1 mRNA levels is very rapid, which in turn implies that the turnover of UCP-1 mRNA is also very rapid. Moreover, a recent study demonstrated that amount of UCP-1 is directly proportional to thermogenesis, and this apparent lack of relationship between UCP-1 mRNA levels and UCP-1 protein levels is explained by the fact that half-life of UCP-1 protein (3-6 days) is much greater than half-life of UCP-1 mRNA (few hours) (Nedergaard & Cannon, 2013). Assuming that UCP-1 functions in 3T3-L1 adipocytes are similar to brown adipocytes, it should decrease the $\Delta\psi$, at least in the short term (Floryk et al., 1999). A decrease in $\Delta\psi$ should decrease ATP synthesis and/or cause the reversal of the ATP synthase, both of which would impair the mitochondrial ATP generation. However, a previous study in 3T3-L1 adipocytes demonstrated that this increase in UCP-1

reverses the ATPsynthase activity leading to ATP hydrolysis and the transport of protons out of the inner mitochondria (Si et al., 2007). This proton efflux, which contributes to the membrane gradient at the expense of ATP, could explain the apparent lack of difference between the Δψ of cells exposed to 50 μM CDCA and control, observed in our study. On the other hand, brown adipocytes can compensate for the decrease in Δψ by up regulating β-oxidation and the TCA cycle, to generate extra NADH and $FADH_2$ for OXPHOS (Senocak et al., 2007). Since mitochondrial mass and oxidative capacity require activation of both nuclear and mitochondrial-encoded genes (Palmeira et al., 2007), COX content was determined. The content in both proteins increased for 10 μM and 50 μM CDCA (Figure 23, 24) wasn't statistically significant; and the nuclear and mitochondrial genomes seemed to be perfectly regulated since the ratio is approximately 1 (Figure 25). qPCR analysis showed increased expression of COX IV and of two biomarkers of mitochondrial biogenesis, PGC-1α and TFAM (Figure 28). To understand if the increased content and mRNA levels of these mitochondrial biomarkers would be representative of an increase in oxidative capacity, COX activity was assessed. The results showed no difference between control and cells exposed do CDCA. Based on these results seems that CDCA do not affect MRC activity. Moreover seems that these cells in spite of expressing UCP-1 do not behave as brown adipocytes.

Since this work aims to understand if CDCA regulates the TG/ (GL+FFA) cycle, the expression of genes involved in this cycle was determined. The most notable differences were in the expression of PPARα, PPARγ, GLUT4 and PEPCK in cells exposed to 50 μM CDCA, being significant in the latter (Figure 28). So contrarily to what been demonstrated by Kazuyuki Y. and colleagues in hepatocytes (Yamagata et al., 2004), our results demonstrated that CDCA increase significantly activity of PEPCK in adipocytes. This suggests that glyceroneogenesis, FFA re-esterification, and lipid deposition is augmented in these cells (Franckhauser et al., 2002). Furthermore, we demonstrated that expression of GLUT4 and PPARγ is also increase in 3T3-L1 in presence of 50 μM CDCA, as previously demonstrated by Shen and colleagues (Shen et al., 2008). The role of GLUT4 in obesity and T2DM is still unclear, however it is known that is downregulated in this conditions, and over-expressing of this receptor leads to an enhance disposal and tolerance in adipose tissue (Shen et al., 2008; Cariou et al., 2006; Vankoningsloo et al., 2005).

Taking into account these results, we could say that glyceroneogenesis is increased, since PEPCK activity correlates directly with its expression level (Ellero-

Simatos et al., 2011). This situation leads to an augmented in glycerol-3-phosphate availability and consequently in FFA re-esterification (Franckhauser et al., 2002; Olswang et al., 2002). This is consistent to the increase in PPARγ and FAS, since up-regulation of these genes stimulates enzymes involved in FFA uptake and TG synthesis, respectively (Vidal-Puig et al., 1996; Guan et al., 2002b; Olswang et al., 2002). However, the observed decrease in TG accumulation in cells treated with CDCA (Figure 20), suggests that despite of lipid deposition being favored, these lipids are being consumed. The augment in PPARα expression corroborates with this hypothesis, since this factor when co-expressed with PGC-1α, induces the expression of FFA oxidation enzymes in 3T3-L1 cells (Vega et al., 2000); and when rats are exposed to a PPARα activator, the expression of genes involved in FFA uptake and β-oxidation are increased (Christodoulides & Vidal-Puig, 2010). Moreover the slightly increase in CPT1α seems to be also in agreement with a possible increase in β-oxidation.

In order to confirm these results, TG/ (GL+FFA) activity was followed by NMR through deposition of labeled compounds, [U-$^{2}H_{5}$] glycerol and [U-^{13}C] glucose. Firstly, DNL was evaluated, since elevated synthesis of lipids is associated to obesity (Wang et al., 2013; McDevitt et al., 2001). Our results demonstrated no significant differences in terms of relative DNL contributions (~20% in each experimental condition), however absolute measures of DNL show that the addition of CDCA leads to a significant reduction in absolute lipid synthesis and concomitantly the overall de novo synthesis of fatty acids is also reduced (Figure 30). On the other hand, an increase in lipolysis followed by re-esterification of FFA was observed, i.e. a more pronounced turnover of the TG, in presence of CDCA. This demonstrates that there is an increment in the “futile” cycling (Figure 31), which is decreased in situations of obesity and T2DM (Prentki & Madiraju, 2008; Prentki & Madiraju, 2012; Reshef et al., 2003). To further this idea, glyceroneogenesis is increased in presence of CDCA, based either in increase of PEPCK expression (Figure 28) as in the increase of the doubly labelled glyceryl isotopomer in TG pool of cell lipidic extracts (Figure 32).

Thus, this increase in TG/ (GL+FFA) activity, leads to an augmented availability of FFA in adipocytes, which could favor their oxidation. However there is no significant oxidation of unenriched fatty acids in the adipocytes in any of the experimental conditions (Figure 34). This might be a surprising result assuming the higher TG turnover (Figure 31), the increase in PPARα expression (Figure 28) and the reduction in TG accumulation (Figure 20), seen in CDCA treated cells. However one must consider the fact that these

cells are specialized in lipid synthesis and not in lipid degradation/oxidation (Large et al., 2004). The reduction in lipid content can thus only be explained by their export to the medium.

Another surprising conclusion is that ratios of C4Q/C4D45 are higher in glutamine C4 than in glutamate (Figure 34). Since glutamine is derived from glutamate, such controversial finding suggests the occurrence of metabolic compartmentation within adipocytes, i.e. distinct intracellular pools of glutamine and glutamate that are not in equilibrium, as previously demonstrated (Patel et al., 1982). The sizes of these pools are noticeably in the same order of magnitude and do not justify the differences in labelling patterns. Further studies will be required to shed some light into these compartmentation issues but their interest is undoubtedly warranted by the inimitability of its behavior. This same compartmentation issues are absent when analysing the lactate and alanine pools (Figure 34 and 36).

Concluding, there are three major conclusions that can be drawn: 1) CDCA leads to a decrease in TG accumulation in 3T3-L1 adipocytes; 2) CDCA leads to an increase in UCP-1 content; 3) CDCA leads to an increase in glyceroneogenesis that consequently leads to an increase in TG/ (GL+FFA) cycle activity. Indeed, these results show that administration of CDCA seems to be an attractive therapy to obesity and T2DM. On the other hand, a question still remains, what leads to a reduction in TG accumulation? CDCA up-regulates genes involved in β-oxidation and mitochondrial biogenesis, but there are no differences in fatty acid oxidation between control and cell exposed to CDCA. A possible explanation is that lipids are being exported to the medium. However this is an *in vitro* study, it would be interesting understand the destination of this lipids *in vivo*. Finally the possible occurrence of metabolic compartmentalization opens new perspectives in futures works.

Bibliography

Abdelkarim, M. et al., 2010. The Farnesoid X Receptor Regulates Adipocyte Differentiation and Function by Promoting Peroxisome Proliferator-activated Receptor- γ and Interfering with the Wnt/β-Catenin Pathways. *Biological Chemistry*, 285, pp.36759–36767.

Abel, E.D. et al., 2001. Adipose-selective targeting of the GLUT4 gene impairs insulin action in muscle and liver. *Nature*, 409(6821), pp.729–733.

Alfadda, A. a & Sallam, R.M., 2012. Reactive oxygen species in health and disease. *Journal of biomedicine & biotechnology*, 2012, p.14.

Attardi, G. & G., S., 1988. Biogenesis of mitochondria. *Cell*, 4, pp.289–333.

Azzu, V. & Brand, M.D., 2010. The on-off switches of the mitochondrial uncoupling proteins. *Trends in biochemical sciences*, 35(5), pp.298–307.

Balistreri, C.R., Caruso, C. & Candore, G., 2010. The Role of Adipose Tissue and Adipokines in Obesity-Related Inflammatory Diseases. *Mediators of Inflammation*, 2010, p.19.

Barbatelli, G. et al., 2010. The emergence of cold-induced brown adipocytes in mouse white fat depots is determined predominantly by white to brown adipocyte transdifferentiation. *American Journal of Physiology, Endocrinology and Metabolism*, 298, pp.1244–1253.

Bengtsson, J. et al., 2001. Mitochondrial transcription factor A and respiratory complex IV increase in response to exercise training in humans. *European journal of physiology*, 443(1), pp.61–6.

Berger, J. et al., 1999. Novel Peroxisome Proliferator-activated Receptor (PPAR) γ and PPARδ Ligands Produce Distinct Biological Effects. *The Journal of biological chemistry*, 274, pp.6718–6725.

Berger, J. et al., 1996. Thiazolidinediones produce a conformational change in peroxisomal proliferator-activated receptor-gamma: binding and activation correlate with antidiabetic actions in db/db mice. *The Journal of Endocrinology*, 137(10), pp.4189–4195.

Bradford, B.L. et al., 1993. Development of obesity in transgenic mice after genetic ablation of brown adipose tissue. *Nature*, 336, pp.740–742.

Brautigan, D.L., Ferguson-Miller, S. & Margoliash, E., 1978. Mitochondrial cytochrome c: preparation and activity of native and chemically modified cytochromes c. *Methods in enzymology*, 53(0076-6879), pp.128–64.

Bray, G. a, 2004. Medical consequences of obesity. *The Journal of clinical endocrinology and metabolism*, 89(6), pp.2583–9.

Brito, M.N. et al., 1999. Brown adipose tissue triacylglycerol synthesis in rats adapted to a high-protein, carbohydrate-free diet. *The American journal of physiology*, 276(4 Pt 2), pp.R1003–9.

Brito, M.N., Brito, N.A. & Migliorini, H., 1992. Thermogenic Capacity of Brown Adipose Tissue Is Reduced in Rats Fed a High Protein, Carbohydrate-Free Diet. *The Journal of Nutrition*, pp.2081–2086.

Cahová, M., Vavrínková, H. & Kazdová, L., 2007. Glucose-fatty acid interaction in skeletal muscle and adipose tissue in insulin resistance. *Physiological research*, 56(1), pp.1–15.

Cariou, B. et al., 2011. Fasting plasma chenodeoxycholic acid and cholic acid concentrations are inversely correlated with insulin sensitivity in adults. *Nutrition & metabolism*, 8(1), p.48.

Cariou, B. et al., 2006. The Farnesoid X Receptor Modulates Adiposity and Peripheral Insulin Sensitivity in Mice. *The Journal of Biological Chemistry*, 281, pp.11039–11049.

Carrière, A. et al., 2003. Inhibition of preadipocyte proliferation by mitochondrial reactive oxygen species. *FEBS Letters*, 550(1-3), pp.163–167.

Carrière, A. et al., 2004. Mitochondrial reactive oxygen species control the transcription factor CHOP-10/GADD153 and adipocyte differentiation: a mechanism for hypoxia-dependent effect. *The Journal of biological chemistry*, 279(39), pp.40462–9.

Carrière, A. et al., 2009. Preconditioning by mitochondrial reactive oxygen species improves the proangiogenic potential of adipose-derived cells-based therapy. *Journal of the American Heart Association*, 29(7), pp.1093–9.

Casteilla, L. et al., 2008. Choosing an Adipose Tissue Depot for Sampling. In K. Yang, ed. *Adipose Tissue Protocols*. Methods in Molecular Biology™. Humana Press, pp. 23–38.

Christodoulides, C. & Vidal-Puig, A., 2010. PPARs and adipocyte function. *Molecular and cellular endocrinology*, 318, pp.61–68.

Cipriani, S. et al., 2010. FXR activation reverses insulin resistance and lipid abnormalities and protects against liver steatosis in Zucker (fa/fa) obese rats. *Journal of lipid research*, 51(4), pp.771–84.

Coutinho, G. et al., 2012. The role of the uncoupling protein 1 (UCP1) on the development of obesity and type 2 diabetes mellitus. *Archives of Endroconology and Metabolism*, pp.215–225.

Dalgaard, L.T. & Pedersen, O., 2001. Uncoupling proteins: functional characteristics and role in the pathogenesis of obesity and Type II diabetes. *Diabetologia*, 44(8), pp.946–65.

Dettmer, K. et al., 2011. Metabolite extraction from adherently growing mammalian cells for metabolomics studies: optimization of harvesting and extraction protocols. *Analytical and bioanalytical chemistry*, 399(3), pp.1127–39.

Dhar, S.S., Johar, K. & Wong-riley, M.T.T., 2013. Bigenomic transcriptional regulation of all thirteen cytochrome c oxidase subunit genes by specificity protein 1. *Open Biology*, 3, pp.1–11.

Duarte, F., 2012. *Dibenzofuran exposure: cellular and mitochondrial damage*. Universidade de Coimbra.

Duran-Sandoval, D. et al., 2004. Glucose regulates the expression of the farnesoid X receptor in liver. *Diabetes*, 53(4), pp.890–8.

Ellero-Simatos, S. et al., 2011. Combined transcriptomic-(1)H NMR metabonomic study reveals that monoethylhexyl phthalate stimulates adipogenesis and glyceroneogenesis in human adipocytes. *Journal of proteome research*, 10(12), pp.5493–502.

Enerbäck, S. et al., 1997. Mice lacking mitochondrial uncoupling protein are cold-sensitive but not obese. *Nature*, 387, pp.90–94.

Ferre, P., 2004. The Biology of Peroxisome Proliferator–Activated Receptors. *American Diabetes Association*, 53(February 2004), pp.43–50.

Fiorucci, S. et al., 2009. Bile-acid-activated receptors: targeting TGR5 and farnesoid-X-receptor in lipid and glucose disorders. *Cell*, 30(11), pp.570–80.

Floryk, D. et al., 1999. Transgenic UCP1 in white adipocytes modulates mitochondrial membrane potential. *FEBS Letters*, 444, pp.206–210.

Franckhauser, S. et al., 2002. Increased fatty acid re-esterification by PEPCK overexpression in adipose tissue leads to obesity without insulin resistance. *Diabetes*, 51(3), pp.624–30.

Frayn, K.N., Arner, P. & Yki-järvinen, H., 2006. Fatty acid metabolism in adipose tissue , muscle and liver in health and disease. In *Assays in Biochmestry*. pp. 89–103.

Frayth, K.N., 2003. *Metabolic Regulation: A Human Perspective* 2nd ed., Blackwell Publisher.

Fridovich, I., 1978. The biology of oxygen radicals. *Science*, 201, pp.875–80.

Furukawa, S. et al., 2004. Increased oxidative stress in obesity and its impact on metabolic syndrome. *The Journal of clinical investigation*, 114(12), pp.1752–1761.

Gesta, S., Tseng, Y.-H. & Kahn, C.R., 2007. Developmental origin of fat: tracking obesity to its source. *Cell*, 131(2), pp.242–56.

Gnaiger*, E. et al., 1998. Mitochondrial Oxygen Affinity, Respiratory Flux Control and Excess Capacity of Cytochrome c Oxidase. *The Journal of Experimental Biology*, 201, pp.1129–1139.

González, A. et al., 2012. Melatonin promotes differentiation of 3T3-L1 fibroblasts. *Journal of pineal research*, 52(1), pp.12–20.

Green, H. & Meuth, M., 1974. An established pre-adipose cell line and its differentiation in culture. *Cell*, 3(2), pp.127–133.

Guan, H.-P. et al., 2002a. A futile metabolic cycle activated in adipocytes by antidiabetic agents. *Nature medicine*, 8(10), pp.1122–8.

Guan, H.-P. et al., 2002b. A futile metabolic cycle activated in adipocytes by antidiabetic agents. *Nature medicine*, 8(10), pp.1122–8.

Hajer, G.R., Haeften, T.W. Van & Visseren, F.L.J., 2008. Adipose tissue dysfunction in obesity, diabetes, and vascular diseases. *European Heart Journal*, 29, pp.2959–2971.

Harper, J.A., Dickinson, K. & Brand, M.D., 2001. Mitochondrial uncoupling as a target for drug development for the treatment of obesity. *Obesity Reviews*, 2(4), pp.255–265.

Harwood, H.J., 2012. The adipocyte as an endocrine organ in the regulation of metabolic homeostasis. *Neuropharmacology*, 63(1), pp.57–75.

Hsiao, A.L. et al., 2005. Pediatric Fatality Following Ingestion of Dinitrophenol: Postmortem Identification of a "Dietary Supplement." *Clinical Toxicology*, 43(4), pp.281–285.

Hsieh, C., Desantis, D. & Croniger, C.M., 2011. Role of Triglyceride / Fatty Acid Cycle in Development of Type 2 Diabetes. In *Role of Triglyceride / Fatty Acid Cycle in Development of Type 2 Diabetes*. pp. 53–64.

Iser, J.H. et al., 1975. Chenodeoxycholic Acid Treatment of Gallstones. *New England Journal of Medicine*, 293(8), pp.378–383.

Jacobsson, a, Cannon, B. & Nedergaard, J., 1987. Physiological activation of brown adipose tissue destabilizes thermogenin mRNA. *FEBS letters*, 224(2), pp.353–6.

Joshi, D.C. & Bakowska, J.C., 2011. Determination of mitochondrial membrane potential and reactive oxygen species in live rat cortical neurons. *Journal of visualized experiments*, (51), pp.2–5.

K. Ramaesh, F.A.B. & Madigan, M. e., 1998. *Effect of bile acids on fibroblast proliferation and viability*,

Kast, H.R. et al., 2001. Farnesoid X-Activated Receptor Induces Apolipoprotein C-II Transcription : a Molecular Bile Acids. *The Journal of Molecular Endroconology*, 15(February), pp.1720–1728.

Katsuma, S., Hirasawa, A. & Tsujimoto, G., 2005. Bile acids promote glucagon-like peptide-1 secretion through TGR5 in a murine enteroendocrine cell line STC-1. *Biochemical and biophysical research communications*, 329(1), pp.386–90.

Keller, M.P. & Attie, A.D., 2010. Physiological insights gained from gene expression analysis in obesity and diabetes. *Annual review of nutrition*, 30(April), pp.341–64.

Kirkinezos, I.G. & Moraes, C.T., 2001. Reactive oxygen species and mitochondrial diseases. *Seminars in cell & developmental biology*, 12(6), pp.449–57.

Knutti, D. & Kralli, A., 2001. PGC-1, a versatile coactivator. *Trends in endocrinology and metabolism: TEM*, 12(8), pp.360–5.

Kopecky, J. et al., 1995. Expression of the mitochondrial uncoupling protein gene from the aP2 gene promoter prevents genetic obesity. *The Journal of clinical investigation*, 96(6), pp.2914–23.

Kusminski, C.M. & Scherer, P.E., 2012. Mitochondrial dysfunction in white adipose tissue. *Trends in endocrinology and metabolism: TEM*, 23(9), pp.435–43.

Large, V. et al., 2004. Metabolism of lipids in human white adipocyte. *Diabetes & metabolism*, 30(4), pp.294–309.

Lee, C.-H., Olson, P. & Evans, R.M., 2003. Minireview: lipid metabolism, metabolic diseases, and peroxisome proliferator-activated receptors. *Journal of Endocrinology*, 144(6), pp.2201–7.

Lee, H.-C. & Wei, Y.-H., 2005. Mitochondrial biogenesis and mitochondrial DNA maintenance of mammalian cells under oxidative stress. *The international journal of biochemistry & cell biology*, 37(4), pp.822–34.

Lefebvre, P. et al., 2009. Role of Bile Acids and Bile Acid Receptors in Metabolic Regulation. *The American journal of physiology*, 89, pp.147–191.

Li, H. et al., 2011. Phosphatidylcholine induces apoptosis of 3T3-L1 adipocytes. *Journal of biomedical science*, 18(1), p.91.

Lichtenbelt, W.D.V.M. et al., 2009. Cold-Activated Brown Adipose Tissue in Healthy Men. *The New England Journal of Medicine*, 360(15), pp.1500–1508.

Listenberger, L.L. et al., 2003. Triglyceride accumulation protects against fatty acid-induced lipotoxicity. *Proceedings of the National Academy of Sciences of the United States of America*, 100(6), pp.3077–82.

Lowe, C.E., Rahilly, O. & Rochford, J.J., 2011. Adipogenesis at a glance. *Journal of Cell Science*.

Ma, K. et al., 2006. Farnesoid X receptor is essential for normal glucose homeostasis. *The Journal of clinical investigation*, 116(4), pp.1102–1109.

Mackall, J.C. et al., 1976. Induction of lipogenesis during differentiation in a “preadipocyte” cell line. *The Journal of biological chemistry*, 251(20), pp.6462–6464.

Maruyama, T. et al., 2006. Targeted disruption of G protein-coupled bile acid receptor 1 (Gpbar1/M-Bar) in mice. *The Journal of endocrinology*, 191(1), pp.197–205.

Matthias, a et al., 2000. Thermogenic responses in brown fat cells are fully UCP1-dependent. UCP2 or UCP3 do not substitute for UCP1 in adrenergically or fatty scid-induced thermogenesis. *The Journal of biological chemistry*, 275(33), pp.25073–81.

McDevitt, R.M. et al., 2001. De novo lipogenesis during controlled overfeeding with sucrose or glucose in lean and obese women. *The American journal of clinical nutrition*, 74(6), pp.737–46.

Mead, J.R., Irvine, S. a & Ramji, D.P., 2002. Lipoprotein lipase: structure, function, regulation, and role in disease. *Journal of molecular medicine*, 80(12), pp.753–69.

Medina-gómez, G., 2012. Mitochondria and endocrine function of adipose tissue. *Best Practice & Research Clinical Endocrinology & Metabolism*, 26(6), pp.791–804.

Mehlem, A. et al., 2013. Imaging of neutral lipids by oil red O for analyzing the metabolic status in health and disease. *Nature Protocols*, 8(6), pp.1149–1154.

Millward, C. a et al., 2010. Phosphoenolpyruvate carboxykinase (Pck1) helps regulate the triglyceride/fatty acid cycle and development of insulin resistance in mice. *Journal of lipid research*, 51(6), pp.1452–63.

Moran, J.H. & Schnellmann, R.G., 1996. A Rapid P-NADH-Linked Fluorescence Assay for Lactate Dehydrogenase in Cellular Death. *Journal of Pharmacological and Toxicological Methods*, 36, pp.41–44.

Moreno-Navarrete, J.M. & Fernández-real, J.M., 2012. Adipocyte Differentiation. In *Adipose Tissue Biology*. pp. 17–39.

Nakae, J. et al., 2003. The Forkhead Transcription Factor Foxo1 Regulates Adipocyte Differentiation. *Cell*, 4(1), pp.119–129.

Nammi, S. et al., 2004. Obesity: an overview on its current perspectives and treatment options. *Nutrition journal*, 3, p.3.

Nedergaard, J. & Cannon, B., 2013. UCP1 mRNA does not produce heat. *Biochimica et biophysica acta*, 1831(5), pp.943–9.

Nicholls, D.G., 1983. The thermogenic mechanism of brown adipose tissue. Review. *Bioscience reports*, 3(5), pp.431–41.

Ntambi, J.M. & Kim, Y., 2000. Adipocyte Differentiation and Gene expression. *The Journal of Nutrition*, 130, pp.3122–3126.

Oakes, N.D., Ljung, B. & Camejo, G., 2002. Correction of dysfunctional fatty acid metabolism using peroxisome proliferator activated receptor gamma agonists. *Journal of the Royal Society of Medicine*, 95(4), pp.33–8.

Ockenga, J. et al., 2012. Plasma bile acids are associated with energy expenditure and thyroid function in humans. *The Journal of clinical endocrinology and metabolism*, 97(2), pp.535–42.

Olswang, Y. et al., 2002. A mutation in the peroxisome proliferator-activated receptor gamma-binding site in the gene for the cytosolic form of phosphoenolpyruvate carboxykinase reduces adipose tissue size and fat content in mice. *Proceedings of the National Academy of Sciences of the United States of America*, 99(2), pp.625–30.

Palmeira, C.M. et al., 2007. Hyperglycemia decreases mitochondrial function: the regulatory role of mitochondrial biogenesis. *Toxicology and applied pharmacology*, 225(2), pp.214–20.

Park, S. et al., 2013. Direct Effect of Chenodeoxycholic Acid on Differentiation of Mouse Embryonic Stem Cells Cultured under Feeder-Free Culture Conditions. *BioMed Research International*, 2013, p.9.

Patel, A.J. et al., 1982. The activities in different neural cell types of certain enzymes associated with the metabolic compartmentation glutamate. *Developmental Brain Research*, 4(1), pp.3–11.

Patel, H. V, Freeman, K.B. & Desautels, M., 1987. Selective loss of uncoupling protein mRNA in brown adipose tissue on deacclimation of cold-acclimated mice. *Biochemistry and Cell Biology*, 65(11), pp.955–959.

Patti, M.-E. & Corvera, S., 2010. The role of mitochondria in the pathogenesis of type 2 diabetes. *Endocrine reviews*, 31(3), pp.364–95.

De Pauw, A. et al., 2009. Mitochondrial (dys)function in adipocyte (de)differentiation and systemic metabolic alterations. *The American journal of pathology*, 175(3), pp.927–39.

Peralta, S., Wang, X. & Moraes, C.T., 2011. Mitochondrial transcription : Lessons from mouse models. *Biochimica et Biophysica Acta (BBA)*, 1819(9-10), pp.961–969.

Peters, J.M. et al., 2003. Bezafibrate is a dual ligand for PPARα and PPARβ: studies using null mice. *Biochimica et Biophysica Acta (BBA)*, 1632, pp.80–89.

Petrovic, N. et al., 2010. Chronic peroxisome proliferator-activated receptor gamma (PPARgamma) activation of epididymally derived white adipocyte cultures reveals a population of thermogenically competent, UCP1-containing adipocytes molecularly distinct from classic brown adipocyt. *The Journal of biological chemistry*, 285(10), pp.7153–64.

Picó, C. et al., 1994. Stabilization of the mRNA for the uncoupling protein thermogenin by transcriptional/translational blockade and by noradrenaline in brown adipocytes

differentiated in culture: a degradation factor induced by cessation of stimulation? *The Biochemical journal*, 302 (Pt 1, pp.81–6.

Pinkus, R., Weiner, L.M. & Daniel, V., 1996. Cell Biology and Metabolism : Role of Oxidants and Antioxidants in the Role of Oxidants and Antioxidants in the Induction of AP-1 , NF -kB , and Glutathione S -Transferase Gene Expression. *The Journal of biological chemistry*, 271, pp.13422–13429.

Porez, G. et al., 2012. Bile acid receptors as targets for the treatment of dyslipidemia and cardiovascular disease. *Journal of lipid research*, 53(9), pp.1723–37.

Powell, A.A. et al., 2001. Bile acid hydrophobicity is correlated with induction of apoptosis and/or growth arrest in HCT116 cells. *Journal of biochemical society*, 356, pp.481–486.

Prawitt, J., Caron, S. & Staels, B., 2011. Bile acid metabolism and the pathogenesis of type 2 diabetes. *Current diabetes reports*, 11(3), pp.160–6.

Prentki, M. & Madiraju, S.R.M., 2008. Glycerolipid metabolism and signaling in health and disease. *Endocrine reviews*, 29(6), pp.647–76.

Prentki, M. & Madiraju, S.R.M., 2012. Glycerolipid/free fatty acid cycle and islet β-cell function in health, obesity and diabetes. *Molecular and cellular endocrinology*, 353(1-2), pp.88–100.

Rasmussen, B.B. et al., 2002. Malonyl coenzyme A and the regulation of functional carnitine palmitoyltransferase-1 activity and fat oxidation in human skeletal muscle. *The Journal of Clinical Investigation*, 110(11), pp.1687–1693.

Rasouli, N. & Kern, P. a, 2008. Adipocytokines and the metabolic complications of obesity. *The Journal of clinical endocrinology and metabolism*, 93(11 Suppl 1), pp.S64–73.

Reaven, G., 2004. The metabolic syndrome or the insulin resistance syndrome? Different names, different concepts, and different goals. *Endocrinology and Metabolism Clinics of North America*, 33(2), pp.283–303.

Redinger, R.N., 2009. Fat storage and the biology of energy expenditure. *Laboratory and clinical medicine*, 154(2), pp.52–60.

Reshef, L. et al., 1970. A Possible Physiological Role for Glyceroneogenesis in Rat Adipose Tissue. *The Journal of biological chemistry*, 245, pp.5979–5984.

Reshef, L. et al., 2003. Glyceroneogenesis and the triglyceride/fatty acid cycle. *The Journal of biological chemistry*, 278(33), pp.30413–6.

Rizzo, G. et al., 2006. The Farnesoid X Receptor Promotes Adipocyte Differentiation and Regulates Adipose Cell Function in Vivo. *Molecular Pharmacology*, 70(4), pp.1164–1173.

Rolo, A.P. et al., 2004. Role of Mitochondrial Dysfunction in Combined Bile Acid-Induced Cytotoxicity: The Switch Between Apoptosis and Necrosis. *Toxicological Sciences*, 79(1), pp.196–204.

Rolo, A.P. & Palmeira, C.M., 2006. Diabetes and mitochondrial function: Role of hyperglycemia and oxidative stress. *Toxicology and Applied Pharmacology*, 212(2), pp.167–178.

Rolo, A.P., Palmeira, C.M. & Wallace, K.B., 2003. Mitochondrially mediated synergistic cell killing by bile acids. *Biochimica et Biophysica Acta (BBA) - Molecular Basis of Disease*, 1637(1), pp.127–132.

Saltiel, a R., 2001. New perspectives into the molecular pathogenesis and treatment of type 2 diabetes. *Cell*, 104(4), pp.517–29.

Scarpellini, E. & Tack, J., 2012. Obesity and metabolic syndrome: an inflammatory condition. *Digestive diseases (Basel, Switzerland)*, 30(2), pp.148–53.

Scarpulla, R.C., 2008. Transcriptional Paradigms in Mammalian Mitochondrial Biogenesis and Function. *Physiological reviews*, 88, pp.611–638.

Schenk, S. & Horowitz, J.F., 2007. Acute exercise increases triglyceride synthesis in skeletal muscle and prevents fatty acid – induced insulin resistance. *The Journal of clinical investigation*, 117(6), pp.18–20.

Schoeller, D. a, 2001. The importance of clinical research: the role of thermogenesis in human obesity. *The American journal of clinical nutrition*, 73(3), pp.511–6.

Schoonjans, K. et al., 1996. PPARα and PPARγ activators direct a distinct tissue-specific transcriptional response via a PPRE in the lipoprotein lipase gene. *The EMBRO Journal*, 15(19), pp.5336–5348.

Schuster, D.P., 2010. Obesity and the development of type 2 diabetes: the effects of fatty tissue inflammation. *Diabetes, metabolic syndrome and obesity : targets and therapy*, 3, pp.253–62.

Semple, R.K., Chatterjee, V.K.K. & Rahilly, S.O., 2006. PPARγ and human metabolic disease. *The Journal of Clinical Investigation*, 116(3), pp.581–589.

Senocak, F.S. et al., 2007. Effect of uncoupling protein-1 expression on 3T3-L1 adipocyte gene expression. *FEBS letters*, 581(30), pp.5865–71.

Sethi, J.K. & Vidal-puig, A.J., 2007. Adipose tissue function and plasticity orchestrate nutritional adaptation. *Journal Of Lipid Research*, 48, pp.1253–1262.

Shen, H. et al., 2008. Farnesoid X Receptor Induces GLUT4 Expression Through FXR Response Element in the GLUT4 Promoter. *Cellular Physiology and Biochemistry*, pp.1–14.

Si, Y. et al., 2007. Effects of forced uncoupling protein 1 expression in 3T3-L1 cells on mitochondrial function and lipid metabolism. *Journal of lipid research*, 48(4), pp.826–36.

Si, Y., Shi, H. & Lee, K., 2009. Metabolic flux analysis of mitochondrial uncoupling in 3T3-L1 adipocytes. *PloS one*, 4(9), p.e7000.

Sikaris, K. a, 2004. The clinical biochemistry of obesity. *The Clinical biochemist. Reviews / Australian Association of Clinical Biochemists*, 25(3), pp.165–81.

Silva, J.E., 2006. Thermogenic Mechanisms and Their Hormonal Regulation. *The American journal of physiology*, 86, pp.435–464.

Sonoda, J. et al., 2007. PGC-1beta controls mitochondrial metabolism to modulate circadian activity, adaptive thermogenesis, and hepatic steatosis. *Proceedings of the National Academy of Sciences of the United States of America*, 104(12), pp.5223–8.

Soumaya, K., 2012. MOLECULAR MECHANISMS OF INSULIN RESISTANCE IN DIABETES. In *Diabetes: An Old Disease, a New Insight*. pp. 240–251.

Staels, B. & Fonseca, V.A., 2009. Bile Acids and Metabolic Regulation - Mechanisms and clinical responses to bile acid sequestration. *DIABETES CARE*, 32(2), pp.237–245.

Strehle, A. et al., 2007. Anti-hyperglycemic activity of a TGR5 agonist isolated from Olea europaea. *Biochemical and biophysical research communications*, 362, pp.793–798.

Student, a K., Hsu, R.Y. & Lane, M.D., 1980. Induction of fatty acid synthetase synthesis in differentiating 3T3-L1 preadipocytes. *The Journal of biological chemistry*, 255(10), pp.4745–50.

Sul, H.S. et al., 2000. Function of pref-1 as an inhibitor of adipocyte differentiation. *International journal of obesity*, 24(4), pp.S15–9.

Taittonen, M. et al., 2009. Functional Brown Adipose Tissue in Healthy Adults. *The New England Journal of Medicine*, 360(15), pp.1518–1525.

Teodoro, J.P., 2007. *Esteatose hepática : Mecanismos mitocondriais relevantes para a função celular*. Faculdade de Ciências e Tecnologia da Universidade de Coimbra.

Teodoro, J.S. et al., 2013. Enhancement of brown fat thermogenesis using chenodeoxycholic acid in mice. *International journal of obesity*, (August 2013), pp.1–8.

Teodoro, J.S., Rolo, A.P. & Palmeira, C.M., 2011. Hepatic FXR: key regulator of whole-body energy metabolism. *Cell Press*, 22(11), pp.458–66.

Thomas, C. et al., 2008. Targeting bile-acid signalling for metabolic diseases. *Nature reviews*, 7(8), pp.678–93.

Thomas, C. et al., 2010. TGR5-mediated bile acid sensing controls glucose homeostasis. *Cell metabolism*, 10(3), pp.167–177.

Tiraby, C. et al., 2003. Acquirement of brown fat cell features by human white adipocytes. *The Journal of biological chemistry*, 278(35), pp.33370–6.

Tontonoz, P., Hu, E. & Spiegelman, B.M., 1994. Stimulation of adipogenesis in fibroblasts by PPARγ2, a lipid-activated transcription factor. *Cell*, 79(7), pp.1147–1156.

Torres, N. et al., 2008. White Adipose Tissue as Endocrine Organ and Its Role in Obesity. *Archives of Medical Research*, 39, pp.715–728.

Turrens, J.F., Alexandre, A. & Lehninger, A.L., 1985. Ubisemiquinone is the electron donor for superoxide formation by complex III of heart mitochondria. *Archives of Biochemistry and Biophysics*, 237(2), pp.408–414.

Valerio, A. et al., 2006. TNF-α downregulates eNOS expression and mitochondrial biogenesis in fat and muscle of obese rodents. *The Journal of clinical investigation*, 116(10), pp.2791–2798.

Vance, D.E., 2002. Adipose tissue and lipid metabolism. In *Biochemistry of Lipids, Lipoproteins and Membranes*. pp. 263–289.

Vankoningsloo, S. et al., 2005. Mitochondrial dysfunction induces triglyceride accumulation in 3T3-L1 cells: role of fatty acid beta-oxidation and glucose. *Journal of lipid research*, 46(6), pp.1133–49.

Vega, R.B., Huss, J.M. & Kelly, D.P., 2000. The coactivator PGC-1 cooperates with peroxisome proliferator-activated receptor alpha in transcriptional control of nuclear genes encoding mitochondrial fatty acid oxidation enzymes. *Molecular and cellular biology*, 20(5), pp.1868–76.

Vichai, V. & Kirtikara, K., 2006. Sulforhodamine B colorimetric assay for cytotoxicity screening. *Nature Protocols*, 1(3), pp.1112–1116.

Vidal-Puig, A. et al., 1996. Regulation of PPAR gamma gene expression by nutrition and obesity in rodents. *The Journal of clinical investigation*, 97(11), pp.2553–61.

Wang, P.-P. et al., 2013. Piromelatine decreases triglyceride accumulation in insulin resistant 3T3-L1 adipocytes: role of ATGL and HSL. *Biochimie*, 95(8), pp.1650–4.

Wang, T. et al., 2010. Respiration in adipocytes is inhibited by reactive oxygen species. *Obesity*, 18(8), pp.1493–502.

Watanabe, M. et al., 2006. Bile acids induce energy expenditure by promoting intracellular thyroid hormone activation. *Nature*, 439(7075), pp.484–9.

Watanabe, M. et al., 2004. Bile acids lower triglyceride levels via a pathway involving FXR , SHP , and SREBP-1c. *The Journal of clinical investigation*, 113(10), pp.1408–1418.

WHO, 1999. Definition , Diagnosis and Classification of Diabetes Mellitus and its Complications. Part 1 Provisional report of a WHO Consultant. *Diabetes Medicines*, 15(7), pp.539–553.

WHO, 2013. WHO Obesity. Available at: http://www.who.int/mediacentre/factsheets/fs311/en/.

Wilson-fritch, L. et al., 2004. Mitochondrial remodeling in adipose tissue associated with obesity and treatment with rosiglitazone. *The Journal of clinical investigation*, 114(9), pp.1281–1289.

Wu, J. et al., 2012. Beige adipocytes are a distinct type of thermogenic fat cell in mouse and human. *Cell*, 150(2), pp.366–76.

Yamagata, K. et al., 2004. Bile acids regulate gluconeogenic gene expression via small heterodimer partner-mediated repression of hepatocyte nuclear factor 4 and Foxo1. *The Journal of biological chemistry*, 279(22), pp.23158–65.

Yehuda-shnaidman, E. et al., 2010. Acute Stimulation of White Adipocyte Respiration by PKA-Induce Lipolysis. *Diabetes Journal*, 59, pp.2474–2483.

Yoneshiro, T. et al., 2013. Recruited brown adipose tissue as an antiobesity agent in humans. *Clinical Investigation*, 123(8), pp.3404–3408.

Zebisch, K. et al., 2012. Protocol for effective differentiation of 3T3-L1 cells to adipocytes. *Analytical biochemistry*, 425(1), pp.88–90.

Zhang, Y. et al., 2004. Peroxisome proliferator-activated regulates triglyceride metabolism by activation of the nuclear receptor FXR. *Genes & Development*, 18, pp.157–169.